Mesoscopic charge quantization

I. L. Aleiner*
NEC Research Institute, 4 Independence Way, Princeton, New Jersey 08540

L. I. Glazman
Theoretical Physics Institute, University of Minnesota, Minneapolis, Minnesota 55455
(Received 20 October 1997)

We study the Coulomb blockade in a chaotic quantum dot connected to a lead by a single channel at nearly perfect transmission. We take into account quantum fluctuations of the dot charge and a finite level spacing for electron states within the dot. Mesoscopic fluctuations of thermodynamic and transport properties in the Coulomb blockade regime exist at any transmission coefficient. In contrast to the previous theories, we show that by virtue of these mesoscopic fluctuations, the Coulomb blockade is not destroyed completely even at perfect transmission. The oscillatory dependence of all the observable characteristics on the gate voltage is preserved, its period is still defined by the charge of a single electron. However, phases of those oscillations at perfect transmission are random; because of the randomness, the Coulomb blockade shows up not in the averages but in the correlation functions of the fluctuating observables (e.g., capacitance or tunneling conductance). This phenomenon may be called ''*mesoscopic charge quantization.*'' [S0163-1829(98)05316-8]

I. INTRODUCTION

The effect of the Coulomb blockade[1–3] in chaotic quantum dots sets an ideal stage for studying the interplay between the quantum chaos and interaction phenomena in a many-electron system. By tuning the connection between the leads and the quantum dot, one can study a rich variety of nontrivial effects. In the weak tunneling limit, discrete charging of the dot results in a sequence of sharp conductance peaks, which carry information about the chaotic motion of noninteracting electrons confined inside an almost closed dot.[4] In the opposite limit of wide channels, charge quantization does not occur, and quantum chaos of free electrons in an open billiard may be studied.[5] In a broad intermediate region, the charge quantization is gradually destroyed, and the chaotic electron motion is affected by fluctuations of charge of the cavity. The modern experimental technique[3,6,7] allows one to continuously traverse these regimes.

The effect of charging is conventionally described by the Hamiltonian[2]

$$\hat{H}_C=\frac{E_C}{2}\left(\frac{\hat{Q}}{e}-\mathcal{N}\right)^2, \quad E_C=\frac{e^2}{C}, \tag{1.1}$$

where C is the total capacitance of the dot, the dimensionless parameter $\mathcal{N}$ is related to the gate voltage V_g, and gate capacitance C_g by $\mathcal{N}=V_g/eC_g$, and $\hat{Q}$ is the dot charge. Usually, charging energy E_C is much larger than the one-electron mean level spacing of the dot, Δ. If the connection of the dot with the leads is weak and temperature T is small, $T\ll E_C$, the charge is well quantized for almost all $\mathcal{N}$ except narrow vicinities of the charge degeneracy points (half-integer $\mathcal{N}$). The behavior of the differential capacitance of the cavity, $d\langle Q\rangle/dV_g$, and of the conductance through the cavity is quite different for the system tuned to the immediate vicinity of charge degeneracy points (Coulomb blockade peaks), or away from those points (Coulomb blockade valleys). The statistics of the peaks can be related to the properties of a single electron energy and wave function,[4] so that the distribution functions for these quantities can be extracted from the well-known random matrix theory (RMT).[8,9] The transport in the valleys occurs by virtual transitions of an electron via excited states of the dot.[10] The statistics of the conductance in this case was recently obtained in Ref. 11 and was confirmed experimentally in Ref. 12.

All the aforementioned results were obtained neglecting quantum fluctuations of the charge of the cavity. These fluctuations grow with the increase of the coupling between the dot and lead.[13] Then, the difference between the peaks and valleys becomes less pronounced and eventually instead of the peak structure, one observes only a weak periodic modulation.[14] Clearly, this modulation can be described neither by the properties of the single-electron wave function nor by the lowest-order virtual transitions via the excited states.

The case of almost perfect transmission of a one-channel point contact connecting the quantum dot with the lead (see Fig. 1) was analyzed by Matveev[14] and Flensberg[15] in the framework of an effective one-dimensional Hamiltonian. Employing the bosonization technique, they showed that the Coulomb blockade disappears completely if the transmission

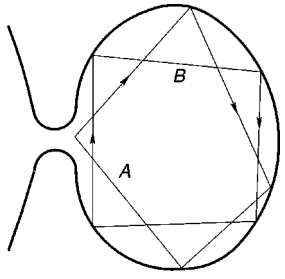

FIG. 1. Schematic view of a quantum dot connected to a lead. Periodic orbit A encounters the entrance to the dot once, $n_A=1$, and periodic orbit B does not encounter the entrance, $n_B=0$.

coefficient of the point contact is exactly unity $r=0$ and $\Delta=0$. The explicit dependence of the differential capacitance of the system on $\mathcal{N}$, and on the small reflection coefficient $0<|r|^2\ll 1$ was obtained by Matveev.[14] It is important to emphasize that the Coulomb blockade in this situation is nonperturbative in charging energy effect and it cannot be revealed in the standard Hartree-Fock or random phase approximations.

The properties of a quantum dot connected to reservoir by a channel were analyzed in a series of papers of Büttiker and collaborators.[16,17] They have used the random phase approximation to calculate the frequency dependence of the linear response of the current I through the channel to bias $Ve^{i\omega t}$ applied to the reservoir: $I=G(\omega)V$. In this approach, the admittance $C=-\mathrm{Im}(dG/d\omega)|_{\omega\to 0}$ coincides by construction with the thermodynamic capacitance of the noninteracting electrons. The quantum corrections and mesoscopic fluctuations of this quantity then can be analyzed by using the distribution of the Wigner delay times of the noninteracting system.[17] This approach is perfectly valid for a large number of channels, but for a single channel, there is no parameter justifying it. We will see below that the results obtained by a well-controlled procedure are significantly different (see Secs. V and VI).

In this paper, we account for both the strong quantum charge fluctuations, and the chaotic electron motion within the dot. We will show that backscattering of electrons from the walls of the dot into the channel connecting it to the lead results in residual Coulomb blockade oscillations of observables with the gate voltage. In the limit of perfect channel transmission, the relative magnitude of the differential capacitance oscillations is $\sqrt{\Delta/E_C}$ and $(\Delta/E_C)\ln^2(E_C/\Delta)$ for the spinless and for spin-1/2 cases, respectively. If the second lead is attached to the cavity by a weak tunnel junction with conductance $G_0\ll e^2/\hbar$, the two-terminal conductance G can be measured. The average value of the conductance is suppressed by the Coulomb blockade, but it remains finite even at zero temperature, $\langle G\rangle\simeq G_0\Delta/E_C$. Fluctuations of the conductance are of the order of its average. This resembles the result for the elastic co-tunneling in the weak coupling regime.[10,11] However, the dependence of the conductance of the gate voltage is no longer a sequence of deep valleys and sharp peaks, but rather a weakly oscillating function.

For a finite reflection coefficient in the channel ($|r|^2\neq 0$), we found a new contribution, in addition to the averaged differential capacitance calculated in Ref. 14. This contribution is fluctuating and provides, in particular, the dependence of the differential capacitance on the magnetic field.

The paper is organized as follows. In Sec. II, we qualitatively discuss the mesoscopic fluctuations of the differential capacitance for spinless electrons. Section III is devoted to the formulation of the model and derivation of the effective action representation. We will also discuss the conditions of applicability of the model. Section IV describes the bosonization procedure. Calculation of the ground-state energy and differential capacitance is performed in Sec. V. The tunneling conductance in a strongly asymmetric setup (one channel is reflectionless, and the other junction is of conductance $G_0\ll e^2/\hbar$) is studied in Sec. VI. Our findings are summarized in the Conclusion.

II. QUALITATIVE DISCUSSION

Let us consider first a completely opened channel ($r=0$). In the limit $\Delta\to 0$, the electron charge of the dot varies with the gate voltage as $\langle Q\rangle=e\mathcal{N}$, to assure the minimum of the electrostatic energy.[14] The interaction (1.1) depends only on the number of electrons crossing the dot-channel boundary. Therefore, the properties of the ground state can be characterized by the asymptotic behavior of the wave functions far from the entrance to the dot. This behavior is described by the scattering phase, and at low energies can be understood from the following qualitative argument.

Entrance of an additional electron with energy ϵ (all the energies will be measured from the Fermi level) into the dot requires energy E_C. Therefore, the electron may spend in the dot time of the order of $\hbar/E_C$, and then the extra charge of the dot has to relax. There are two processes that lead to the relaxation of the charge: (i) the elastic process where the same electron leaves the dot; and (ii) the inelastic process where some other electron is emitted from the dot. At low energies the probability of the inelastic process is as small as $(\epsilon/E_C)^2$, by virtue of the smallness of the phase volume. (The last statement assumes the Fermi liquid behavior at low energies and, as we will see later, is valid only for a spinless one-channel case.) Therefore, we may consider only the elastic process. The same consideration is applicable also to an electron leaving the dot. Thus we conclude that the low-energy properties of the system can be mapped onto the dot effectively decoupled from the channel, and the phase of the scattering amplitude from the entrance of the dot is given by the Friedel sum rule

$$\delta=\pi\langle Q\rangle/e=\pi\mathcal{N}. \tag{2.1}$$

Equation (2.1) can be applied to electrons incident from inside the dot, as well as to electrons incident from the channel. The outlined description resembles closely the Nozieres description of the unitary limit in the one-channel Kondo problem.[18]

The outlined above qualitative picture based on the introduction of scattering phase δ is somewhat intuitive; it will be verified by a calculation in Sec. IV. Here instead of rigorous proof, we demonstrate that this scheme reproduces the result

$$E_g(\mathcal{N})\simeq|r|E_C\cos 2\pi\mathcal{N} \tag{2.2}$$

obtained by Matveev[14] for the ground-state energy $E_g(\mathcal{N})$ of spinless electrons in the limit of zero level spacing in the dot. Then, we apply the scheme to find the corrections to the ground-state energy arising from a finite Δ. Those corrections will result in the mesoscopic fluctuations of the ground-state energy.

We start with considering the limit $\Delta=0$. First, we put also $|r|=0$ and calculate the density of electrons in the channel $\rho(x)$. Then we take into account the scattering potential $V(x)$ that generates $r\neq 0$, in the first order of perturbation theory,

$$E_g(\mathcal{N})=\int dx\,\rho(x)V(x). \tag{2.3}$$

As we discussed, the Coulomb interaction leads to the perfect reflection of an electron at low energies; wave functions

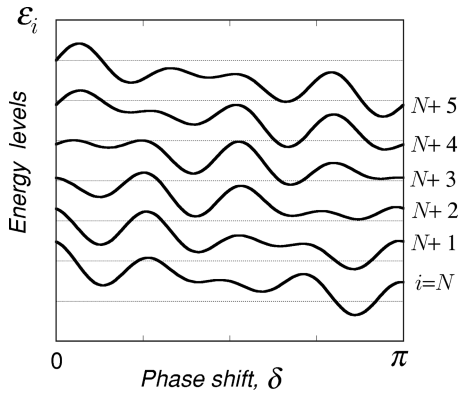

FIG. 2. Evolution of the energy levels of the quantum dot with the scattering phase δ.

have the form $\psi_k(x)=\cos(k|x|-\delta)$, with phase shift δ given by Eq. (2.1). It leads to the Friedel oscillation of the electron density $\rho(x)=\Sigma_{v_F|k-k_F|\lesssim E_C}|\psi_k(x)|^2$, where v_F and k_F are the Fermi velocity and Fermi wave vector, respectively. We obtain

$$\rho(x)=\begin{cases}\dfrac{E_C}{v_F}\cos(2k_F|x|-2\delta), & |x|<v_F/E_C\\ \dfrac{\sin(2k_F|x|-2\delta)}{|x|}, & |x|>v_F/E_C.\end{cases} \tag{2.4}$$

Here we omitted the irrelevant constant part of the electron density. Substituting Eq. (2.4) into Eq. (2.3), assuming the magnitude of the potential around $x=0$ smaller than v_F/E_C, and using the standard expression $|r|=|\tilde{V}(2k_F)|/v_F$, we obtain formula (2.2). Here $\tilde{V}(k)$ is the Fourier transform of the potential $V(x)$.

Having verified the suggested scheme for the case $\Delta=0$, we proceed with evaluation of the ground-state energy of a finite dot connected to a reservoir by a perfect channel. According to the above discussion, the channel is effectively decoupled from the dot due to the charging effect even though $r=0$. Therefore, we have to relate the ground-state energy of a closed dot to the scattering phase δ of Eq. (2.1). For a chaotic dot, this problem is equivalent to finding a variation of the eigenenergies by introduction of impurity potential $V(\mathbf{r})=(1/\pi\nu)\delta(\mathbf{r})\tan\delta$, where ν is the averaged density of states per unit area. The relevant contribution to the ground-state energy is given by

$$E_g=\sum_{-E_C\lesssim\xi_i<0}[\xi_i(\delta)+\mu], \tag{2.5}$$

where ξ_i are the eigenenergies measured from the Fermi level μ. As soon as the scattering phase changes by π, one more level enters under the Fermi level. Evolution of the energy levels with changing δ is shown schematically in Fig. 2. The position of the level $\xi_i(\delta)$ satisfies the gluing condition

$$\xi_i(\delta+\pi)=\xi_{i+1}(\delta). \tag{2.6}$$

From Eq. (2.5) and Eq. (2.6) we see that the ground-state energy depends almost periodically on δ:

$$E_g(\delta)=E_g(\delta+\pi)+O(\Delta). \tag{2.7}$$

As we will see below, the amplitude of the oscillation of the ground-state energy with δ is much larger than the mean level spacing and we will neglect the last term in Eq. (2.7).

In order to estimate the amplitude of the oscillations, we recall that the correlation function of the level velocities is given by[19]

$$\langle\partial_\delta\epsilon_i\rangle=\frac{\Delta}{\pi},\quad \langle\partial_\delta\epsilon_i\partial_\delta\epsilon_j\rangle=\delta_{ij}\frac{2}{\beta}\left(\frac{\Delta}{\pi}\right)^2, \tag{2.8}$$

where $\beta=1,2$ for the orthogonal and unitary ensembles, respectively, and $\langle\cdots\rangle$ stands for the ensemble averaging. Formula (2.8) can be easily understood from the first-order perturbation theory. At $\delta\ll1$, we have $\epsilon_i(\delta)\approx\epsilon_i(0)+(\delta/\pi\nu)|\psi_i^2(0)|$. For a chaotic system the exact wave functions ψ_i can be presented in the form

$$|\psi_i(0)|^2=\frac{1+b_i}{\mathcal{A}},$$

where the area of the dot $\mathcal{A}$ appears due to the normalization condition, and b_i characterizes the fluctuations of the chaotic wave functions. In accordance with the Porter-Thomas distribution,[8]

$$\langle b_i\rangle=0;\quad \langle b_ib_j\rangle=\frac{2}{\beta}\delta_{ij}.$$

Estimating the mesoscopic fluctuations of the ground-state energy (2.5) with the help of Eq. (2.8), we obtain for $\delta\ll1$

$$\langle[E_g(\delta)-E_g(0)]^2\rangle=\Delta^2\left(\frac{\delta}{\pi}\right)^2\sum_{-E_C\lesssim\xi_i,\xi_j<0}\frac{2}{\beta}\delta_{ij}\approx\Delta E_C\delta^2. \tag{2.9}$$

As we have already explained, energy (2.5) is a periodic function of δ with period π. On the other hand, for $\delta\lesssim1$, Eq. (2.9) is valid. Therefore the characteristic amplitude of the oscillations is of the order of $\sqrt{E_C\Delta}$, and it is plausible to assume that the correlation function of energies at two different parameters $\mathcal{N}_1,\mathcal{N}_2$ takes the form

$$\langle E_g(\mathcal{N}_1)E_g(\mathcal{N}_2)\rangle\approx\Delta E_C\cos2\pi(\mathcal{N}_1-\mathcal{N}_2), \tag{2.10}$$

where we use Eq. (2.1). It is important to notice that the variation of the energy of the ground state is much larger than the mean level spacing Δ. This observation enabled us not to consider in particular the variation of the chemical potential with changing δ, because it would generate a correction of the order of the level spacing only.

In order to explain the functional form of the correlation function (2.10) and make our argumentation more precise, it is instructive to evaluate the shift of the energy levels starting from the Gutzwiller trace formula.[20] The energy of the ground state is given by

$$E_g=-\int_{-\infty}^{0}d\epsilon N(\epsilon)K(\epsilon/E_C), \tag{2.11}$$

where ϵ is measured from the Fermi level, and $N(\epsilon)$ is the integrated density of states, $N(\epsilon)=\Sigma_i\theta(\epsilon-\epsilon_i)$. Here $K(x)$ is

some function that decays rapidly at $x>1$, so only the states that can be described within the Fermi liquid theory contribute into the δ-dependent part of the ground-state energy [cf. Eq. (2.5)].

The integrated density of states can be expressed as a sum over the classical periodic orbits:[20]

$$N(\epsilon,\delta)=\mathrm{Re}\sum_j R_j(\epsilon)\exp\left[\frac{i}{\hbar}S_j(\epsilon)+2in_j\delta\right]. \quad (2.12)$$

Here R_j is the weight associated with jth orbit, S_j is the reduced action for this orbit. The last term in the exponent in Eq. (2.12) characterizes the reflection from the entrance of the cavity, and n_j is the number of such reflections for jth orbit; see Fig. 1. We have omitted the mean value of $N(\epsilon)$, which is independent of the phase shift (2.1).

Integrated density of states (2.12) is a strongly oscillating function of energy, which vanishes upon ensemble (or energy) averaging. However, it contributes to the fluctuations of the density of states:

$$\langle N(\epsilon_1,\delta_1)N(\epsilon_2,\delta_2)\rangle = 2\,\mathrm{Re}\sum_j |R_j|^2\exp\left[\frac{i}{\hbar}(S_j(\epsilon_1)-S_j(\epsilon_2))+2in_j(\delta_1-\delta_2)\right], \quad (2.13)$$

and we neglected the energy dependence of the preexponential factors R_j because it occurs on the energy scale of the order of the Fermi energy. In the double sum over the periodic orbits, arising in Eq. (2.13), one can retain only diagonal terms[21] because different orbits have different actions; the nondiagonal terms oscillate strongly and vanish upon averaging. The factor of 2 in Eq. (2.13) originates from the fact that the electron trajectory j and the trajectory time reversed to j have the same action.

In order to calculate the correlation function of mesoscopic fluctuations of ground-state energies (2.11), we use Eq. (2.13) and expand the action as $S_j(\epsilon_1)-S_j(\epsilon_2)=(\epsilon_1-\epsilon_2)t_j$, with t_j being the period of jth orbit. After integration over energies $\epsilon_{1,2}$, we find

$$\langle E_g(\delta_1)E_g(\delta_2)\rangle = 2E_C^2\sum_j |R_j|^2\widetilde{K}\left(\frac{E_C t_j}{\hbar}\right)\cos[2n_j(\delta_1-\delta_2)], \quad (2.14)$$

where $\widetilde{K}(y)=\left|\int_{-\infty}^{0}dx\,K(x)e^{ixy}\right|^2$ is a function decaying at $y>1$.

Coefficients $|R_j|^2$ have a very simple physical meaning, and are related to the classical probability $P(t)dt$ to find a periodic orbit with a period within the interval $[t;t+dt]$:

$$\sum_j |R_j|^2\cdots\to\frac{1}{2\pi^2}\int_0^\infty\frac{dt}{t}P(t)\cdots. \quad (2.15)$$

In the same fashion, we obtain from Eq. (2.14):

$$\langle E_g(\delta_1)E_g(\delta_2)\rangle = \frac{E_C^2}{\pi^2}\sum_n \int_0^\infty\frac{dt}{t}\widetilde{K}\left(\frac{E_C t}{\hbar}\right)P_n(t)\cos[2n(\delta_1-\delta_2)]. \quad (2.16)$$

The classical probability $P_n(t)$ differs from $P(t)$ by satisfying an additional constraint: the corresponding periodic orbits are reflected from the dot entrance exactly n times; $\Sigma_n P_n(t)=P(t)$.

In general, $P_n(t)$ depends on a particular shape of the dot. However, if the motion is chaotic, $P_n(t)$ becomes universal,

$$P_n(t)=\frac{(t\Delta/\hbar)^n}{n!}e^{-t\Delta/\hbar}, \quad (2.17)$$

for the periods t much larger than the ergodic time $\hbar/E_T$. Energy E_T associated with the time scale at which the classical dynamics becomes ergodic is the counterpart of the Thouless energy for the diffusive system. Typically $E_T\gtrsim E_C$, therefore we adopt the approximation $E_T\gg E_C\gg\Delta$. According to Eq. (2.14), the characteristic period of the semiclassical trajectory is of the order of $\hbar/E_C$, which is much smaller than the Heisenberg time $\hbar/\Delta$. Therefore, when calculating the oscillatory part of the correlation function of the ground-state energies, it suffices to keep in Eq. (2.16) only the contribution of the trajectories reaching the entrance only once. As the result, we obtain an expression similar to our estimate (2.10),

$$\langle E_g(\mathcal{N}_1)E_g(\mathcal{N}_2)\rangle=\alpha\Delta E_C\cos 2\pi(\mathcal{N}_1-\mathcal{N}_2), \quad (2.18)$$

where we have used Eq. (2.1). The numerical coefficient $\alpha=(1/\pi^2)\int_0^\infty dx\,\widetilde{K}(x)$ depends on the particular form of function $\widetilde{K}$, and cannot be found within the simple consideration.

Let us now discuss the correlation of the ground-state energies as a function of magnetic field. The magnetic flux threading a periodic orbit adds a phase $\phi_j=A_jH/\Phi_0$ to the action in each term j in the Gutzwiller formula (2.12), where A_j is the directed area under the trajectory, H is the applied magnetic field, and Φ_0 is the flux quantum. Correspondingly, formula (2.14) is modified to

$$\langle E_g(\delta_1,H_1)E_g(\delta_2,H_2)\rangle = 2E_C^2\sum_j |R_j|^2\widetilde{K}\left(\frac{E_C t_j}{\hbar}\right)\times\cos\left(\frac{H_1A_j}{\Phi_0}\right)\cos\left(\frac{H_2A_j}{\Phi_0}\right)\cos[2n_j(\delta_1-\delta_2)]. \quad (2.19)$$

In analogy with Eq. (2.16), we transform Eq. (2.19) to

$$\langle E_g(\delta_1,H_1)E_g(\delta_2,H_2)\rangle = \frac{E_C^2}{\pi^2}\sum_n\int dA\int_0^\infty\frac{dt}{t}P_n(t;A)\times\widetilde{K}\left(\frac{E_C t}{\hbar}\right)\cos\left(\frac{H_1A}{\Phi_0}\right)\cos\left(\frac{H_2A}{\Phi_0}\right)\cos[2n(\delta_1-\delta_2)], \quad (2.20)$$

where $P_n(t;A)dA$ differs from probability $P_n(t)$ by one more constraint: the directed area swept by a trajectory lies within the interval $[A;A+dA]$.

In a chaotic system, the probability $P_n(t;A)$ factorizes:

$$P_n(t;A)=P_n(t)p(t;A). \quad (2.21)$$

Here $P_n(t)$ is defined by Eq. (2.17), and the distribution function of the areas is Gaussian:

$$p(t;A)=\frac{1}{2\sqrt{\pi\langle A^2(t)\rangle}}\exp\left\{-\frac{A^2}{4\langle A^2(t)\rangle}\right\},$$
$$\langle A^2(t)\rangle=\frac{E_T t}{\hbar}\mathcal{A}^2. \tag{2.22}$$

The formula for $\langle A^2(t)\rangle$ shows that the typical area under the electron trajectory differs from the area of the dot $\mathcal{A}$, and grows as $\sqrt{t}$. This law is applicable at the time scale exceeding the ergodic time $\hbar/E_T$, and reflects the time dependence of r.m.s. of the random winding number for the trajectory of an electron bouncing off the walls of the dot.

As we already discussed, the characteristic time an electron spends in the dot is $\hbar/E_C$. The characteristic area accumulated during this time is $\sqrt{E_T/E_C}$. A magnetic field produces an appreciable effect if a flux penetrating through this area is of the order of Φ_0. Thus, the correlation magnetic field is controlled by the charging energy:

$$H_c=\frac{\Phi_0}{\mathcal{A}}\sqrt{\frac{E_C}{2\pi E_T}}. \tag{2.23}$$

Using Eqs. (2.20)–(2.22), we find the correlation function

$$\langle E_g(\mathcal{N}_1,H_1)E_g(\mathcal{N}_2,H_2)\rangle=E_C\Delta\sum_{\gamma=+,-}\Lambda_E\left(\frac{H_\gamma^2}{H_c^2}\right)\cos 2\pi n, \tag{2.24}$$

where we introduced the shorthand notation $H_\pm=H_1\pm H_2$ and $n=\mathcal{N}_1-\mathcal{N}_2$. Calculation of the exact form of the dimensionless function $\Lambda_E(x)=\int_0^\infty dy\, e^{-xy}\tilde{K}(y)$, and of the numerical coefficient in Eq. (2.23), requires more involved treatment, which is a subject of the following sections.

Equations (2.18) and (2.24) constitute the main qualitative result of this section. We were able to demonstrate the oscillations of the ground-state energy with the applied gate voltage. The phase of those oscillations is random, so that the oscillations can be revealed only in the correlation functions. Unfortunately, these simple qualitative arguments are not sufficient for finding the precise form of the correlation functions. Moreover, the assumption of the Fermi-liquid behavior is valid only for the spinless electrons. It is known that the low-energy behavior of the $s=1/2$ electrons is equivalent[14] to that of the two-channel Kondo problem in its strong-coupling fixed point displaying a non-Fermi-liquid behavior. Quantitative study of the system in this case will be presented later; see Sec. V B.

III. THE MODEL

The main difficulty of the problem is in the nonperturbative nature of the Coulomb blockade effect. Derivation of an effective one-dimensional model is our first step in overcoming this difficulty. The interaction energy (1.1) depends only on the total number of electrons in the dot. The change of this number is associated with electrons propagating through the channel. Because the dynamics of the channel is one dimensional, the charging effects of the system can be considered on the basis of a one-dimensional Hamiltonian.[14,15] However, the original problem was at least two dimensional, so backscattering of the electrons by the walls of the dot cannot be accounted for by the one-dimensional Hamiltonian. Instead, of an effective Hamiltonian, we were able to find an effective action that depends only on the electron variables of the one-dimensional channel. If there was no interaction, such an approach would have no advantage; however, in the presence of interaction it becomes very powerful. The interaction will be exactly accounted for by means of bosonization, see Sec. IV.

Electrons are backscattered into the channel by the walls of the dot at random times, therefore the action we derive in Sec. III A has a nonlocal in time, random term. This term, however, can be treated perturbatively by virtue of the small parameter, $\Delta/E_c\ll 1$. With the help of the action, calculation of the correlation functions of energies and differential capacitances can be performed by the standard diagrammatic methods.[19] At energies less than E_T the averages become universal. In this regime, it is also possible to formulate the model starting from the random matrix Hamiltonian,[22] see Sec. III B.

The applicability of the description of the interaction by Eq. (1.1), i.e., of the constant-interaction model, is discussed in Sec. III C. We will show that the corrections to this description are of the order of $1/g$, where $g\gg 1$ is the dimensionless conductance of the dot.

A. ''Conventional'' formulation

We start with the Hamiltonian of the system,

$$\hat{H}=\hat{H}_F+\hat{H}_C, \tag{3.1}$$

where $\hat{H}_F$ is the Hamiltonian of noninteracting electrons,

$$\hat{H}_F=\int d\mathbf{r}\left[\frac{1}{2m}\nabla\psi^\dagger\nabla\psi+[-\mu+U(\mathbf{r})]\psi^\dagger\psi\right]. \tag{3.2}$$

The potential $U(\mathbf{r})$ describes the confinement of electrons to the dot and channel.

The interaction Hamiltonian $\hat{H}_C$ is given by Eq. (1.1), and the charge of the dot is

$$\frac{\hat{Q}}{e}=\int_{\text{dot}} d\mathbf{r}\ \psi^\dagger\psi, \tag{3.3}$$

where the integration is performed within the dot. Of course, the boundary separating the dot from the lead is not defined. However, this ambiguity can be absorbed into the definition of dimensionless gate voltage $\mathcal{N}$.

For the purpose of the evaluation it is more convenient, however, to change the definition of the charge. Noticing that the total number of particles in the system is an integer number that can be added to the parameter $\mathcal{N}$ without affecting any periodic in $\mathcal{N}$ observables, we write

$$\frac{\hat{Q}}{e}=-\int_{\text{channel}} d\mathbf{r}\ \psi^\dagger\psi. \tag{3.4}$$

To calculate the ground-state energy, we start with the thermodynamic potential,

$$\Omega = -\frac{1}{\beta}\ln(\mathrm{Tr}e^{-\beta\hat{H}}), \tag{3.5}$$

where temperature $T=1/\beta$.

We evaluate the trace in two steps, $\mathrm{Tr}\cdots=\mathrm{Tr}_1\mathrm{Tr}_2\cdots$, where 1 and 2 indicate the fermionic operators belonging to the channel and dot, respectively. Because all of the interaction is attributed to the channel [see Eq. (3.4)], the charging energy operator is not affected by the summation in the dot, and can be omitted in the intermediate formulas. The noninteracting Hamiltonian (3.2) can be presented as $\hat{H}_F=\hat{H}_1+\hat{H}_2+\hat{H}_{12}$, where $\hat{H}_1$ and $\hat{H}_2$ are the noninteracting Hamiltonians of the channel and of the dot, respectively, and $\hat{H}_{12}$ connects the dot with the channel. Thus, we write

$$\begin{aligned}\mathrm{Tr}_2 e^{-\beta\hat{H}_F} &= \mathrm{Tr}_2 e^{-\beta(\hat{H}_1+\hat{H}_2+\hat{H}_{12})}\\ &= e^{-\beta\hat{H}_1}\mathrm{Tr}_2[e^{-\beta\hat{H}_2}T_\tau e^{-\int_0^\beta d\tau\hat{H}_{12}(\tau)}]\\ &= e^{-\beta\Omega_2}e^{-\beta\hat{H}_1}T_\tau e^{(1/2)\int_0^\beta d\tau_1\int_0^\beta d\tau_2\langle\hat{H}_{12}(\tau_1)\hat{H}_{12}(\tau_2)\rangle_2}.\end{aligned} \tag{3.6}$$

Here $\hat{H}_{12}(\tau)=e^{\tau(\hat{H}_1+\hat{H}_2)}\hat{H}_{12}e^{-\tau(\hat{H}_1+\hat{H}_2)}$ is the interaction representation of the Hamiltonian connecting the dot and lead, T_τ stands for the chronological ordering, and $\Omega_2=-T\ln\mathrm{Tr}_2e^{-\beta\hat{H}_2}$ is the thermodynamic potential of noninteracting electrons in the dot. Averaging $\langle\cdots\rangle_2$ over the electronic variables of the dot is defined by the relation $\langle\cdots\rangle_2=e^{\beta\Omega_2}\mathrm{Tr}_2(e^{-\beta\hat{H}_2}\cdots)$. The thermodynamic potential Ω_2 does not depend on $\mathcal{N}$, and it will be omitted.

The operator Eq. (3.6) depends only on the electron variables of the channel. The evaluation of the last factor in Eq. (3.6) is performed in Appendix A. This yields

$$\begin{aligned}\frac{1}{2}\langle\hat{H}_{12}(\tau_1)\hat{H}_{12}(\tau_2)\rangle_2 &= -\overline{\psi}(\tau_1;0)\psi(\tau_2;0)\\ &\times\frac{1}{4m^2}\int dy\,dy'\,\phi(y)\phi(y')\partial^2_{xx'}\mathcal{G}(\tau_1-\tau_2;\mathbf{r},\mathbf{r}'),\end{aligned} \tag{3.7}$$

where $\psi(\tau;x)=e^{\tau\hat{H}_1}\psi(x)e^{-\tau\hat{H}_1}$ are the one-dimensional fermionic operators of the channel in the interaction representation, $\overline{\psi}(\tau)=\psi^\dagger(-\tau)$, and $\mathcal{G}$ is the exact Matsubara Green function of the closed dot subjected to the zero boundary condition. The wave function $\phi(y)$ describes the transverse motion in the single-mode channel, and the coordinates x, x' in the derivative of the Green function $\mathcal{G}$ are set to $+0$.

The detailed behavior of the Green function $\mathcal{G}$ depends on the particular shape of the dot. It is convenient to separate the fluctuating part of the Green function, $\mathcal{G}=\overline{\mathcal{G}}+\widetilde{\mathcal{G}}$, and to combine the sample-independent proportional to $\overline{\mathcal{G}}$ part of $\langle\hat{H}_{12}(\tau_1)\hat{H}_{12}(\tau_2)\rangle_2$ with the Hamiltonian H_1 in Eq. (3.6).

We rewrite Eq. (3.7) in the form

$$\begin{aligned}\langle\hat{H}_{12}(\tau_1)\hat{H}_{12}(\tau_2)\rangle_2 &= \overline{\langle\hat{H}_{12}(\tau_1)\hat{H}_{12}(\tau_2)\rangle_2}\\ &-2\overline{\psi}(\tau_1;0)\psi(\tau_2;0)L(\tau_1-\tau_2),\end{aligned} \tag{3.8}$$

where kernel L is given by

$$L(\tau)=\frac{1}{4m^2}\int dy\,dy'\,\phi(y)\phi(y')\partial^2_{xx'}\widetilde{\mathcal{G}}(\tau;\mathbf{r},\mathbf{r}'). \tag{3.9}$$

One can check by a direct calculation that

$$e^{-\beta\hat{H}_1}T_\tau e^{(1/2)\int_0^\beta d\tau_1\int_0^\beta d\tau_2\overline{\langle\hat{H}_{12}(\tau_1)\hat{H}_{12}(\tau_2)\rangle_2}}\propto\mathrm{Tr}_> e^{-\beta\hat{H}_{1D}}, \tag{3.10}$$

where $\mathrm{Tr}_>$ stands for the trace of the one-dimensional fermionic operators on the positive half axis, and

$$\hat{H}_{1D}=\int_{-\infty}^{\infty}dx\left[\frac{1}{2m}\nabla\psi^\dagger\nabla\psi-\mu\psi^\dagger\psi\right] \tag{3.11}$$

is the one-dimensional Hamiltonian defined on the whole real axis. The proportionality coefficient in Eq. (3.10) does not contribute to any observable quantity and we omit it. We substitute Eq. (3.8) into Eq. (3.6), use Eq. (3.10), restore the charging energy [see Eq. (3.4)], and obtain

$$\mathrm{Tr}e^{-\beta\hat{H}}\propto\mathrm{Tr}(e^{-\beta\hat{H}_0}T_\tau e^{-\hat{S}}). \tag{3.12}$$

The one-dimensional effective Hamiltonian is given by

$$\hat{H}_0=\hat{H}_{1D}+E_C\left(\mathcal{N}+\int_{-\infty}^{0}:\psi^\dagger\psi:dx\right)^2, \tag{3.13}$$

where $:\cdots:$ stands for the normal ordering. The effective action $\hat{S}$ in Eq. (3.12),

$$\hat{S}=\int_0^\beta d\tau_1 d\tau_2 L(\tau_1-\tau_2)\overline{\psi}(\tau_1;0)\psi(\tau_2;0), \tag{3.14}$$

has kernel L defined by Eq. (3.9). If the electrons with spin are considered, the summation over spin indices is implied in the above formulas.

As we are interested in the dynamics of the system at energies much smaller than the Fermi energy, we can linearize the spectrum of one-dimensional fermions. Writing $\psi(x)=e^{-ik_Fx}\psi_L(x)+e^{ik_Fx}\psi_R(x)$, where ψ_L and ψ_R are the left- and right-moving fermions, respectively, we obtain from Eqs. (3.11) and (3.13):

$$\begin{aligned}\hat{H}_0 &= iv_F\int_{-\infty}^{\infty}dx\{\psi_L^\dagger\partial_x\psi_L-\psi_R^\dagger\partial_x\psi_R\}\\ &+\frac{E_C}{2}\left(\int_{-\infty}^{0}dx:\psi_L^\dagger\psi_L+\psi_R^\dagger\psi_R:+\mathcal{N}\right)^2,\end{aligned} \tag{3.15}$$

where v_F is the Fermi velocity in the channel. In Eq. (3.15) the fermionic fields are assumed to be smooth on the scale of the Fermi wavelength. The action has the following form in terms of the left- and right-movers:

$$\hat{S}=\int_0^\beta d\tau_1 d\tau_2 L(\tau_1-\tau_2)$$
$$\times[\bar{\psi}_L(\tau_1)+\bar{\psi}_R(\tau_1)][\psi_L(\tau_2)+\psi_R(\tau_2)]. \quad (3.16)$$

Finite reflection in the channel can be taken into account by adding to the Hamiltonian (3.15) one more term:

$$\hat{H}_{bs}=|r|v_F[\psi_L^\dagger(0)\psi_R(0)+\psi_R^\dagger(0)\psi_L(0)], \quad (3.17)$$

where $|r|^2\ll 1$ is the reflection coefficient. The thermodynamic potential $\Omega(\mathcal{N})$ can be found from

$$\Omega(\mathcal{N})=-T\ \ln\ \mathrm{Tr}(e^{-\beta(\hat{H}_0+\hat{H}_{bs})}T_\tau e^{-\hat{S}}). \quad (3.18)$$

The differential capacitance $C_{\mathrm{diff}}(\mathcal{N})$ of the system is then given by

$$C_{\mathrm{diff}}(\mathcal{N})=C\left(1-\frac{1}{E_C}\frac{\partial^2\Omega}{\partial\mathcal{N}^2}\right). \quad (3.19)$$

Equations (3.15) and (3.17) were first suggested in Refs. 14 and 15.

So far we succeeded in reducing the original problem to the effective one-dimensional problem, where all the features of the chaotic motion of electrons in the dot are incorporated into the nonlocal in time action. The action fluctuates strongly from sample to sample, and we should study the statistics of these fluctuations.

1. Statistics of $L(\tau)$

It is convenient to use the Lehmann representation for the function $L(\tau)$ of Eq. (3.9):

$$L(\tau)=\int_{-\infty}^{\infty}\frac{dt}{2\pi}[L^R(t)-L^A(t)]\frac{\pi T}{\sinh[\pi T(t+i\tau)]}, \quad (3.20)$$

where the retarded and advanced kernels $L^{R,A}$ are given by Eq. (3.9), with $\tilde{\mathcal{G}}$ replaced by the exact advanced and retarded Green functions $\tilde{\mathcal{G}}^{R,A}$, respectively. It is well known that the averaged products of the type $\overline{\tilde{\mathcal{G}}^R\tilde{\mathcal{G}}^R}$ and $\overline{\tilde{\mathcal{G}}^A\tilde{\mathcal{G}}^A}$ vanish, and the products of the retarded and advanced Green functions can be expressed in terms of the classical propagators—diffusons $\mathcal{P}^D$ and Cooperons $\mathcal{P}^C$,

$$\overline{\tilde{\mathcal{G}}^R_{H_1}(t_1;\mathbf{r}_1^+,\mathbf{r}_2^+)\tilde{\mathcal{G}}^A_{H_2}(t_2;\mathbf{r}_2^-,\mathbf{r}_1^-)}=2\pi\nu\delta(t_1+t_2)$$
$$\times\mathcal{F}(\mathbf{r}_1^+,\mathbf{r}_1^-)\mathcal{F}(\mathbf{r}_2^+,\mathbf{r}_2^-)\mathcal{P}^D(t_1;\mathbf{R}_1,\mathbf{R}_2), \quad (3.21a)$$

$$\overline{\tilde{\mathcal{G}}^R_{H_1}(t_1;\mathbf{r}_1^+,\mathbf{r}_2^+)\tilde{\mathcal{G}}^A_{H_2}(t_2;\mathbf{r}_1^-,\mathbf{r}_2^-)}=2\pi\nu\delta(t_1+t_2)$$
$$\times\mathcal{F}(\mathbf{r}_1^+,\mathbf{r}_1^-)\mathcal{F}(\mathbf{r}_2^+,\mathbf{r}_2^-)\mathcal{P}^C(t_1;\mathbf{R}_1,\mathbf{R}_2), \quad (3.21b)$$

$$\mathcal{F}(\mathbf{r}_1,\mathbf{r}_2)=\mathrm{Im}\frac{\overline{G^A}}{\pi}=J_0(k_F|\mathbf{r}_1-\mathbf{r}_2|)-J_0(k_F|\mathbf{r}_1-\hat{\mathcal{R}}\mathbf{r}_2|),$$

where $J_0(x)$ is the zeroth Bessel function, $\mathbf{r}_i^\pm=\mathbf{R}_i\pm\mathbf{r}_i/2$, and k_F is the Fermi wave vector. Point $\hat{\mathcal{R}}\mathbf{r}$ is the coordinate of the image charge created by the charge in the point $\mathbf{r}$, so that the propagators (3.21) satisfy proper zero boundary conditions. Green functions here are taken at different values of magnetic fields H_1, H_2. In Eqs. (3.21), $\nu=m/2\pi$ is the density of states per unit area. Equations (3.21) are valid if the arguments of the Green functions are close to each other pairwise: $|r_{1,2}|$ must be much smaller than the elastic mean free path for a diffusive dot, and much smaller than the dot size for a ballistic dot. The boundary is assumed to be smooth on the scale of the Fermi wavelength.

Retarded classical propagators in the diffusive dot satisfy diffusionlike equations[23]

$$\left\{\frac{\partial}{\partial t}-D\left[\nabla+\frac{ie}{c}\begin{pmatrix}\mathbf{A}_1-\mathbf{A}_2\\ \mathbf{A}_1+\mathbf{A}_2\end{pmatrix}\right]^2\right\}\begin{Bmatrix}\mathcal{P}^D\\ \mathcal{P}^C\end{Bmatrix}=\delta(\mathbf{R}_1-\mathbf{R}_2), \quad (3.22)$$

where D is the diffusion coefficient, and the vector potentials $\mathbf{A}_{1,2}$ are defined so that $\nabla\times\mathbf{A}_{1,2}=H_{1,2}$. For a ballistic dot, Eqs. (3.22) should be substituted by the corresponding Liouville (or, to be more precise, Perron-Frobenius) equation, and Eq. (3.21) should be somewhat changed.[24] However, in the universal limit considered in this paper, there is no difference between the ballistic and diffusive dots.

The universal limit corresponds to a large time scale at which the semiclassical electron orbit covers all the available phase space. At such a time scale, the classical probabilities no longer depend on the coordinate and acquire the form

$$\mathcal{P}^{D,C}=\frac{1}{\mathcal{A}}\theta(t)e^{-t/\tau_H^{D,C}}, \quad (3.23)$$

where $\theta(x)$ is the step function, $\mathcal{A}$ is the area of the dot, and the decay times associated with the magnetic field are given by

$$\frac{1}{\tau_H^{D,C}}=E_T\left(\frac{\Phi_1\mp\Phi_2}{\Phi_0}\right)^2. \quad (3.24)$$

Here $\Phi_0=e/c\hbar$ is the flux quantum, $\Phi_{1,2}=\mathcal{A}H_{1,2}$ are the fluxes through the dot corresponding to the fields H_1 and H_2, and the Thouless energy E_T is of the order of $\hbar D/\mathcal{A}$ for a diffusive dot, and of the order of $\hbar v_F/\sqrt{\mathcal{A}}$ for a ballistic dot.

The correlation functions of the retarded and advanced parts of the kernel L can be expressed, with the help of Eqs. (3.9) and (3.21), in terms of the diffuson and Cooperon. The kernel L [see Eq. (3.9)] depends on the Green function at coinciding spatial arguments. Therefore, both pairings leading to the diffuson and Cooperon upon averaging should be taken into account. In the universal regime [see Eq. (3.23)] integrals in the transverse direction in Eq. (3.9) can be calculated using the normalization condition $\int dy\,\phi^2(y)=1$. As a result, we find

$$\langle L^R_{H_1}(t_1)L^A_{H_2}(t_2)\rangle=\frac{v_F^2\Delta}{2\pi}\delta(t_1+t_2)\theta(t_1)$$
$$\times\{e^{-t_1/\tau_H^D}+e^{-t_1/\tau_H^C}\}, \quad (3.25)$$

where $\Delta=1/(\nu\mathcal{A})$ is the mean level spacing of the dot. Averages of the type $\overline{L^R L^R}$ vanish. Because we are interested in times smaller than the Heisenberg time $\hbar/\Delta$, the higher moments can be decoupled by using the Wick theorem and the pair correlation functions are defined by Eq. (3.25).

B. Random matrix formulation

We start by dividing the entire system into two parts, the leads and the dot. In general, the Hamiltonian $\hat{H}$ of the system can be represented as

$$\hat{H}=\hat{H}_L+\hat{H}_D+\hat{H}_{LD}. \tag{3.26}$$

The Hamiltonian of the leads is of the form

$$\hat{H}_L=v_F\sum_{k,j}\, k\psi^\dagger_{k,j}\psi_{k,j}, \tag{3.27}$$

where we linearized the electron spectrum in the leads, and measured all the energies from the Fermi level. Index k is the longitudinal momentum in a mode propagating along the channel connected to the dot, and index $j=1,\ldots,N$ labels these modes (summation over spin indices is implied whenever it is necessary). For the sake of simplicity, we assume the same Fermi velocity in all the modes, the general case can be reduced to Eq. (3.27) by the corresponding rescaling. Hamiltonian $\hat{H}_D=\hat{H}_n+\hat{H}_C$ of the dot consists of the noninteracting part

$$\hat{H}_n=\sum_{\alpha,\beta}\,\mathcal{H}_{\alpha,\beta}\psi^\dagger_\alpha\psi_\beta, \tag{3.28}$$

and the interaction term $\hat{H}_C$, which is described by the Hamiltonian (1.1) with the charge $\hat{Q}$ given by

$$\frac{\hat{Q}}{e}=\sum_{\alpha}\,\psi^\dagger_\alpha\psi_\alpha. \tag{3.29}$$

(In this subsection, we reserve greek and latin letters for labeling the fermionic states in the dot and in the leads, respectively.) For definiteness, we restrict the discussion to the case of the orthogonal ensemble; generalization to other cases is straightforward. Elements $\mathcal{H}_{\alpha,\beta}$ in Eq. (3.28) form a real random Hermitian matrix $\mathcal{H}$ of size $M\times M$, $(M\to\infty)$, belonging to the Gaussian ensemble

$$P(\mathcal{H})\propto\exp\left(-\frac{\pi^2}{4\Delta^2 M}\mathrm{Tr}\mathcal{H}^2\right), \tag{3.30}$$

where Δ is the mean level spacing near the center of the band. Finally, Hamiltonian $\hat{H}_{LD}$ in Eq. (3.26) describes the coupling of the dot to the leads, and has the form

$$\hat{H}_{LD}=\sum_{k,j,\alpha}\,(W_{\alpha,j}\psi^\dagger_\alpha\psi_{k,j}+\mathrm{H.c.}), \tag{3.31}$$

where the coupling constant $W_{\alpha,j}$ is a real $M\times N$ matrix W.

Let us list the needed averaged quantities corresponding to the Gaussian ensemble Eq. (3.30). The averaged density of states is given by the semicircle law

$$\rho(\epsilon)=\overline{\mathrm{Tr}\,\delta(\epsilon-\mathcal{H})}=\mathrm{Re}\frac{1}{\Delta}\sqrt{1-\left(\frac{\pi\epsilon}{\Delta M}\right)^2}. \tag{3.32}$$

We will need only properties of the system at energies ϵ much smaller than the width of the band $\Delta N/\pi$, and we will neglect the energy dependence of the averaged density of states. The average of the Green functions $\mathcal{G}^{R,A}(\epsilon)=(\epsilon-\mathcal{H}\pm i0)^{-1}$ has the form

$$\overline{\mathcal{G}^{R,A}_{\alpha,\beta}}=\mp i\pi\delta_{\alpha\beta}\frac{1}{M\Delta}. \tag{3.33}$$

Random matrix counterparts of the diffusion and Cooperon propagators (3.21) can be written as

$$\overline{\mathcal{G}^R_{\alpha,\beta}(\epsilon+\omega)\mathcal{G}^A_{\gamma,\delta}(\epsilon)}=\frac{2\pi}{M\Delta}[\mathcal{P}^D(\omega)\,\delta_{\alpha\delta}\delta_{\beta\gamma}+\mathcal{P}^C(\omega)\,\delta_{\alpha\gamma}\delta_{\beta\delta}],$$

$$\mathcal{P}^D(\omega)=\mathcal{P}^C(\omega)=\frac{1}{M}\,\frac{1}{-i\omega+0}, \tag{3.34}$$

where $\tilde{\mathcal{G}}=\mathcal{G}-\bar{\mathcal{G}}$. Averages of the type $\overline{\tilde{\mathcal{G}}^R\tilde{\mathcal{G}}^R}$ and $\overline{\tilde{\mathcal{G}}^A\tilde{\mathcal{G}}^A}$ vanish. Formulas (3.32)–(3.34) have the accuracy $\sim 1/M$ and they neglect the oscillatory ω dependences on the scale of the order of Δ. This accuracy, however, is sufficient for us because, as we already discussed, the relevant results are contributed by the energy strip of the width $E_C\gg\Delta$.

Our purpose now is to derive the effective action theory similar to Eqs. (3.15)–(3.18) starting from the random matrix model. Before doing so, let us review some useful properties of the system (3.26) in the absence of the interaction, $E_C=0$. In this case, electron transmission at energy ϵ is completely characterized by $N\times N$ scattering matrix $S(\epsilon)$:

$$S(\epsilon)=1-2\pi i\nu W^\dagger[\epsilon-\mathcal{H}+i\pi\nu WW^\dagger]^{-1}W, \tag{3.35}$$

where $\nu=1/(2\pi v_F)$ is the one-dimensional density of states in the leads. Coupling matrix W can be represented in the form

$$W=\sqrt{\frac{\Delta M}{\pi^2\nu}}UO\tilde{W}, \tag{3.36}$$

where U is an orthogonal $M\times M$ matrix, $\tilde{W}$ is a real $N\times N$ matrix, and O is an $M\times N$ matrix, $O_{\alpha j}=\delta_\alpha j, 1\leqslant\alpha\leqslant N$. Because the distribution function (3.26) is invariant under rotations $\mathcal{H}\to U\mathcal{H}U^\dagger$, matrix U in Eq. (3.36) can be omitted. Substituting Eq. (3.36) into Eq. (3.35) and performing ensemble averaging with the help of Eq. (3.33), we obtain for the average scattering matrix

$$\bar{S}=\frac{1-\tilde{W}^\dagger\tilde{W}}{1+\tilde{W}^\dagger\tilde{W}}. \tag{3.37}$$

At $\tilde{W}^\dagger\tilde{W}=1$ the average scattering matrix vanishes; see Eq. (3.37). It indicates that matrix S belongs to the circular ensemble (corresponding to the regime of ''ideal contacts''). Deviation of $\tilde{W}^\dagger\tilde{W}$ from a unit matrix can be attributed to the scattering on the contacts between the leads and the dot. This scattering is described by a unitary symmetric $2N\times 2N$ matrix

$$S_c=\begin{pmatrix} r & t^\dagger \\ t & r' \end{pmatrix} \tag{3.38}$$

with $N\times N$ matrices r,r',t being defined by

$$r=\frac{1-\widetilde{W}^\dagger\widetilde{W}}{1+\widetilde{W}^\dagger\widetilde{W}},\quad r'=-\widetilde{W}\frac{1-\widetilde{W}^\dagger\widetilde{W}}{1+\widetilde{W}^\dagger\widetilde{W}}\widetilde{W}^{-1},$$
$$t=\widetilde{W}\frac{2}{1+\widetilde{W}^\dagger\widetilde{W}}. \tag{3.39}$$

The explicit relations between the coupling matrices W and the scattering matrix in the contacts (3.38) were first obtained by Brouwer.[25]

Now we turn to the derivation of the effective action. For technical reasons [see discussion above Eq. (3.4)], we replace the charge operator (3.29) with

$$\frac{\hat{Q}}{e}=-\sum_{k,j}\psi^\dagger_{k,j}\psi_{k,j}. \tag{3.40}$$

After this replacement, the Hamiltonian of the system becomes quadratic in fermionic operators of the dot, so that this part of the system can be integrated out:

$$\mathrm{Tr}_D e^{-\beta\hat{H}}=\mathrm{Tr}_D e^{-\beta(\hat{H}_L+\hat{H}_C+\hat{H}_n+\hat{H}_{LD})}$$
$$=e^{-\beta(\hat{H}_L+\hat{H}_C)}e^{-\beta\Omega_n}T_\tau e^{\frac{1}{2}\int_0^\beta d\tau_1 d\tau_2\langle\hat{H}_{LD}(\tau_1)\hat{H}_{LD}(\tau_2)\rangle_D}. \tag{3.41}$$

Here $\hat{H}_{LD}(\tau)$ is the interaction representation of the coupling operator $\hat{H}_{LD}$ and averaging over Hamiltonian of the dot is defined as $\langle\cdots\rangle_D=e^{\beta\Omega_D}\mathrm{Tr}_D(e^{-\beta\hat{H}_n}\cdots)$. The thermodynamic potential $\Omega_D=T\ \ln\mathrm{Tr}e^{-\beta\hat{H}_n}$ of the closed dot is independent of the gate voltage $\mathcal{N}$ and it will be omitted.

The average in the last factor in Eq. (3.41) is calculated with the help of Eq. (3.31) and of the definition of the Matsubara Green function for the closed dot:

$$\mathcal{G}_{\alpha\beta}(\tau)=-\langle T_\tau\psi_\alpha(\tau)\overline{\psi}_\beta(0)\rangle_D=\sum_{\omega_n}e^{i\omega_n\tau}\left[\frac{1}{i\omega_n-\mathcal{H}}\right]_{\alpha\beta}, \tag{3.42}$$

where $\psi_\alpha(\tau)=e^{\hat{H}_n\tau}\psi_\alpha e^{-\hat{H}_n\tau}$, $\overline{\psi}(\tau)=\psi^\dagger(-\tau)$, and $\omega_n=\pi T(2n+1)$ is the fermionic Matsubara frequency. The result is

$$\langle\hat{H}_{LD}(\tau_1)\hat{H}_{LD}(\tau_2)\rangle_2$$
$$=-\sum_{k_1,k_2,j_1,j_2}\overline{\psi}_{k_1,j_1}(\tau_1)$$
$$\times[W^\dagger\mathcal{G}(\tau_1-\tau_2)W]_{j_1j_2}\psi_{k_2,j_2}(\tau_2). \tag{3.43}$$

We separate the averaged part of the Green function $\mathcal{G}=\overline{\mathcal{G}}+\widetilde{\mathcal{G}}$, use Eqs. (3.33) and (3.36), and obtain the Fourier transform of the kernel in Eq. (3.44),

$$W\mathcal{G}(i\omega_n)W^\dagger=-i\frac{\mathrm{sgn}\ \omega_n}{\pi\nu}\widetilde{W}^\dagger\widetilde{W}+\frac{\Delta M}{\pi_2\nu}\widetilde{W}^\dagger\widetilde{\mathcal{G}}(i\omega_n)\widetilde{W}. \tag{3.44}$$

The first term in the right-hand side of Eq. (3.44) does not contain any information about the dot, and its frequency dependence is the same as of the Green function of free chiral fermions. It is, therefore, possible (and very convenient) to transform this part of the action to the Hamiltonian form by introducing fictitious fermionic fields $b_{k,j}, j=1,\ldots,N$. Then, Eq. (3.41) acquires the form

$$\mathrm{Tr}_D e^{-\beta\hat{H}}\propto\mathrm{Tr}_b(e^{-\beta\hat{H}_{\mathrm{eff}}}T_\tau e^{-\hat{S}}); \tag{3.45}$$

the omitted $\mathcal{N}$-independent proportionality coefficient is irrelevant. The effective Hamiltonian $\hat{H}_{\mathrm{eff}}$ is given by

$$\hat{H}_{\mathrm{eff}}=v_F\sum_{j,k}k(\psi^\dagger_{k,j}\psi_{k,j}+b^\dagger_{k,j}b_{k,j})$$
$$+\frac{1}{\pi\nu}\sum_{k_1,k_2;j_1,j_2}[b^\dagger_{k_1,j_1}w_{j_1j_2}\psi_{k_2,j_2}+\mathrm{H.c.}]$$
$$+E_C\left(\sum_{k,j}\psi^\dagger_{k,j}\psi_{k,j}+\mathcal{N}\right)^2, \tag{3.46}$$

where $w_{j_1j_2}$ are the elements of the Hermitian matrix w defined as

$$w=(\widetilde{W}^\dagger W)^{1/2}. \tag{3.47}$$

Action $\mathcal{S}$ has the form

$$\mathcal{S}=4\sum_{k_1,k_2;j_1,j_2}\int_0^\beta d\tau_1 d\tau_2\overline{\psi}_{k_1,j_1}(\tau_1)$$
$$\times L_{j_1j_2}(\tau_1-\tau_2)\psi_{k_2,j_2}(\tau_2), \tag{3.48}$$

where the kernel L is a $N\times N$ matrix given by

$$L(\tau)=\frac{\Delta M}{4\pi^2\nu}\widetilde{W}^\dagger\widetilde{\mathcal{G}}(\tau)\widetilde{W}. \tag{3.49}$$

Equation (3.45) can be easily checked by tracing out fermions b and using the relation

$$\sum_{k_1,k_2}\langle T_\tau b_{k_1,j_1}(\tau)\overline{b}_{k_2,j_2}(0)\rangle=i\pi\nu\delta_{j_1j_2}\sum_{\omega_n}e^{i\omega_n\tau}\mathrm{sgn}\ \omega_n.$$

Hamiltonian $\hat{H}_{\mathrm{eff}}$ can be rewritten in a more familiar form. Introducing the Fourier transform of the fermionic fields $\psi_j(x)=\Sigma_k e^{-ikx}\psi_{j,k}$ and $b_j(x)=\Sigma_k e^{-ikx}b_{j,k}$, we obtain from Eq. (3.46)

$$\hat{H}_{\mathrm{eff}}=iv_F\sum_j\int_{-\infty}^{\infty}dx(\psi^\dagger_j\partial_x\psi_j+b^\dagger_j\partial_x b_j)$$
$$+\frac{1}{\pi\nu}\sum_{j_1,j_2}[b^\dagger_{j_1}(0)w_{j_1j_2}\psi_{j_2}(0)+\mathrm{H.c.}]$$
$$+E_C\left(\sum_j\int_\infty^\infty dx\,\psi^\dagger_j\psi_j+\mathcal{N}\right)^2. \tag{3.50}$$

We are interested in the case of almost open ideal contacts, $\|w-1\|\ll 1$. In this case, it is natural to change the variables

and reveal the small parameter of the perturbation theory. Introducing left- and right-moving fermions,

$$\psi_j(x)=\psi_{L,j}(x)\,\theta(-x)+\psi_{R,j}(-x)\,\theta(x),$$

$$b_j(x)=i[\psi_{R,j}(-x)\,\theta(-x)-\psi_{L,j}(x)\,\theta(x)]$$

(the ambiguity of this definition at the origin should be resolved as $\psi(0)=[\psi(+0)+\psi(-0)]/2$), we obtain from Eq. (3.50)

$$\hat{H}_{\rm eff}=\hat{H}_0+\hat{H}_{bs}, \tag{3.51a}$$

$$\hat{H}_0=iv_F\sum_j\int_{-\infty}^{\infty}dx(\psi^\dagger_{L,j}\partial_x\psi_{L,j}-\psi^\dagger_{R,j}\partial_x\psi_{R,j})+E_C\left(\sum_j\int_{-\infty}dx{:}\psi^\dagger_{L,j}\psi_{L,j}+\psi^\dagger_{R,j}\psi_{R,j}{:}+\mathcal{N}\right)^2, \tag{3.51b}$$

$$\hat{H}_{bs}=-i\sum_{ij}r_{ij}\psi^\dagger_{L,i}\psi_{R,j}+\text{H.c.}, \tag{3.51c}$$

$$\hat{S}=\sum_{ij}\int_0^\beta d\tau_1 d\tau_2 L_{ij}(\tau_1-\tau_2)\times[\overline{\psi}_{L,i}(\tau_1;0)+\overline{\psi}_{R,i}(\tau_1;0)][\psi_{L,j}(\tau_2;0)+\psi_{R,j}(\tau_2;0)]. \tag{3.51d}$$

Here we neglected the terms related to the discontinuities of the fermionic field at the origin, which induces higher-order terms in r, and approximated reflection matrix $r\approx 1-w$, as follows from Eqs. (3.47) and (3.39) for $\|r\|\ll 1$. Within the same approximation we can put $\widetilde{W}=1$ in Eq. (3.49). Formulas (3.51) are analogous to Eqs. (3.15)–(3.18) derived in a previous subsection.

Finally, we have to study the statistics of the kernel (3.49), which can be expressed in terms of its advanced and retarded counterparts by Lehmann formula (3.20). Performing time Fourier transform of Eq. (3.34), and using $\nu=1/(2\pi v_F)$, we obtain

$$\langle L^R_{ij}(t_1)L^A_{rs}(t_2)\rangle=\frac{v_F^2\Delta}{2\pi}\delta(t_1+t_2)\,\theta(t_1)\times\{\delta_{is}\delta_{jr}+\delta_{ir}\delta_{js}\}. \tag{3.52}$$

For the one-mode lead this result agrees with the zero magnetic field version of Eq. (3.25).

The statistics of the kernel at different magnetic fields can be obtained by adding a purely imaginary Hermitian matrix to the original matrix $\mathcal{H}$ in Eq. (3.28).[9,26] This would lead to the result analogous to the exponential decay in Eq. (3.25). We will not describe details of such calculation here, and refer the reader to the extensive literature on parametric correlations.[28,29]

C. Applicability of the model

So far, we were using a very simple model of the interaction (1.1), which ascribes all the interaction effects to the variation of the number of particles in the dot. However, a natural question arises: what is the accuracy of this approximation? One may even think that the effects considered in this paper are completely washed out by remaining interaction terms that we neglected.

The purpose of this subsection is to show that the simple model (1.1) of interactions in the dot leaves out only small, $\propto 1/g$, effects, where $g=E_T/\Delta$ is the dimensionless conductance of the cavity (E_T is the Thouless energy). For a diffusive dot in the metallic regime, and for a ballistic nonintegrable dot the conductance is large, $g\gg 1$. Mesoscopic charge quantization is adequately described by the model of interaction (1.1), as long as $g\gg 1$, and the number of modes propagating to the lead is much smaller than g. In other words, ergodic time of the dot $\hbar/E_T$ should be much larger than the escape time of the electron from the dot.

The electrons in the dot are described by the Hamiltonian $\hat{H}=\hat{H}_n+\hat{H}_{\rm int}$, where the noninteracting part of the Hamiltonian, $\hat{H}_n$, is given by Eq. (3.25). The validity of the random matrix theory for $\hat{H}_n$ for the energy scale smaller than the Thouless energy was proven in Ref. 21 for chaotic systems and in Ref. 30 for diffusive systems.

The general form of the interaction Hamiltonian is

$$\hat{H}_{\rm int}=\frac{1}{2}\sum V_{\alpha\beta\gamma\delta}\psi^\dagger_{\alpha,\sigma_1}\psi^\dagger_{\beta,\sigma_2}\psi_{\gamma,\sigma_2}\psi_{\delta,\sigma_1}. \tag{3.53}$$

In this subsection, we will write explicitly the spin indices σ for the fermionic operators. The interaction Hamiltonian (1.1) corresponds to the approximation of the matrix V by

$$V\approx E_C\delta_{\alpha\delta}\delta_{\beta\gamma}. \tag{3.54}$$

Our goal now is to show that all the other matrix elements as well as the mesoscopic fluctuations of matrix elements (3.54) are small. Some of these calculations already appeared in the literature,[31,32] however, we will present brief derivation to make this paper self-contained.

The easiest way to study the statistics of the one-electron wave function $\phi_\alpha(\mathbf{r})$ is to relate them to the Green function and then use Eq. (3.21). By definition of the retarded and advanced Green functions we have

$$G^A_\epsilon(\mathbf{r}_1,\mathbf{r}_2)-G^R_\epsilon(\mathbf{r}_1,\mathbf{r}_2)=2\pi i\sum_\alpha\phi_\alpha(\mathbf{r}_1)\phi_\alpha(\mathbf{r}_2)\,\delta(\epsilon-\epsilon_\alpha), \tag{3.55}$$

where we assumed no magnetic field for simplicity. At given energy ϵ only one function contributes into the sum in Eq. (3.55), so that the statistics of the Green functions is related to that of the wave functions. Furthermore, it is known that there is no correlation between level statistics and wave function in the lowest order in $1/g$, see, e.g., Ref. 30, so we can neglect the level correlations and average δ function in Eq. (3.55) independently. As a result, we can estimate

$$\phi_\alpha(\mathbf{r}_1)\phi_\alpha(\mathbf{r}_2)\approx\frac{\Delta}{2\pi i}[G^A_{\epsilon_\alpha}(\mathbf{r}_1,\mathbf{r}_2)-G^R_{\epsilon_\alpha}(\mathbf{r}_1,\mathbf{r}_2)]. \tag{3.56}$$

Now we can use Eq. (3.55) and (3.21) to study the average of different momenta of the matrix elements:

$$V_{\alpha\beta\gamma\delta}=\int d\mathbf{r}_1 d\mathbf{r}_2 V(\mathbf{r}_1-\mathbf{r}_2)\phi_\alpha(\mathbf{r}_1)\phi_\beta(\mathbf{r}_1)\phi_\gamma(\mathbf{r}_2)\phi_\delta(\mathbf{r}_2).$$

Averaging this matrix element itself with the help of Eq. (3.56), we obtain

$$\overline{V_{\alpha\beta\gamma\delta}}=V^{(0)}_{\alpha\beta\gamma\delta}+V^{(1/g)}_{\alpha\beta\gamma\delta}. \tag{3.57}$$

The first term in Eq. (3.57) comes from the product of the averaged Green functions

$$\mathrm{Im}\overline{G^A(\mathbf{r}_1,\mathbf{r}_2)}=\pi\nu\langle e^{i\mathbf{k}(\mathbf{r}_1-\mathbf{r}_2)}\rangle_{\mathrm{FS}},$$

and it is given by

$$V^{(0)}_{\alpha\beta\gamma\delta}=E_C\delta_{\alpha\delta}\delta_{\beta\gamma}+F\Delta(\delta_{\alpha\gamma}\delta_{\beta\delta}+\delta_{\alpha\beta}\delta_{\gamma\delta}),$$

$$E_C=\frac{1}{\mathcal{A}^2}\int d\mathbf{r}_1 d\mathbf{r}_2 V(\mathbf{r}_1-\mathbf{r}_2), \tag{3.58}$$

$$F=\nu\langle\widetilde{V}(\mathbf{k})\rangle_{\mathrm{FS}}.$$

Here $\mathcal{A}$ is the area of the dot, $\langle\cdots\rangle_{\mathrm{FS}}$ stands for the averaging over directions of the wave vector on the Fermi surface, ν is the averaged density of states per unit area and per one spin in the dot, and $\widetilde{V}(\mathbf{k})$ is the Fourier transform of the two-particle interaction $V(\mathbf{r})$.

Charging energy E_C in Eq. (3.58) is related to the zero mode of the interaction potential. This mode cannot redistribute the electrons within the dot and that is why it is not screened (the redistribution of the electrons between the dot and the leads is taken into account by the model). As the result, E_C is much larger than the mean level spacing. On the other hand, coefficient F includes only nonzero modes that are perfectly screened, $V(k)=V_0(k)/[1+2\nu V_0(k)]$, where $V_0(k)$ is the bare potential. (The use of the static screening here is possible because the screening is established during the characteristic time of the plasmon propagation through the dot, which is much smaller than $\hbar/E_T$.) Therefore, we estimate $F\leqslant 1/2$, so that the last two terms introduce a correction only of the order of level spacing, and may be neglected. [We will not consider here the case of the attractive interaction when the third term in Eq. (3.58) renormalizes to infinity due to the interaction in the Cooper channel.]

The second term in Eq. (3.57) originates from the product of the retarded and advanced Green functions; see Eqs. (3.21). In the absence of magnetic field, diffuson and Cooperon propagators coincide, and their spectral expansion for a diffusive system is

$$\mathcal{P}_\omega(\mathbf{r}_1,\mathbf{r}_2)=\frac{1}{(-i\omega+0)\mathcal{A}}+\sum_{\gamma_\mu\neq 0}\frac{f^*_\mu(\mathbf{r}_1)f_\mu(\mathbf{r}_2)}{-i\omega+\gamma_\mu}, \tag{3.59}$$

where γ_μ and $f_\mu(\mathbf{r})$ are the corresponding eigenvalues and eigenfunctions. For a diffusive system, $\gamma_\mu=DQ_\mu^2$, where D is the diffusion constant, and wave vectors Q_μ depend on the shape of the system. For a rectangular diffusive dot of the size $L_x\times L_y$, one finds $Q^2=\pi^2(n_x^2/L_x^2+n_y^2/L_y^2)$ with $n_x,n_y>0$ being integer numbers. For chaotic systems, γ_μ are the eigenvalues of the Perron-Frobenius operator. The zero mode in Eq. (3.59) corresponds to the conservation of the number particles, and all the other modes describe the relaxation of any initial inhomogeneous distribution function by virtue of classical chaotic dynamics, $\mathrm{Re}\,\gamma_\mu>0$. If the system is integrable, or there are some additional symmetries of the system, other zero modes appear, however, we disregard such a possibility and consider only diffusive or classically chaotic systems.

Using Eqs. (3.21), (3.56), and (3.59), and taking into account that all the energies are smaller than the Thouless energy (or, in other words, the lowest nonzero eigenvalue of diffusion or Perron-Frobenius operator), $|\epsilon_\alpha|\ll\gamma_1$, we find

$$V^{(1/g)}_{\alpha\beta\gamma\delta}=\frac{\Delta}{g}[2F_1\delta_{\alpha\delta}\delta_{\beta\gamma}+(F_2+F_1)(\delta_{\alpha\gamma}\delta_{\beta\delta}+\delta_{\alpha\beta}\delta_{\gamma\delta})], \tag{3.60}$$

where the dimensionless conductance of the system is defined as

$$g=\mathrm{Re}\frac{\gamma_1}{\Delta}, \tag{3.61}$$

and is assumed to be much larger than unity. Dimensionless coefficients in Eq. (3.60) are given by

$$F_i=\frac{\mathrm{Re}\,\gamma_1}{\pi}\sum_{\gamma_\mu\neq 0}\frac{F_i^\mu}{\gamma_\mu},\quad i=1,2,$$

$$F_1^\mu=\nu\langle\widetilde{V}(\mathbf{k})\rangle_{\mathrm{FS}}, \tag{3.62}$$

$$F_2^\mu=\nu\int d\mathbf{r}_1 d\mathbf{r}_2 V(\mathbf{r}_1-\mathbf{r}_2)f^*_\mu(\mathbf{r}_1)f_\mu(\mathbf{r}_2).$$

For the screened interaction potential, coefficients $F^\mu_{1,2}=1/2$ and, therefore, $F_{1,2}$ are of the order of unity for chaotic systems and of the order of $(1/4\pi^2)\ln(L/l)$ for the diffusive dot. Here L is the size of the dot and l is the transport elastic mean free path. Thus, we have shown that the corrections to the average matrix element (3.54) are parametrically small for the metallic regime.

Now, we wish to show that the fluctuations of the matrix elements are small. Indeed, with the help of Eq. (3.21), we obtain for a generic (i.e., with no pairwise equal indices) matrix element:

$$\overline{(V_{\alpha\beta\gamma\delta})^2}=c\left(\frac{\Delta}{g}\right)^2. \tag{3.63}$$

The numerical coefficient c for the diffusive system is given by

$$c=\left(\frac{\gamma_1}{\pi}\right)^2\sum_{\gamma_\mu\neq 0}\{2(F_1^\mu)^2+(F_2^\mu)^2\}\left(\mathrm{Re}\frac{1}{\gamma_\mu}\right)^2$$

[where coefficients $F^\mu_{1,2}$ are defined in Eq. (3.62)] and it is of the order of unity, so that the matrix elements are small at $g\gg 1$. For chaotic systems, the expression for c is more cumbersome, but still have a similar structure. In the case of ''diagonal'' [in the sense of Eq. (3.60)] matrix elements, the average in Eq. (3.63) should be replaced by the corresponding variance.

The main conclusion of this section is contained in Eqs. (3.60) and (3.63). These equations clearly show that the Cou-

lomb blockade type interaction (1.1) is a parametrically justified description for the dynamics of the system at energies smaller than the Thouless energy.

Closing this subsection, let us mention numerical works that have been performed recently.[33,34] These papers addressed either dirty diffusive systems with a small number of electrons,[33] $g \simeq 1$, or classically localized states[34] and are not relevant for the metallic regime $g \gg 1$ we are dealing with. We believe that the large quantum dots studied in Refs. 5–7 belong to the metallic regime.

IV. BOSONIZATION PROCEDURE

Equations (3.15)–(3.18) reduce the initial system consisting of a dot and a single-mode channel to the effective one-dimensional model. To treat the interaction in the model [the second term in Eq. (3.15)], we follow Ref. 14, and use the bosonization technique. In the bosonic variables, the entire Hamiltonian (3.15) becomes quadratic. The price for this convenience is a strongly nonlinear form that the backscattering terms acquire [in the language of left and right movers, those are the terms $\propto \psi_L^\dagger \psi_R$ in Eqs. (3.16) and (3.17)]. Fortunately, the typical value of the kernel (3.9) is small ($\sim \Delta/E_C$), and this enables us to use the perturbation theory, which will be presented in Secs. V and VI. In this section we present a bosonization procedure in a form most suitable for our purposes.

A. Spinless electrons

One-dimensional fermionic fields can be presented in the form[35]

$$\psi_R(x) = \frac{\hat{\eta}}{\sqrt{2\pi\lambda}} e^{i\hat{\varphi}_R(x)}, \quad \psi_L(x) = \frac{\hat{\eta}}{\sqrt{2\pi\lambda}} e^{-i\hat{\varphi}_L(x)}, \tag{4.1}$$

where λ is the high-energy cutoff of the order of the Fermi wavelength, and $\hat{\eta} = \hat{\eta}^\dagger, \hat{\eta}^2 = 1$ is the Majorana fermion; its significance will be discussed later. One-dimensional bosonic fields $\hat{\varphi}_{L,R}(x)$ satisfy the following commutation relations:

$$[\hat{\varphi}_L(x), \hat{\varphi}_L(y)] = -i\pi \mathrm{sgn}(x-y), \tag{4.2a}$$

$$[\hat{\varphi}_R(x), \hat{\varphi}_R(y)] = i\pi \mathrm{sgn}(x-y), \tag{4.2b}$$

$$[\hat{\varphi}_R(x), \hat{\varphi}_L(y)] = -i\pi. \tag{4.2c}$$

It is easy to check, using Eqs. (4.2), that the fermionic fields (4.1) obey the standard commutation relations. The expressions for the densities of left and right movers are

$$:\psi_L^\dagger(x)\psi_L(x): = \frac{1}{2\pi}\partial_x \varphi_L(x),$$
$$:\psi_R^\dagger(x)\psi_R(x): = \frac{1}{2\pi}\partial_x \varphi_R(x). \tag{4.3}$$

With the help of Eq. (4.3), Hamiltonian (3.15) can be bosonized as

$$\hat{H}_0 = \frac{v_F}{4\pi}\int_{-\infty}^{\infty} dx \left[\left(\frac{\partial\hat{\varphi}_L}{\partial x}\right)^2 + \left(\frac{\partial\hat{\varphi}_R}{\partial x}\right)^2 \right]$$
$$+ \frac{E_C}{8\pi^2}[\hat{\varphi}_L(0) + \hat{\varphi}_R(0) + 2\pi\mathcal{N}]^2. \tag{4.4}$$

The relations (4.2a) and (4.2b) ensure the fermionic commutation relations within the species ψ_L and ψ_R. The commutation relation (4.2c) guarantees the anticommutation relation of ψ_L with ψ_R and the commutation relations

$$\left[\int_{-\infty}^{0} \psi_R^\dagger\psi_R + \psi_L^\dagger\psi_L dx; \psi_{R,L}^\dagger(y) \right] = \psi_{R,L}^\dagger(y)\,\theta(-y).$$

The backscattering Hamiltonian (3.17) takes the form

$$\hat{H}_{\mathrm{bs}} = \frac{|r| v_F}{\pi\lambda} \cos[\hat{\varphi}_L(0) + \hat{\varphi}_R(0)]. \tag{4.5}$$

The bosonized version of the effective action Eq. (3.16) is

$$\hat{S} = \frac{1}{2\pi\lambda}\int_0^\beta d\tau_1 d\tau_2 L(\tau_1-\tau_2)\,\hat{\eta}(\tau_1)\,\hat{\eta}(\tau_2)$$
$$\times [e^{i\hat{\varphi}_L(\tau_1)} + e^{-i\hat{\varphi}_R(\tau_1)}][e^{-i\hat{\varphi}_L(\tau_2)} + e^{i\hat{\varphi}_R(\tau_2)}], \tag{4.6}$$

where bosonic operators are taken at the origin $x = 0$. Majorana fermion η does not enter the effective Hamiltonian, and therefore it is not a dynamical field. Its role in the effective action is to take care of the difference in the definition of the operation of chronological ordering for the fermionic and bosonic operator. The equality

$$\langle T_\tau \hat{\eta}(\tau_1)\,\hat{\eta}(\tau_2)\rangle = \mathrm{sgn}(\tau_1-\tau_2), \tag{4.7}$$

and Wick's theorem, preserves the definition of chronological ordering for fermions in Eq. (3.18).

It is convenient to separate the part of the bosonic sector not affected by the Coulomb interaction and introduce a new field $\hat{\varphi}_+, \hat{\varphi}_-, \hat{\Phi}$ with the commutation relations

$$[\hat{\varphi}_+(x), \hat{\varphi}_+(y)] = -i\pi \mathrm{sgn}(x-y), \tag{4.8a}$$

$$[\hat{\varphi}_-(x), \hat{\varphi}_-(y)] = -i\pi \mathrm{sgn}(x-y), \tag{4.8b}$$

$$[\hat{\Phi}, \hat{\varphi}_-(x)] = [\hat{\varphi}_+(x), \hat{\varphi}_-(y)] = 0, \tag{4.8c}$$

$$[\hat{\Phi}, \hat{\varphi}_+(x)] = i\pi. \tag{4.8d}$$

We express operators (4.2) in terms of new fields (4.8) as

$$\hat{\varphi}_L(x) = \frac{\hat{\varphi}_+(x) + \hat{\varphi}_-(x) + \hat{\Phi}}{\sqrt{2}} - \pi\mathcal{N},$$
$$\hat{\varphi}_R(x) = \frac{\hat{\varphi}_+(-x) - \hat{\varphi}_-(-x) - \hat{\Phi}}{\sqrt{2}} - \pi\mathcal{N}, \tag{4.9}$$

where c number $\pi\mathcal{N}$ is incorporated into the definition of the field. It is easy to see that the commutation relations (4.2) are

preserved. In the new variables, the Hamiltonian (4.4) is independent on the gate voltage (i.e., on $\mathcal{N}$):

$$\hat{H}_0=\frac{v_F}{4\pi}\int_{-\infty}^{\infty}dx\left[\left(\frac{\partial\hat{\varphi}_+}{\partial x}\right)^2+\left(\frac{\partial\hat{\varphi}_-}{\partial x}\right)^2\right]+\frac{E_C}{4\pi^2}\hat{\varphi}_+^2(0). \tag{4.10}$$

All the $\mathcal{N}$ dependence is transferred now to the backscattering term in the Hamiltonian:

$$\hat{H}_{\rm bs}=\frac{|r|v_F}{\pi\lambda}\cos[\sqrt{2}\hat{\varphi}_+(0)-2\pi\mathcal{N}], \tag{4.11}$$

and to the action $\hat{S}$, which is contributed to by the return trajectories of electrons after multiple scattering within the dot:

$$\hat{S}=\frac{1}{2\pi\lambda}\int_0^\beta d\tau_1 d\tau_2 L(\tau_1-\tau_2)\,\hat{\eta}(\tau_1)\,\hat{\eta}(\tau_2) \tag{4.12}$$

$$\times\exp\left[i\frac{\hat{\varphi}_-(\tau_1)-\hat{\varphi}_-(\tau_2)}{\sqrt{2}}\right]\exp\left[i\frac{\hat{\Phi}(\tau_1)-\hat{\Phi}(\tau_2)}{\sqrt{2}}\right]$$

$$\times\cos\left[\frac{\hat{\varphi}_+(\tau_1)}{\sqrt{2}}+\frac{\pi}{4}-\pi\mathcal{N}\right]\cos\left[\frac{\hat{\varphi}_+(\tau_2)}{\sqrt{2}}+\frac{\pi}{4}-\pi\mathcal{N}\right].$$

If one neglects such trajectories altogether,[14] then the Coulomb blockade oscillations apparently vanish in the limit $r=0$ (no backscattering in the channel). However, if return trajectories (i.e., a finite value of Δ/E_C) are taken into account, the Coulomb blockade oscillations exist, even if $r=0$. The $\mathcal{N}$ dependence of the action (4.12) and Hamiltonian (4.11) clearly shows that the period of the oscillations does not depend on the details of the system. This periodic dependence is a direct consequence of the discreteness of the electron charge.

We are going to develop perturbation theory in $\hat{S}$ and $\hat{H}_{\rm bs}$. Every order of the perturbation theory is expressed in terms of the correlators of the bosonic field governed by the quadratic Hamiltonian (4.10). The necessary correlation functions are

$$\mathcal{D}_-(\tau)=\langle T_\tau\hat{\varphi}_-(\tau)\hat{\varphi}_-(0)\rangle, \tag{4.13a}$$

$$\mathcal{D}_+(\tau)=\langle T_\tau\hat{\varphi}_+(\tau)\hat{\varphi}_+(0)\rangle, \tag{4.13b}$$

$$\mathcal{D}_\Phi(\tau)=\langle T_\tau\hat{\Phi}(\tau)\hat{\Phi}(0)\rangle, \tag{4.13c}$$

$$\mathcal{D}_{\Phi+}(\tau)=\langle T_\tau\hat{\Phi}(\tau)\hat{\varphi}_+(0)\rangle, \tag{4.13d}$$

where averages are calculated with respect to Hamiltonian $\hat{H}_0$ and all the bosonic fields are taken at $x=0$.

Standard calculation presented in Appendix B yields for $T\ll E_C$ and $\tau\gtrsim\lambda/v_F\simeq 1/\epsilon_F$:

$$\mathcal{D}_\Phi(\tau)-\mathcal{D}_\Phi(0)=-\frac{1}{2}\int_0^\infty dx\,e^{-x}\ln\left[\frac{\sin(i2\pi x/E_c+\tau)\pi T\,\sin(-i2\pi x/E_c+\tau)\pi T}{\sinh^2\left(\dfrac{2\pi^2Tx}{E_c}\right)}\right], \tag{4.14a}$$

$$\mathcal{D}_-(\tau)-\mathcal{D}_-(0)=\ln\left(\frac{\lambda}{v_F}\frac{\pi T}{|\sin\,\pi T\tau|}\right), \tag{4.14b}$$

$$\mathcal{D}_+(0)=\ln\left(\frac{2\pi v_F}{\lambda E_C e^{\mathbf{C}}}\right), \tag{4.14c}$$

$$\mathcal{D}_+(\tau)-\mathcal{D}_+(0)=[\mathcal{D}_-(\tau)-\mathcal{D}_-(0)]-[\mathcal{D}_\Phi(\tau)-\mathcal{D}_\Phi(0)], \tag{4.14d}$$

$$\mathcal{D}_{\Phi+}(\tau)=\frac{i}{2}\int_0^\infty dx\;e^{-x}\frac{2\pi^2T}{E_C}\left[\cot\left(i\frac{2\pi x}{E_c}+\tau\right)\pi T+\cot\left(-i\frac{2\pi x}{E_c}+\tau\right)\pi T\right], \tag{4.14e}$$

where $\mathbf{C}\approx 0.577$ is the Euler constant.

To conclude this subsection, let us prove the assumption of Sec. II about the Fermi-liquid behavior of the system at low energies. In order to do this, we will calculate the fermionic Green functions, $\langle\psi_L^\dagger(\tau)\psi_L(0)\rangle$ and $\langle\psi_R^\dagger(\tau)\psi_L(0)\rangle$, using the definitions (4.1), (4.9), and the results (4.14). Averaging over the bosonic fields similar to the well-known calculation of the Debye-Waller factor, yields

$$\langle\psi_L^\dagger(\tau)\psi_L(0)\rangle=\frac{1}{2\pi\lambda}\exp\left\{\frac{1}{2}[\mathcal{D}_-(\tau)-\mathcal{D}_-(0)]\right\}\exp\left\{\frac{1}{2}[\mathcal{D}_+(\tau)-\mathcal{D}_+(0)]\right\}\exp\left\{\frac{1}{2}[\mathcal{D}_\Phi(\tau)-\mathcal{D}_\Phi(0)]\right\}$$

$$\times\exp\left\{\frac{1}{2}[\mathcal{D}_{\Phi+}(\tau)+\mathcal{D}_{\Phi+}(-\tau)]\right\} \tag{4.15a}$$

$$\langle \psi_R^\dagger(\tau)\psi_L(0)\rangle = \frac{e^{i2\pi\mathcal{N}}}{2\pi\lambda}\exp\left\{-\frac{1}{2}[\mathcal{D}_+(\tau)+\mathcal{D}_+(0)]\right\}$$
$$\times\exp\left\{\frac{1}{2}[\mathcal{D}_-(\tau)-\mathcal{D}_-(0)]\right\}\exp\left\{\frac{1}{2}[\mathcal{D}_\Phi(\tau)-\mathcal{D}_\Phi(0)]\right\}\exp\left\{\frac{1}{2}[\mathcal{D}_{\Phi+}(\tau)-\mathcal{D}_{\Phi+}(-\tau)]\right\}. \quad (4.15b)$$

Substituting Eqs. (4.14) into Eq. (4.15), we obtain

$$\langle \psi_L^\dagger(\tau)\psi_L(0)\rangle = \frac{1}{2\pi v_F}\frac{\pi T}{\sin\pi T\tau}, \quad (4.16a)$$

$$\langle \psi_R^\dagger(\tau)\psi_L(0)\rangle = \frac{e^{i2\pi\mathcal{N}}}{2\pi v_F}K(\tau), \quad (4.16b)$$

$$K(\tau) = \frac{\pi T}{\sin\pi T\tau}\exp\left\{-\int_0^\infty dx\, e^{-(E_C/2\pi^2T)x}\coth(x+i\pi\tau T)\right\}.$$

The Green function (4.16a) is not affected by interactions at all. The reason is that it is taken at coinciding arguments ($x_1=x_2=0$), e.g., outside the interaction region. Because $\langle\psi_L^\dagger(\tau)\psi_L(0)\rangle$ describes propagation of a chiral particle, the information about interaction is never carried back to the observation point $x=0$. The Green function (4.16b) acquires the free-fermion form at $\tau>E_C^{-1}$, which corresponds to the energies below the charging energy (note that $T\ll E_C$). In this energy range, $\langle\psi_R^\dagger(\tau)\psi_L(0)\rangle$ corresponds to a free fermion completely reflected from the dot. The phase factor $\exp(i2\pi\mathcal{N})$ in Eq. (4.16b) represents the scattering phase $\pi\mathcal{N}$, which agrees with the Friedel sum rule (2.1). Thus, our intuitive picture of Sec. II is proven by explicit calculation of the fermionic propagators.

B. Electrons with spin

Similarly to the spinless case, we start here with the bosonization of electron operators:

$$\psi_{R,\alpha}(x) = \frac{\hat\eta_\alpha}{\sqrt{2\pi\lambda}}\exp\left(i\frac{\hat\varphi_R^\rho(x)+\alpha\hat\varphi_R^\sigma(x)}{\sqrt{2}}\right),$$
$$\psi_{L,\alpha}(x) = \frac{\hat\eta_\alpha}{\sqrt{2\pi\lambda}}\exp\left(-i\frac{\hat\varphi_L^\rho(x)+\alpha\hat\varphi_L^\sigma(x)}{\sqrt{2}}\right), \quad (4.17)$$

where index $\alpha=\pm1$ denotes the spin projections, and the Majorana fermions $\eta_{\pm1}$ satisfy the anticommutation relations $\{\eta_{+1},\eta_{-1}\}=0$. Boson fields $\hat\varphi_{L,R}^\rho$ and $\hat\varphi_{L,R}^\sigma$ corresponding to the charge and spin degrees of freedom, respectively, satisfy the following commutation relations:

$$[\hat\varphi_L^i(x),\hat\varphi_L^j(y)] = -i\pi\,\mathrm{sgn}(x-y)\,\delta_{ij}, \quad (4.18a)$$

$$[\hat\varphi_R^i(x),\hat\varphi_R^j(y)] = i\pi\,\mathrm{sgn}(x-y)\,\delta_{ij}, \quad (4.18b)$$

$$[\hat\varphi_R^i(x),\hat\varphi_L^j(y)] = -i\pi\,\delta_{ij}, \quad i,j=\rho,\sigma. \quad (4.18c)$$

As in the case of spinless fermions, it is convenient to introduce even and odd modes $\hat\varphi_\pm^{\rho,\sigma}$ for the charge and spin sectors, and two x-independent fields, $\Phi^{\rho,\sigma}$ analogous to Eq. (4.9):

$$\hat\varphi_L^i(x) = \frac{\hat\varphi_+^i(x)+\hat\varphi_-^i(x)+\hat\Phi^i-\delta_{i\rho}\pi\mathcal{N}}{\sqrt{2}}, \quad i=\rho,\sigma$$
$$\hat\varphi_R^i(x) = \frac{\hat\varphi_+^i(-x)-\hat\varphi_-^i(-x)-\hat\Phi^i-\delta_{i\rho}\pi\mathcal{N}}{\sqrt{2}}. \quad (4.19)$$

The commutation relations for the new fields within the charge and spin sectors coincide with Eqs. (4.8); fields of different sectors commute with each other. In terms of the new fields, Hamiltonian (3.15) acquires the form independent of dimensionless gate voltage $\mathcal{N}$:

$$\hat H_0 = \frac{v_F}{4\pi}\sum_{i=\rho,\sigma}\sum_{\gamma=\pm}\int_{-\infty}^{\infty}dx\left(\frac{\partial\hat\varphi_\gamma^i}{\partial x}\right)^2+\frac{E_C}{2\pi^2}[\hat\varphi_+^\rho(0)]^2. \quad (4.20)$$

The backscattering Hamiltonian (3.17) takes the form

$$\hat H_{\mathrm{bs}} = \frac{2|r|v_F}{\pi\lambda}\cos[\hat\varphi_+^\rho(0)-\pi\mathcal{N}]\cos\hat\varphi_+^\sigma(0), \quad (4.21)$$

and the effective action (3.16) can be rewritten as

$$\hat S = \frac{1}{\pi\lambda}\int_0^\beta d\tau_1 d\tau_2 L(\tau_1-\tau_2)\sum_{\alpha=\pm1}\hat\eta_\alpha(\tau_1)\hat\eta_\alpha(\tau_2)e^{(i/2)\alpha[\hat\varphi_-^\sigma(\tau_1)-\hat\varphi_-^\sigma(\tau_2)]}e^{(i/2)\alpha[\hat\Phi^\sigma(\tau_1)-\hat\Phi^\sigma(\tau_2)]}$$
$$\times e^{(i/2)[\hat\varphi_-^\rho(\tau_1)-\hat\varphi_-^\rho(\tau_2)]}e^{(i/2)[\hat\Phi^\rho(\tau_1)-\hat\Phi^\rho(\tau_2)]}\left\{\cos\left[\frac{\hat\varphi_+^\rho(\tau_1)+\hat\varphi_+^\rho(\tau_2)}{2}+\alpha\frac{\hat\varphi_+^\sigma(\tau_1)+\hat\varphi_+^\sigma(\tau_2)}{2}-\pi\mathcal{N}\right]\right.$$
$$\left.-\sin\left[\frac{\hat\varphi_+^\rho(\tau_1)-\hat\varphi_+^\rho(\tau_2)}{2}+\alpha\frac{\hat\varphi_+^\sigma(\tau_1)-\hat\varphi_+^\sigma(\tau_2)}{2}\right]\right\}. \quad (4.22)$$

Similarly to Eq. (4.13), we introduce the relevant bosonic correlation functions

$$\mathcal{D}^i_-(\tau)=\langle T_\tau\hat{\varphi}_-(\tau)^i\hat{\varphi}_-(0)^i\rangle, \tag{4.23a}$$

$$\mathcal{D}^i_+(\tau)=\langle T_\tau\hat{\varphi}^i_+(\tau)\hat{\varphi}^i_+(0)\rangle, \tag{4.23b}$$

$$\mathcal{D}^i_\Phi(\tau)=\langle T_\tau\hat{\Phi}^i(\tau)\hat{\Phi}^i(0)\rangle, \tag{4.23c}$$

$$\mathcal{D}^i_{\Phi+}(\tau)=\langle T_\tau\hat{\Phi}^i(\tau)\hat{\varphi}^i_+(0)\rangle, \tag{4.23d}$$

where index $i=\rho,\sigma$ labels charge and spin sectors, respectively, bosonic fields are taken at $x=0$, and averaging is performed over the Hamiltonian $\hat{H}_0$ given by Eq. (4.20).

The calculation of these propagators can be performed immediately by noticing that the spin sector of the Hamiltonian (4.20) corresponds to the free bosons, and the charge sector differs from Eq. (4.10) only by replacement $E_C\to 2E_C$. Thus, we obtain

$$\mathcal{D}^\rho_\Phi(\tau)-\mathcal{D}^\rho_\Phi(0)=-\frac{1}{2}\int_0^\infty dx\,e^{-x}\ln\left[\frac{\sin(i\pi x/E_c+\tau)\pi T\,\sin(-i\pi x/E_c+\tau)\pi T}{\sinh^2\left(\dfrac{\pi^2Tx}{E_c}\right)}\right],\quad \mathcal{D}^\sigma_\Phi=0, \tag{4.24a}$$

$$\mathcal{D}^\rho_-(\tau)-\mathcal{D}^\rho_-(0)=\mathcal{D}^\sigma_\pm(\tau)-\mathcal{D}^\sigma_\pm(0)=\ln\left(\frac{\lambda}{v_F}\frac{\pi T}{|\sin\,\pi T\tau|}\right), \tag{4.24b}$$

$$\mathcal{D}^\rho_+(0)=\ln\left(\frac{\pi v_F}{\lambda E_C e^{\mathbf{C}}}\right), \tag{4.24c}$$

$$\mathcal{D}^\rho_+(\tau)-\mathcal{D}^\rho_+(0)=[\mathcal{D}^\rho_-(\tau)-\mathcal{D}^\rho_-(0)]-[\mathcal{D}^\rho_\Phi(\tau)-\mathcal{D}^\rho_\Phi(0)], \tag{4.24d}$$

$$\mathcal{D}^\rho_{\Phi+}(\tau)=\frac{i}{2}\int_0^\infty dx\,e^{-x}\frac{\pi^2T}{E_C}\left[\cot\left(i\frac{\pi x}{E_c}+\tau\right)\pi T+\cot\left(-i\frac{\pi x}{E_c}+\tau\right)\pi T\right],\quad \mathcal{D}^\sigma_{\Phi+}(\tau)=\frac{i\pi}{2}\,\mathrm{sgn}\,\tau, \tag{4.24e}$$

where $\mathbf{C}\approx 0.577$ is the Euler constant.

As we will see below (see also Ref. 14) the main contribution to the observable quantities is associated with the time scale $\tau\gtrsim 1/E_C$. At this time scale the effective theory can be further simplified. The mode $\hat{\varphi}^\rho_+$ is ''pinned'' due to the charging energy, see Eq. (4.20). Therefore, the amplitude of quantum fluctuations of this mode is finite [see Eq. (4.24c)] and the correlation function $\mathcal{D}^\rho_+(\tau)$ decreases rapidly at $\tau\gtrsim 1/E_C$, as it follows from Eqs. (4.24d), (4.24b), and (4.24a). The decrease of correlations means that the average of a product, $\langle e^{i\hat{\varphi}^\rho_+(\tau_1)}\cdots e^{i\hat{\varphi}^\rho_+(\tau_n)}\rangle$, can be replaced by the product of averages, $\langle e^{i\hat{\varphi}^\rho_+(\tau_1)}\rangle\cdots\langle e^{i\hat{\varphi}^\rho_+(\tau_n)}\rangle$, if the intervals between the times $\tau_1,\ldots,\tau_n$ exceed $1/E_C$. In other words, the operator functions of $\hat{\varphi}^\rho_+$ in Eq. (4.22) can be substituted with c numbers, according the rule

$$e^{i\hat{\varphi}^\rho_+}\to e^{-\frac{1}{2}\mathcal{D}^\rho_+(0)}. \tag{4.25}$$

On the other hand, it follows from Eqs. (4.24a) and (4.24b) that at $\tau>1/E_C$

$$\langle T_\tau[\hat{\varphi}^\rho_-(\tau)+\hat{\Phi}^\rho(\tau)-\hat{\varphi}^\rho_-(0)-\hat{\Phi}^\rho(0)]^2\rangle = -2\ln\left[\frac{\pi\lambda}{v_F E_C e^{\mathbf{C}}}\left(\frac{\pi T}{\sin\,\pi T\tau}\right)^2\right],$$

which means that such correlation function will be preserved if we introduce another free bosonic field $\hat{\varphi}_\rho(x)$, with commutation relation $[\hat{\varphi}_\rho(x);\hat{\varphi}_\rho(y)]=-i\pi\,\mathrm{sgn}(x-y)$, and substitute

$$\hat{\varphi}^\rho_-(x=0)+\hat{\Phi}^\rho\to\sqrt{2}\hat{\varphi}_\rho(x=0). \tag{4.26}$$

After substitutions (4.25) and (4.26), Hamiltonian (4.20) becomes just a Hamiltonian of three free bosonic fields

$$\hat{H}_0=\int_{-\infty}^\infty dx\left[\left(\frac{\partial\hat{\varphi}_\rho}{\partial x}\right)^2+\left(\frac{\partial\hat{\varphi}^\sigma_+}{\partial x}\right)^2+\left(\frac{\partial\hat{\varphi}^\sigma_-}{\partial x}\right)^2\right], \tag{4.27}$$

backscattering term acquires the form[14]

$$\hat{H}_{\mathrm{bs}}=\frac{2|r|}{\pi}\left(\frac{E_C e^{\mathbf{C}}v_F}{\pi\tilde{\lambda}}\right)^{1/2}\cos\,\pi\mathcal{N}\cos\,\hat{\varphi}^\sigma_+(0), \tag{4.28}$$

and the effective action is given by

$$\hat{S}=\frac{1}{\pi\tilde{\lambda}}\int_0^\beta d\tau_1 d\tau_2 L(\tau_1-\tau_2)\sum_{\alpha=\pm 1}\hat{\eta}_\alpha(\tau_1)\hat{\eta}_\alpha(\tau_2)e^{(i/2)\alpha[\hat{\varphi}_-^\sigma(\tau_1)-\hat{\varphi}_-^\sigma(\tau_2)]}e^{(i/2)\alpha[\hat{\Phi}^\sigma(\tau_1)-\hat{\Phi}^\sigma(\tau_2)]}e^{(i/\sqrt{2})[\hat{\varphi}_\rho(\tau_1)-\hat{\varphi}_\rho(\tau_2)]}$$
$$\times\left\{\cos\left[\alpha\frac{\hat{\varphi}_+^\sigma(\tau_1)+\hat{\varphi}_+^\sigma(\tau_2)}{2}-\pi\mathcal{N}\right]+\cos\left[\frac{\pi}{4}+\alpha\frac{\hat{\varphi}_+^\sigma(\tau_1)-\hat{\varphi}_+^\sigma(\tau_2)}{2}\right]\right\}. \tag{4.29}$$

Correlation functions of the free bosonic fields are given by

$$\mathcal{D}_\rho(\tau)-\mathcal{D}_\rho(0)=\mathcal{D}_\pm^\sigma(\tau)-\mathcal{D}_\pm^\sigma(0)=\ln\left(\frac{\tilde{\lambda}}{v_F}\frac{\pi T}{|\sin\ \pi T\tau|}\right), \tag{4.30}$$

where the cutoff $\tilde{\lambda}$ is of the order of v_F/E_C because the charging energy E_C is the largest energy scale, which can be considered with the help of Hamiltonian (4.27). It is easy to check also by an explicit calculation that at time differences larger than E_C^{-1} correlation functions of the electron operators evaluated with the help of the Hamiltonians (4.20) and (4.27) respectively coincide.

V. THERMODYNAMICS OF THE "OPEN" DOT

Coulomb blockade can be investigated experimentally[37,38] by measuring the differential capacitance of a dot, see Eq. (3.19). In the regime of a developed blockade (weak tunneling between the dot and the electron reservoir), $C_{\rm diff}(\mathcal{N})$ exhibits sharp peaks at half-integer values of $\mathcal{N}$. In the opposite limit of no backscattering, the differential capacitance is an $\mathcal{N}$-independent constant, $C_{\rm diff}(\mathcal{N})=C$. It was shown in Ref. 14 that weak reflection from a scatterer in the channel leads to the capacitance oscillations with a phase depending on the exact position of the scatterer. In this section we demonstrate that even at $r=0$, the differential capacitance still depends on $\mathcal{N}$ due to the electron backscatterings from inside the dot, which are described by the action $\hat{S}$. The randomness of the backscattering events results in the randomness of the phase of the capacitance oscillations. We will relate the statistics of $C_{\rm diff}(\mathcal{N})$ with the one of kernel $L(\tau)$.

The starting point for the calculation of the capacitance is Eq. (3.18) for the thermodynamic potential. In principle, Eq. (3.18) enables one to consider the backscattering off a barrier in the channel ($\hat{H}_{\rm bs}\neq 0$), as well as off the dot ($\hat{S}\neq 0$). In the limit of weak backscattering, the perturbation theory in $\hat{H}_{\rm bs}$ and $\hat{S}$ can be used to calculate $C_{\rm diff}(\mathcal{N})$. The case of $\hat{S}=0$ was considered by Matveev.[14] He has shown that for spinless fermions, a nonvanishing result appears in the first-order perturbation theory, whereas for the spin-1/2 electrons this order gives zero result. Similarly, it is sufficient to account for the scatterings from inside the cavity in the first order of the perturbation theory for spinless fermions, but in the case of spin-1/2 electrons we have to expand the thermodynamic potential (3.18) up to the second order in $\hat{S}$, if $\hat{H}_{\rm bs}=0$.

Backscattering in the channel leads to a finite modulation of the average differential capacitance. The modulation amplitude can be estimated[14] by expansion of Eq. (3.18) to the second order in $\hat{H}_{\rm bs}$ in the spin-1/2 case. Electron scattering from inside the dot leads to the capacitance fluctuations superimposed on this modulation. The two contributions to the capacitance are not additive: the nonzero result appears only in the second-order in perturbations to the Hamiltonian $\hat{H}_0$, when one expands Eq. (3.18). In the domain of a relatively strong backscattering in the channel, $|r|^2\gtrsim\Delta/E_C$, the leading term in fluctuations is proportional to the product of $\hat{H}_{\rm bs}$ and $\hat{S}$. We address the capacitance fluctuations at finite $|r|$ in the end of this section.

A. Spinless fermions

1. Reflectionless contact

The first-order expansion of Eq. (3.18) in $\hat{S}$ yields

$$\delta\Omega=T\langle T_\tau\hat{S}\rangle. \tag{5.1}$$

We substitute Eq. (4.12) into Eq. (5.1), retain only $\mathcal{N}$-dependent terms, and obtain with the help of Eqs. (4.14):

$$\delta\Omega=\frac{1}{2\pi v_F}\int_0^\beta d\tau L(\tau)[e^{i2\pi\mathcal{N}}K(\tau)+\text{c.c.}], \tag{5.2}$$

where function $K(\tau)$ is defined in Eq. (4.16b). To perform the integration over τ, we use the Lehmann representation (3.20) of the kernel L:

$$\delta\Omega=\frac{1}{2\pi v_F}\int_{-\infty}^{\infty}\frac{dt}{2\pi}[L^R(t)-L^A(t)]$$
$$\times\int_0^\beta d\tau\frac{\pi T}{\sinh[\pi T(t+i\tau)]}[e^{i2\pi\mathcal{N}}K(\tau)+\text{c.c.}]. \tag{5.3}$$

The integration over τ here can be now performed with the help of analytic properties of function $K(\tau)$. As it follows from Eq. (4.16b), the function $K(\tau)$ is analytic in the lower semiplane Im $\tau<0$. To calculate the integral of the first term in the brackets, we deform the contour of integration over τ as shown in Fig. 3.

Because of the periodicity of the integrand, the integrals over the parts of the contour running parallel to the imaginary axis cancel out. As the result, only the pole contribution at $\tau=it$ remains at $t<0$. At $t>0$ the pole contribution disappears. The second term in Eq. (5.3) is integrated by using

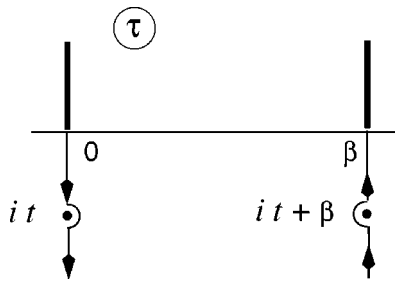

FIG. 3. The integration contour used in the evaluation of $\delta\Omega$ in the spinless case, see Eq. (5.3). Branch cuts of $K(\tau)$ are shown by thick lines.

$K(\tau)^* = -K(-\tau)$ for the real τ. With the help of the explicit expression (4.16b) for the function $K(\tau)$, we find

$$\delta\Omega(\mathcal{N}) = \frac{1}{2\pi i v_F}\int_0^\infty dt \frac{\pi T}{\sinh(\pi T t)} \times \exp\left[-\int_0^\infty dx\, e^{-x}\frac{2\pi^2 T}{E_C}\coth\left(\frac{2\pi x}{E_C}+t\right)\pi T\right] \times [L^R(t)e^{-i2\pi\mathcal{N}} - L^A(-t)e^{i2\pi\mathcal{N}}]. \tag{5.4}$$

Finally, at low temperatures $T \ll E_C$, the $\mathcal{N}$-dependent correction takes the form:

$$\delta\Omega(\mathcal{N}) = \frac{1}{2\pi i v_F}\int_0^\infty \frac{dt}{t}\exp\left[-\int_0^\infty dx \frac{e^{-x}}{x+(E_C/2\pi)t}\right] \times [L^R(t)e^{2\pi i\mathcal{N}} - L^A(-t)e^{-2\pi i\mathcal{N}}]. \tag{5.5}$$

Equation (5.5) relates the Coulomb blockade oscillation to the exact free-electron Green function in the dot. The variation of $\delta\Omega$ with the gate voltage is harmonic, however, its phase and amplitude are random quantities. To reveal this oscillatory dependence in the average quantities, one has to find the correlation function $\overline{\delta\Omega(\mathcal{N}_1)\delta\Omega(\mathcal{N}_2)}$. At low temperatures, Eqs. (5.5) and (3.25) lead directly to the result (2.24) with the dimensionless function Λ_E given by

$$\Lambda_E(x) = \frac{1}{(2\pi)^4}\Lambda(x), \tag{5.6}$$

$$\Lambda(x) = \int_0^\infty \frac{dy}{y^2}\exp[-xy + 2e^y Ei(-y)],$$

where $Ei(x) = \int_{-\infty}^x e^t dt/t$ is the exponential integral function.[40] The correlation function of the differential capacitances (3.19) for different values of the gate voltage and magnetic field is given by

$$\frac{\overline{\delta C_{\rm diff}(1)\,\delta C_{\rm diff}(2)}}{C^2} = \frac{2\Delta}{E_C}\left[\Lambda\left(\frac{H_-^2}{H_c^2}\right)+\Lambda\left(\frac{H_+^2}{H_c^2}\right)\right]\cos 2\pi n, \tag{5.7}$$

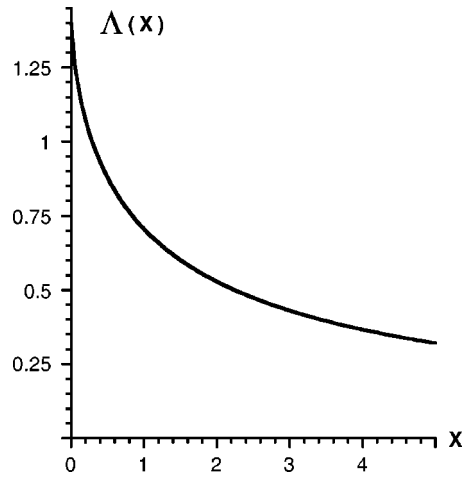

FIG. 4. Function $\Lambda(x)$ determining correlation of differential capacitances at different values of magnetic fields, see Eqs. (5.7) and Eq. (5.6).

where we use the shorthand notations $i \equiv \mathcal{N}_i, H_i$, $n = \mathcal{N}_1 - \mathcal{N}_2$, and $H_\pm = H_1 \pm H_2$. Correlation magnetic field H_c is controlled by the charging energy and it is given by Eq. (2.23).

The variance of the capacitance fluctuations at $H=0$ is two times larger than in the unitary limit ($H \gg H_c$). The dimensionless crossover function $\Lambda(x)$ is plotted in Fig. 4.

Correlation between the capacitances at different magnetic fields is suppressed if H_- exceeds H_c. In our approximation, the correlation ''length'' n_c in the dimensionless gate voltage is infinite. To find n_c, one should take into account that varying the gate voltage affects the chemical potential of electrons in the dot by the level spacing each time $\mathcal{N}$ changes by one. If the chemical potential is shifted by E_C, a completely new set of levels determines the kernel L, thus suppressing the correlations. This results in the estimate $n_c \simeq E_C/\Delta$. Another effect that leads to the decrease of the correlation function at large n is the variation of the dot shape with the gate voltage.

2. Finite reflection in the contact

At finite backscattering in the contact, $r \neq 0$, Hamiltonian (4.11) should be taken into account:

$$\delta\Omega(\mathcal{N}) = \langle \hat{H}_{\rm bs}\rangle.$$

Calculating this average with the help of Eq. (4.14c), and using Eq. (3.19), we arrive at the result for the oscillating contribution of the averaged capacitance,

$$\frac{\overline{\delta C(\mathcal{N})}}{C} = 2e^{\mathbf{C}}|r|\cos 2\pi\mathcal{N}. \tag{5.8}$$

This result was first obtained in Ref. 14.

Average of the action Eq. (5.1) simply adds to this result. Thus, we conclude that finite reflection in this order of perturbation theory does not affect the mesoscopic fluctuations of the capacitance; see Eq. (5.7). We will see below that this is qualitatively different from the electrons with spin where finite reflection in the contact leads to the increase of the mesoscopic fluctuations of the differential capacitance.

B. Electrons with spin

1. Reflectionless contact

In the case of spin-1/2 fermions, the charging energy pins only one out of four modes. Fluctuations in the spin mode are not suppressed; see Eq. (4.27). These fluctuations average action (4.29) to zero. To obtain a finite result for the $\mathcal{N}$-dependent part of the thermodynamic potential, we have to expand Ω up to the second order in $\hat{S}$:

$$\delta\Omega = -\tfrac{1}{2}T\langle T_\tau \hat{S}^2\rangle. \tag{5.9}$$

Upon the substitution of Eq. (4.29) into Eq. (5.9), we use the expressions (4.30) to perform the averaging over $\hat{H}_0$. This cumbersome albeit straightforward calculation yields for the $\mathcal{N}$-dependent part of the thermodynamic potential:

$$\delta\Omega = \frac{1}{(2\pi v_F)^2}\int_0^\beta d\tau_1 d\tau_2 d\tau_3 L(\tau_1)L(\tau_2)\sum_{\gamma=\pm 1} e^{-i2\pi\gamma\mathcal{N}}\frac{\pi T}{[\sin\,\pi T(\tau_1+i\gamma 0)\sin\,\pi T(\tau_2+i\gamma 0)]^{1/2}}$$
$$\times\frac{\pi T}{[\sin\,\pi T(\tau_1+\tau_3+i\gamma 0)\sin\,\pi T(\tau_2-\tau_3+i\gamma 0)]^{1/2}}. \tag{5.10}$$

As in Sec. V A, it is convenient to use the Lehmann representation (3.20) for the kernel L:

$$\delta\Omega = \frac{1}{(2\pi v_F)^2}\int_{-\infty}^{\infty}\frac{dt_1}{2\pi}\frac{dt_2}{2\pi}[L^R(t_1)-L^A(t_1)][L^R(t_2)-L^A(t_2)]\int_0^\beta d\tau_1 d\tau_2 d\tau_3\frac{\pi T}{\sinh\,\pi T(t_1+i\tau_1)}\frac{\pi T}{\sinh\,\pi T(t_2+i\tau_2)}$$
$$\times\sum_{\gamma=\pm 1} e^{-i2\pi\gamma\mathcal{N}}\frac{\pi T}{[\sin\,\pi T(\tau_1+i\gamma 0)\sin\,\pi T(\tau_2+i\gamma 0)]^{1/2}}\frac{\pi T}{[\sin\,\pi T(\tau_1+\tau_3+i\gamma 0)\sin\,\pi T(\tau_2-\tau_3+i\gamma 0)]^{1/2}}. \tag{5.11}$$

The evaluation of the integrals over τ_1 and τ_2 here is similar to the procedure employed for the evaluation of the integral over τ in Sec. V A. Upon the integration, we find

$$\delta\Omega = \frac{1}{(2\pi v_F)^2}\int_{-\infty}^{\infty}\frac{dt_1}{2\pi}\frac{dt_2}{2\pi}(L^R(t_1)L^R(t_2)e^{-i2\pi\mathcal{N}}$$
$$+L^A(t_1)L^A(t_2)e^{i2\pi\mathcal{N}})\frac{\pi T}{[\sinh(\pi T t_1)\sinh(\pi T t_2)]^{1/2}}$$
$$\times\int_0^\beta d\tau_3\frac{\pi T}{[\sinh\,\pi T(t_1-i\tau_3)\sinh\,\pi T(t_2+i\tau_3)]^{1/2}}. \tag{5.12}$$

Integral over τ_3 can be easily evaluated with the help of the formula

$$\int_0^\pi\frac{d\phi}{[\sinh(x-i\phi)\sinh(y+i\phi)]^{1/2}} = 4e^{-|x+y|}\mathbf{K}(e^{-|x+y|}),$$

where $\mathbf{K}(k)$ is the complete elliptic integral of the first kind.[40] We find for $\delta\Omega$:

$$\delta\Omega = \frac{1}{(\pi v_F)^2}\int_0^\infty\frac{dt_1 dt_2\pi T}{[\sinh(\pi T t_1)\sinh(\pi T t_2)]^{1/2}}$$
$$\times[L^R(t_1)L^R(t_2)e^{-i2\pi\mathcal{N}}+\text{c.c.}]e^{-\pi T(t_1+t_2)}$$
$$\times\mathbf{K}(e^{-\pi T(t_1+t_2)}). \tag{5.13}$$

In the derivation of Eq. (5.13), we have utilized the reduced version of action [see Eq. (4.29)], which is valid only on a relatively long time scale larger than $1/E_C$. Now, we average the product of two thermodynamic potentials with the help of Eq. (3.25). As we will see shortly, the result of the averaging is logarithmically divergent at large t. The divergence should be cut off at $t_{1,2}\gtrsim 1/E_C$. Without violating the logarithmical accuracy, we can use also asymptotic expansion of the elliptic integral $\mathbf{K}(k) = -\ln\sqrt{1-k^2}$. We obtain

$$\overline{\delta\Omega(1)\delta\Omega(2)} = \frac{2\Delta^2}{(2\pi)^6}\cos 2\pi n$$
$$\times\int_{1/E_C}^\infty\frac{dt_1 dt_2\pi^2 T^2}{\sinh\,\pi T t_1\,\sinh\,\pi T t_2}$$
$$\times\left[\ln\frac{1}{T^2(t_1+t_2)^2}\right]^2$$
$$\times[e^{-t_1/\tau_D}+e^{-t_1/\tau_C}][e^{-t_2/\tau_D}+e^{-t_2/\tau_C}]. \tag{5.14}$$

Here, as in Eq. (5.7), we use the shorthand notation $i = H_i, \mathcal{N}_i$, and $n = \mathcal{N}_1 - \mathcal{N}_2$. The diffuson and Cooperon decay times τ_D and τ_C are related to the magnetic field values H_1, H_2 by Eq. (3.24). Now we can use Eq. (3.19) to find the correlation function of the differential capacitances. In the leading logarithmic approximation we obtain

$$\frac{\overline{\delta C_{\rm diff}(1)\,\delta C_{\rm diff}(2)}}{C^2}=\frac{8}{3\pi^2}\frac{\Delta^2}{E_C^2}\ln^4\left(\frac{E_C}{T}\right)\cos 2\pi n \times\sum_{\gamma=\pm}\left[1-4\left(\frac{\ln\max(1;[H_\gamma/H_c^<]^2)}{\ln(E_C/T)}\right)^3+\cdots\right], \tag{5.15}$$

where the fields $H_\pm=H_1\pm H_2$ are assumed to be small compared to the correlation field H_c given by Eq. (2.23). The new temperature-dependent correlation field appearing in Eq. (5.15) is given by

$$H_c^<=\frac{\Phi_0}{\mathcal{A}}\sqrt{\frac{T}{2\pi E_T}}, \tag{5.16}$$

with Φ_0, $\mathcal{A}$, and E_T being the flux quantum, the geometrical area of the dot, and the Thouless energy, respectively. Unlike the scale H_c, the characteristic field $H_c^<$ is independent on the charging energy. This smaller field scale appears due to the existence of the ''free'' excitation mode φ_+^σ, which is not pinned by the effect of charging.

With the increase of the number of channels in the dot-lead junction, the number of free modes also increases. The role of charging (which still pins only one mode), and therefore of the field H_c, in the correlation functions should vanish gradually. The dependence of the correlation functions on the magnetic field at $H<H_c$ becomes a power law rather than logarithmic; however, this power law is still nontrivial, and approaches Fermi-liquid results only in the limit of an infinite number of channels.

If $H_\pm\gtrsim H_c$, [the charging correlation field H_c is given by Eq. (2.23)], the correlation function of the fluctuation starts decreasing much faster, $\propto 1/H_\pm^4$. Therefore, in order to get the representative statistics of the capacitance fluctuations, averaging should be performed in the interval of magnetic fields larger than the magnetic field determined by the charging energy (2.23). Finally, in the limit of a strong field, $H_1=H_2\gtrsim H_c$ (unitary limit), the variance $\overline{\delta C_{\rm diff}^2}$ of the differential capacitance becomes four times smaller than at $H=0$.

Our results for the correlation functions diverge logarithmically at $T\to 0$. At lower temperatures the pinning of the spin mode described by action $\hat{S}$ should be taken into account. A variational estimate[39] shows that T at low temperatures should be replaced by $\Delta\,\ln(E_C/\Delta)$ in the above results for $H_c^<$ and for the correlation function. We will elaborate on this point more in the end of the following subsection.

2. Finite reflection in the contact

The main effect of the backscattering in the channel is that the Coulomb blockade appears already in the averaged capacitance.[14] Taking into account backscattering Hamiltonian (4.28) in the second-order perturbation theory, we obtain from Eq. (3.19)

$$\delta C(\mathcal{N})=\frac{8e^{\mathbf{C}}}{\pi}|r|^2\,\cos 2\pi\mathcal{N}\ln\left(\frac{E_C}{T}\right). \tag{5.17}$$

Due to the finite level spacing Δ, this result acquires mesoscopic fluctuations. As we already mentioned in the introduction to this section, at $r\neq 0$ the leading term in fluctuations of the thermodynamic potential is first order in both $\hat{H}_{\rm bs}$ and $\hat{S}$,

$$\delta\Omega=-T\left\langle T_\tau\int_0^\beta d\tau\hat{H}_{\rm bs}(\tau)\hat{S}\right\rangle. \tag{5.18}$$

To calculate the average over the unperturbed state, we use the bosonized representation of $\hat{H}_{\rm bs}$ and $\hat{S}$ given by Eqs. (4.28) and (4.29), respectively, and then the expressions (4.30) for the correlation functions of the boson fields. Then, similar to Sec. V A, we switch to the Lehmann representation (3.20) for the kernel $L(\tau)$ to obtain

$$\delta\Omega=\frac{2\sqrt{e^{\mathbf{C}}}|r|\sqrt{E_C}}{\pi^2\sqrt{\pi}v_F}\cos(\pi\mathcal{N})\int_{-\infty}^{\infty}\frac{dt}{2\pi}[L^R(t)-L^A(t)]\int_0^\beta\frac{d\tau_1 d\tau_2(\pi T)^2}{\sinh[\pi Tt+i\pi T(\tau_1-\tau_2)][\sin(\pi T\tau_1)\sin(\pi T\tau_2)]^{1/2}} \times\sum_{\gamma=\pm 1}\frac{(\pi T)^{1/2}}{[\sin\,\pi T(\tau_2-\tau_1+i\gamma 0)]^{1/2}}e^{-i\pi\gamma(\mathcal{N}-1/4)}. \tag{5.19}$$

Here only the $\mathcal{N}$-dependent part of the thermodynamic potential is taken into account. Integral over τ_1 in Eq. (5.19) is determined by the contribution of the pole at $\tau_1=\tau_2-it$, which can be easily calculated:

$$\delta\Omega=\frac{2\sqrt{e^{\mathbf{C}}}|r|\sqrt{E_C}}{\pi^2\sqrt{\pi}v_F}\cos(\pi\mathcal{N})\int_{-\infty}^{\infty}\frac{dt(\pi T)^{1/2}}{[-i\sinh(\pi Tt)]^{1/2}}[L^A(t)e^{i\pi(\mathcal{N}-1/4)}+L^R(t)e^{-i\pi(\mathcal{N}-1/4)}] \times\int_0^\beta d\tau_2\frac{\pi T}{[\sin(\pi T\tau_2)\sin(\pi T\tau_2+it)]^{1/2}}. \tag{5.20}$$

Integration over τ_2 is now very similar to the one we performed over the variable τ_3 in Eq. (5.12), and we find for $\delta\Omega$:

$$\delta\Omega=\frac{2\sqrt{e^{\mathbf{C}}}|r|\sqrt{E_C}}{\pi^2\sqrt{\pi}v_F}\cos(\pi\mathcal{N})\int_{-\infty}^{\infty}\frac{(\pi T)^{1/2}\ln(1/T^2t^2)dt}{[-i\,\sinh(\pi Tt)]^{1/2}}[L^A(t)e^{i\pi\mathcal{N}}+L^R(t)e^{-i\pi\mathcal{N}}]. \tag{5.21}$$

From Eq. (5.21), with the help of Eqs. (3.25) and (3.19), we find the correlation function of mesoscopic fluctuation of the capacitances:

$$\frac{\overline{\delta C_{\rm diff}(1)\,\delta C_{\rm diff}(2)}}{C^2}=\frac{32e^{\mathbf{C}}}{3\pi^2}\frac{|r|^2\Delta}{E_C}\ln^3\left(\frac{E_C}{T}\right)\cos 2\pi n\sum_{\gamma=\pm}\left[1-\left(\frac{\ln\max(1;[H_\gamma/H_c^<]^2)}{\ln(E_C/T)}\right)^3\right], \tag{5.22}$$

where $i=H_i,\mathcal{N}_i$, $n=\mathcal{N}_1-\mathcal{N}_2$, and $H_\pm=H_1\pm H_2$. Correlation field $H_c^<$ is defined in Eq. (5.16). The amplitude of fluctuations at a partial transmission of the channel is parametrically larger than at $r=0$, cf. Eq. (5.15). Furthermore, in the unitary limit the variance of the differential capacitance is suppressed only by a half of its zero-field value. This similarity with the case of spinless fermions is due to the backscattering in the channel, which leads to pinning of the spin mode.

Result (5.22) is valid at relatively high temperatures. As shown by Matveev,[14] the divergences should be cut at energy $\epsilon^*\simeq|r|^2E_C\cos^2\pi\mathcal{N}$, which corresponds to the pinning energy of the spin mode. The higher-order corrections in backscattering[14] show that at $T\lesssim|r|^2E_C$ the logarithmic growth of fluctuations saturates. Simultaneously, the correlation functions start to depend not only on the difference $\mathcal{N}_1-\mathcal{N}_2$, but also on each of these arguments separately. This weaker logarithmic dependence is beyond the scope of this paper. For an estimate of the differential capacitance variance at low temperature, one may replace $\ln(E_C/T)$ by $\ln(1/|r|^2)$ in Eq. (5.22).

Finally, we elaborate on the estimate of the characteristic energy scale that controls the low-temperature cutoff for the reflectionless contact. Comparing Eq. (5.17) with Eq. (5.21), or Eq. (5.21) with Eq. (5.15), we observe that the reflectionless case results can be obtained from formulas with finite reflection coefficient by putting $|r|^2\mapsto(\Delta/E_C)\ln(E_C\Delta)$. It would correspond to the energy of pinning of the spin mode $\epsilon^*\simeq\Delta\ln(E_C/\Delta)$, which agrees with our variational estimate.[39]

VI. TUNNELING CONDUCTANCE OF THE ''OPEN'' DOT

In the previous section, we considered in detail the thermodynamics of the dot with one almost open channel, and studied mesoscopic effects related to the discreteness of the charge. However, the majority of experimental work deals not with thermodynamics, but rather with transport through a dot. The Coulomb blockade shows up as an oscillatory gate voltage dependence of the conductance of the dot connected with two leads.

The case of small transparency of the channels connecting the dot with leads is well studied.[2,4,10,11] The conductance in the valleys can be represented as the sum of two physically different contributions—elastic and inelastic cotunneling.[10] During the *elastic* cotunneling process, an electron enters the dot, spends there a time $\simeq\hbar/E_C$, and then leaves the dot. Without interaction, this electron would be able to spend a time of the order of $\hbar/\Delta$. As the result, the conductance in the Coulomb blockade valleys is suppressed by a factor of Δ/E_C. During the *inelastic* cotunneling process,[36] an electron enters the dot, spends there a time $\simeq\hbar/E_C$, and then another electron leaves the dot. In this case, the final state contains an extra, in comparison with the initial state, two-particle excitation. This means that the phase volume of the final state is small as T^2; therefore, the elastic contribution dominates at $T\lesssim(E_C\Delta)^{1/2}$.

Conductance of the dot connected to each reservoir by an almost perfect channel was studied, in the limit $\Delta/E_C\to0$, by Furusaki and Matveev.[27] They concluded that even small reflection in any of the channels leads to a dramatic suppression of the conductance of the system. At any gate voltage, except the discrete points of charge degeneracy, they obtained a T^2 law that closely resembles the behavior of inelastic cotunneling in the weak tunneling regime. Pursuing the analogy with the weak tunneling regime further, it is natural to expect that there should be another nonvanishing at $T\to0$ contribution from a counterpart of the elastic cotunneling mechanism. Studying this contribution is the goal of this section.[41]

Similar to Ref. 27, two limiting cases may be distinguished. In the first case both channels are either open or have the same reflection coefficient. This case is technically difficult to consider. Instead, we concentrate on the properties of the strongly asymmetric setup; one point contact (left in Fig. 5) has the transparency close to unity and the other contact (right in Fig. 5) has a very small conductance $G_R\ll e^2/\pi\hbar$. This case can be realized experimentally by a corresponding adjustment of the voltages on the gates forming

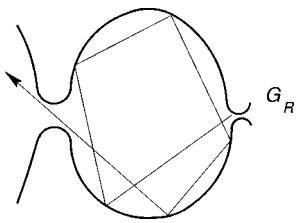

FIG. 5. Schematic view of the asymmetric two-terminal setup. The left point contact has one channel almost open and the conductance of the right point contact G_R is much smaller than $e^2/2\pi\hbar$. One of the electron trajectories contributing to the elastic cotunneling is also shown.

point contacts.[43] Moreover, it follows from the scaling arguments[27] that the asymmetry of contacts is a relevant perturbation. In the case $\Delta=0$, the strongly asymmetric limit corresponds to the fixed point of a system with an infinitesimally small initial asymmetry. Therefore we can expect that at $\Delta/E_C \ll 1$, this limit adequately describes dots with a finite initial degree of asymmetry.

A. General formalism

For calculation of such tunneling conductance, we have to modify derivation of Secs. III A and III B in order to take into account the tunneling between the dot and the second lead. In comparison with Hamiltonian (3.1), the total Hamiltonian of the system acquires two additional terms,

$$\hat{H}=\hat{H}_F+\hat{H}_C+\hat{H}_M+\hat{H}_T. \tag{6.1}$$

Here $\hat{H}_F$ describes the electron motion in the dot and in the left lead and is given by Eq. (3.2), interaction Hamiltonian $\hat{H}_C$ is given by Eq. (1.1), and $\hat{H}_M$ is the Hamiltonian of free electrons in the right lead

$$\hat{H}_M=\sum_p \xi_p \hat{a}_p^\dagger \hat{a}_p. \tag{6.2}$$

Tunneling Hamiltonian $\hat{H}_T$ describes the weak coupling between the right lead and the dot,

$$\hat{H}_T=v_t \hat{\psi}^\dagger(\mathbf{r}_t)\sum_p \hat{a}_p+\text{H.c.}, \tag{6.3}$$

where $\mathbf{r}_t$ is the coordinate of the tunneling contact, $\hat{\psi}^\dagger(\mathbf{r})$ is the electron wave function in the lead, and v_t is the coupling constant which will be later related to the tunneling conductance of the contact G_R.

Because $G_R \ll e^2/(2\pi\hbar)$, we can consider the tunneling current I as the function of applied voltage V in the second order of perturbation theory in tunneling Hamiltonian (6.3). This gives us the standard result[44]

$$I(eV)=i[J(i\Omega_n \to eV+i0)-J(i\Omega_n \to eV-i0)], \tag{6.4}$$

where $\Omega_n=2\pi T n$ is the bosonic Matsubara frequency, and Matsubara current J is defined as

$$J(i\Omega_n)=e v_t^2 \nu \int_0^\beta d\tau\, e^{-i\Omega_n \tau}\mathcal{G}_M(\tau)\Pi(\tau). \tag{6.5}$$

Here ν is the one-electron density of states per unit area and per one spin in the dot, $\mathcal{G}_M$ is the Green function of the electrons in the leads,

$$\mathcal{G}_M \equiv -\sum_{p_1,p_2}\langle T_\tau \hat{a}_{p_1}(\tau)\hat{a}_{p_2}^\dagger(0)\rangle = \nu_M \frac{\pi T}{\sin\,\pi T\tau}, \tag{6.6}$$

with ν_M being the one-electron density of states per one spin in the lead, and function $\Pi(\tau)$ is given by

$$\Pi(\tau)=\nu^{-1}\langle T_\tau \overline{\psi}(\tau;\mathbf{r}_t)\psi(0;\mathbf{r}_t)\rangle. \tag{6.7}$$

Averages in Eqs. (6.6) and (6.7) are performed with respect to the equilibrium distribution of the system without tunneling. We choose to introduce ν into Eq. (6.4) and into definition (6.6) to make function $\Pi(\tau)$ have dimensionality of energy.

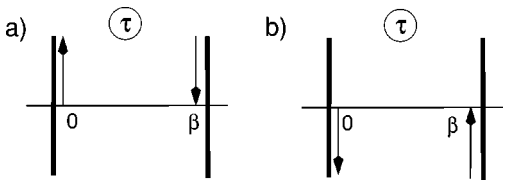

FIG. 6. The integration contour used in the evaluation of the conductance, see Eq. (6.10) for (a) $\Omega_n<0$, and (b) for $\Omega_n>0$. Branch cuts of the analytic continuation of $\Pi(\tau)$ are shown by thick lines.

In the absence of the interaction, $E_C=0$, propagator $\Pi(\tau)$ is nothing but the Green function of the noninteracting system; its ensemble average has a form analogous to Eq. (6.6),

$$\overline{\Pi(\tau)}|_{E_C=0}=\frac{\pi T}{\sin\,\pi T\tau}. \tag{6.8}$$

Then, substitution of Eqs. (6.6) and (6.8) into Eq. (6.5) and analytic continuation (6.4) give the tunneling current $I=sG_RV$ (s is the spin degeneracy), where the tunneling conductance of the contact per one spin is

$$G_R=\frac{2\pi e^2}{\hbar}v_t^2 \nu_M \nu. \tag{6.9}$$

With the help of Eq. (6.9) we can rewrite Eq. (6.5) in terms of the bare conductance of the point contact:

$$J(i\Omega_n)=\frac{G_R}{2\pi e}\int_0^\beta d\tau \frac{\pi T e^{-i\Omega_n\tau}}{\sin\,\pi T\tau}\Pi(\tau). \tag{6.10}$$

As we will see below, function $\Pi(\tau)$ can be analytically continued from the real axis to the complex plane, so that the result is analytic in a strip $0<\mathrm{Re}\ \tau<\beta$, and has branch cuts along Re $\tau=0,\beta$ lines. It allows one to deform the contour of integration as shown in Fig. 6, and to obtain

$$J(i\Omega_n)=\frac{G_R T}{2e}\int_{-\infty}^{\infty} dt\, e^{\Omega_n t}[\theta(-\Omega_n)\theta(t)-\theta(\Omega_n)\theta(-t)] \times\left(\frac{\Pi(it+0)}{\sinh[\pi T(t-i0)]}-\frac{\Pi(it-0)}{\sinh[\pi T(t+i0)]}\right). \tag{6.11}$$

Now the analytic continuation (6.4) can be performed, because the periodicity of the Matsubara Green functions was already taken into account. This gives

$$I(eV)=i\frac{G_R T}{2e}\int_{-\infty}^{\infty} dt\, e^{-ieVt} \times\left[\frac{\Pi(it+0)}{\sinh[\pi T(t-i0)]}-\frac{\Pi(it-0)}{\sinh[\pi T(t+i0)]}\right]. \tag{6.12}$$

Next, we use the analyticity of $\Pi(\tau)$ in the strip $0<\mathrm{Re}\ \tau<\beta$, and shift the integration variable $t\to t-i\beta/2$ in the first term in brackets in Eq. (6.12), and $t\to t+i\beta/2$ in the second term. Bearing in mind that $\Pi(\tau)=-\Pi(\tau+\beta)$, we find

$$I=\left(T\ \sinh\frac{eV}{2T}\right)G_R\int_{-\infty}^{\infty}dt\,e^{-ieVt}\frac{\Pi(it+\beta/2)}{\cosh\ \pi Tt}. \quad (6.13)$$

Linear conductance G is therefore given by

$$G=G_R\int_{-\infty}^{\infty}dt\,\frac{\Pi(it+\beta/2)}{2\cosh\ \pi Tt}. \quad (6.14)$$

Let us turn now to the actual calculation of the function $\Pi(\tau)$. It was shown in Ref. 27 that the interaction drastically affects the form of the function (6.7), however, some contributions were not taken into account. Our purpose is to construct an effective action theory, similar to that of Sec. III, for calculation of $\Pi(\tau)$. Once again, we wish to get rid of the fermionic degrees of freedom of the dot. Similar to Eq. (3.4), it is convenient to rewrite the charge operator in terms of the variables of the channel. However, here we have to keep in mind the fact that the tunneling events described by operators $\psi^{\dagger}(\mathbf{r}_t)$ and $\psi(\mathbf{r}_t)$ change the charge in the system by $+e$ and $-e$. It can be taken into account[27] by introducing three additional operators: Hermitian operator $\hat{n}$, and unitary operators $\hat{F},\hat{F}^{\dagger}$ with the following commutation relations:

$$[\hat{n},\hat{F}^{\dagger}]=\hat{F}^{\dagger}. \quad (6.15)$$

We can definitely choose Hilbert subspace in a way such that operator $\hat{n}$ has integer eigenvalues. Finally, these operators commute with all the fermionic degrees of freedom. Then, we can change the definition of the charge operator [cf. Eq. (3.4)] to

$$\frac{\hat{Q}}{e}=-\int_{\text{channel}}d\mathbf{r}\,\psi^{\dagger}\psi+\hat{n}, \quad (6.16)$$

and rewrite Eq. (6.7) as

$$\Pi(\tau)=\nu^{-1}\langle T_{\tau}\hat{\bar{F}}(\tau)\bar{\psi}(\tau;\mathbf{r}_t)\hat{F}(0)\psi(0;\mathbf{r}_t)\rangle. \quad (6.17)$$

It is easy to see from Eqs. (6.16) and (6.15) that operators $\hat{F}^{\dagger},\hat{F}$ in Eq. (6.17) change the charge by $+e$ and $-e$, respectively, in accordance with the initial definition of charge.

After this manipulation, the Hamiltonian of the system and correlation function (6.17) become quadratic in the fermionic operators of the dot, so that part of the system can be integrated out. We use the identity similar to Eq. (3.6):

$$\begin{aligned}\mathrm{Tr}_2\{e^{-\beta\hat{H}_F}T_{\tau}\bar{\psi}_2(\tau)\psi_2(0)\}&=e^{-\beta\hat{H}_1}\mathrm{Tr}_2[e^{-\beta\hat{H}_2}T_{\tau}\bar{\psi}_2(\tau)\psi_2(0)e^{-\int_0^{\beta}d\tau\hat{H}_{12}(\tau)}]\\&=e^{-\beta\Omega_2}\langle T_{\tau}\bar{\psi}_2(\tau)\psi_2(0)\rangle_2e^{-\beta\hat{H}_1}T_{\tau}e^{1/2\int_0^{\beta}d\tau_1\int_0^{\beta}d\tau_2\langle\hat{H}_{12}(\tau_1)\hat{H}_{12}(\tau_2)\rangle_2}+e^{-\beta\Omega_2}e^{-\beta\hat{H}_1}\\&\times\int_0^{\beta}d\tau_3\int_0^{\beta}d\tau_4T_{\tau}\langle T_{\tau}\bar{\psi}_2(\tau)\hat{H}_{12}(\tau_3)\rangle_2\langle T_{\tau}\psi_2(0)\hat{H}_{12}(\tau_3)\rangle_2e^{1/2\int_0^{\beta}d\tau_1\int_0^{\beta}d\tau_2\langle\hat{H}_{12}(\tau_1)\hat{H}_{12}(\tau_2)\rangle_2},\end{aligned} \quad (6.18)$$

where all $\psi_2^{\dagger},\psi_2$ are the fermionic operators of the dot, and the rest of the notation is the same as that in Eq. (3.6).

The calculation of the product $\langle\hat{H}_{12}(\tau_1)\hat{H}_{12}(\tau_2)\rangle_2$ was performed in Sec. III A [see Eq. (3.7)], and all the steps leading to the derivation of the effective action (3.14) can be repeated here. Calculation of the remaining operator products can be performed along the lines of Appendix A. This yields

$$\begin{aligned}\langle T_{\tau}\psi(\tau_1;\mathbf{r}_t)\hat{H}_{12}(\tau_2)\rangle_2&=-\psi(\tau_2,0)R^*(\tau_1-\tau_2),\\\langle T_{\tau}\bar{\psi}(\tau_1;\mathbf{r}_t)\hat{H}_{12}(\tau_2)\rangle_2&=-\bar{\psi}(\tau_2,0)R(\tau_2-\tau_1),\end{aligned} \quad (6.19)$$

where, similar to Eq. (3.7), $\psi(\tau;x)=e^{\tau\hat{H}_1}\psi(x)e^{-\tau\hat{H}_1}$ are the one-dimensional fermionic operators of the channel in the interaction representation, $\bar{\psi}(\tau)=\psi^{\dagger}(-\tau)$. Kernel R describes the motion of an electron from the tunnel contact to the entrance of the single mode channel, and it is given by

$$R(\tau)=\frac{1}{2m}\int dy\ \phi(y)\partial_x\mathcal{G}(\tau;\mathbf{r},\mathbf{r}_t). \quad (6.20)$$

Here, $\mathcal{G}$ is the exact Matsubara Green function of the closed dot subjected to the zero boundary condition. The wave function $\phi(y)$ describes the transverse motion in the single-mode channel, and the coordinates x in the derivative of the Green function $\mathcal{G}$ is set to $+0$.

Kernel $R(\tau)$ is the random quantity with the zero averages. In the universal regime, products of retarded $R^R(t)$ and advanced $R^A(t)$ counterparts of $R(\tau)$ entering into the Lehmann representation (3.20) have the following nonvanishing averages:

$$\frac{1}{\nu}\langle R^R_{H_1}(t_1)R^A_{H_2}(t_2)\rangle=\Delta v_F\delta(t_1+t_2)\,\theta(t_1)e^{-t_1/\tau_H^C}, \quad (6.21a)$$

$$\frac{1}{\nu}\langle R^R_{H_1}(t_1)[R^R_{H_2}(t_2)]^*\rangle=\Delta v_F\delta(t_1-t_2)\,\theta(t_1)e^{-t_1/\tau_H^D}, \quad (6.21b)$$

where the decay times $\tau_H^{C,D}$ associated with applied magnetic fields $H_{1,2}$ are given by Eq. (3.24). All the higher momenta can be found by using the Wick theorem.[45] Deriving Eq.

(6.21b) we use Eqs. (3.21), (3.23), and the identity $\mathcal{G}^R(t;r_1,r_2)=[\mathcal{G}^A(-t;r_2,r_1)]^*$.

To complete the derivation of the effective theory, we use Eqs. (6.18) and (6.19), introduce left and right moving fermions similarly to Sec. III A, and thus obtain the effective action representation for $\Pi(\tau)$ from Eq. (6.17):

$$\Pi(\tau)=\Pi_{\rm in}(\tau)+\Pi_{\rm el}(\tau), \tag{6.22a}$$

$$\Pi_{\rm in}=-\frac{\mathcal{G}(-\tau;\mathbf{r}_t,\mathbf{r}_t)}{\nu\langle T_\tau e^{-\hat{S}}\rangle}\langle T_\tau e^{-\hat{S}}\hat{\bar{F}}(\tau)\hat{F}(0)\rangle, \tag{6.22b}$$

$$\begin{aligned}\Pi_{\rm el}=&\frac{1}{\nu\langle T_\tau e^{-\hat{S}}\rangle}\int_0^\beta d\tau_1 d\tau_2 R(\tau_1-\tau)R^*(-\tau_2)\\ &\times\langle T_\tau e^{-\hat{S}}\hat{\bar{F}}(\tau)\hat{F}(0)[\overline{\psi_L}(\tau_1)+\overline{\psi_R}(\tau_1)]\\ &\times[\psi_L(\tau_2)+\psi_R(\tau_2)]\rangle.\end{aligned} \tag{6.22c}$$

Here the averaging is performed with respect to the Hamiltonian

$$\begin{aligned}\hat{H}_0=&iv_F\int_{-\infty}^{\infty}dx\{\psi_L^\dagger\partial_x\psi_L-\psi_R^\dagger\partial_x\psi_R\}\\ &+\frac{E_C}{2}\left(\int_{-\infty}^{0}dx{:}\psi_L^\dagger\psi_L+\psi_R^\dagger\psi_R{:}+\mathcal{N}-\hat{n}\right)^2,\end{aligned} \tag{6.23}$$

and action $\hat{S}$ is given by Eq. (3.16). The difference between Eq. (6.23) and Eq. (3.15), is caused by the different definitions of the charge operator in Eqs. (3.4) and (6.16).

Two contributions can be distinguished in the correlation function (6.22). The inelastic contribution (6.22b) was considered in Ref. 27 in the approximation corresponding to $\hat{S}=0$, and with the Green function of the dot $\mathcal{G}$ replaced by its averaged value $\overline{\mathcal{G}}$. The obtained results vanish at low temperatures. The reason for the vanishing is that this term does not allow the introduced electron to leave the dot; the charge of the dot at the moment of tunneling suddenly changes by $+e$ and all the other electrons have to redistribute themselves to accommodate this charge. The logarithmic divergence of the imaginary time action corresponding to such evolution (orthogonality catastrophe) completely suppresses this contribution at $T\to 0$. Conversely, the second contribution, $\Pi_{\rm el}$ from Eq. (6.22c), contains the kernel $R(\tau)$, which promotes an electron from the tunneling contact to the channel. Because the very same tunneling electron is introduced to and then removed from the dot, there is no need in the redistribution of other electrons, so no orthogonality catastrophe occurs. As a result, the elastic contribution survives at $T\to 0$, analogously to the elastic cotunneling contribution for the weak coupling regime.

In what follows, we will be interested in the low-temperature behavior of the system, so we will retain elastic contribution (6.22c) only. Similarly to Sec. IV results for electrons with spin and spinless electrons differ significantly, and we will consider those two cases separately.

B. Spinless electrons

We follow the lines of Sec. IV A in the bosonization of the chiral fermionic fields. In order to account for the appearance of the operator $\hat{n}$ in the Hamiltonian [compare Eqs. (3.15) with Eq. (6.23)], we change slightly the transformation (4.9):

$$\begin{aligned}\hat{\varphi}_L(x)&=\frac{\hat{\varphi}_+(x)+\hat{\varphi}_-(x)+\hat{\Phi}}{\sqrt{2}}-\pi\mathcal{N}+\pi\hat{n},\\ \hat{\varphi}_R(x)&=\frac{\hat{\varphi}_+(-x)-\hat{\varphi}_-(-x)-\hat{\Phi}}{\sqrt{2}}-\pi\mathcal{N}+\pi\hat{n},\end{aligned} \tag{6.24}$$

where operator $\hat{n}$ commutes with the bosonic fields $\hat{\varphi}_\pm,\hat{\Phi}$. In order to preserve the commutation relation $[\hat{F}^\dagger,\hat{\varphi}_{L,R}]=0$, we change the operator $\hat{F}^\dagger$ as

$$\hat{F}^\dagger\mapsto\hat{F}^\dagger e^{-i\sqrt{2}\hat{\Phi}},\quad \hat{F}\mapsto\hat{F}e^{i\sqrt{2}\hat{\Phi}}, \tag{6.25}$$

The fact that $\hat{F}^\dagger$ commutes with bosonic fields $\hat{\varphi}_{L,R}$ is obvious from Eqs. (6.15) and Eq. (4.8d).

Substitution of Eqs. (4.1), (6.24), and (6.25) into Eqs. (6.22b) yields

$$\Pi_{\rm in}(\tau)=-\frac{\mathcal{G}(-\tau;\mathbf{r}_t,\mathbf{r}_t)}{\nu\langle T_\tau e^{-\hat{S}}\rangle}\langle T_\tau e^{-\hat{S}}\hat{\bar{F}}(\tau)\hat{F}(0)e^{i\sqrt{2}[\hat{\Phi}(0)-\hat{\Phi}(\tau)]}\rangle \tag{6.26a}$$

for the inelastic part of the cotunneling; see also Ref. 27. For the elastic contribution, we find

$$\begin{aligned}\Pi_{\rm el}(\tau)=&\frac{2}{\pi\nu\lambda\langle T_\tau e^{-\hat{S}}\rangle}\int_0^\beta d\tau_1 d\tau_2 R(\tau_1-\tau)R^*(-\tau_2)\\ &\times\left\langle T_\tau e^{-\hat{S}}\hat{\bar{F}}(\tau)\hat{F}(0)e^{(i/\sqrt{2})[2\hat{\Phi}(0)-2\hat{\Phi}(\tau)+\hat{\Phi}(\tau_1)-\hat{\Phi}(\tau_2)]}\hat{\eta}(\tau_1)\hat{\eta}(\tau_2)(-1)^{\hat{n}(\tau_1)+\hat{n}(\tau_2)}\right.\\ &\left.\times\exp\left[i\frac{\hat{\varphi}_-(\tau_1)-\hat{\varphi}_-(\tau_2)}{\sqrt{2}}\right]\prod_{i=1}^{2}\cos\left[\frac{\hat{\varphi}_+(\tau_i)}{\sqrt{2}}+\frac{\pi}{4}-\pi\mathcal{N}\right]\right\rangle.\end{aligned} \tag{6.26b}$$

Averaging in Eqs. (6.26) is performed over the Hamiltonian given by Eq. (4.10), finite backscattering is described by (4.11), and action (4.12) is modified as

$$\hat{S}=\frac{1}{2\pi\lambda}\int_0^\beta d\tau_1 d\tau_2 L(\tau_1-\tau_2)\hat{\eta}(\tau_1)\hat{\eta}(\tau_2)(-1)^{\hat{n}(\tau_1)+\hat{n}(\tau_2)}\exp\left[i\frac{\hat{\varphi}_-(\tau_1)-\hat{\varphi}_-(\tau_2)}{\sqrt{2}}\right]\exp\left[i\frac{\hat{\Phi}(\tau_1)-\hat{\Phi}(\tau_2)}{\sqrt{2}}\right]$$
$$\times\cos\left[\frac{\hat{\varphi}_+(\tau_1)}{\sqrt{2}}+\frac{\pi}{4}-\pi\mathcal{N}\right]\cos\left[\frac{\hat{\varphi}_+(\tau_2)}{\sqrt{2}}+\frac{\pi}{4}-\pi\mathcal{N}\right].$$

We will consider only the elastic contribution (6.26b) because it does not vanish at low temperatures.

1. Reflectionless contact

In the lowest in Δ/E_C approximation we can neglect action $\hat{S}$ in Eq. (6.26b) completely. Then averaging over bosonic fields can be performed with the help of Eqs. (4.13) and (4.14), average of the product Majorana fermions operator is given by Eq. (4.7), and the relevant correlation function of the operators $\hat{n},\hat{F},\hat{F}^\dagger$ is given by

$$\langle T_\tau\hat{F}(\tau)\hat{F}(0)(-1)^{\hat{n}(\tau_1)+\hat{n}(\tau_2)}\rangle=\mathrm{sgn}(\tau-\tau_1)\mathrm{sgn}(\tau-\tau_2). \tag{6.27}$$

Equation (6.27) follows from Eq. (6.15) and from the fact that operators $\hat{n},\hat{F}$ commute with Hamiltonian (4.11) and thus do not have their own dynamics. We obtain

$$\Pi_{\mathrm{el}}(\tau)=\frac{2\pi|K(\tau)|^2}{\nu v_F E_C^2 e^{2\mathbf{C}}}\int_0^\beta d\tau_1 d\tau_2 R(\tau_1-\tau)R^*(-\tau_2)$$
$$\times\left[\frac{\pi T}{\sin\,\pi T(\tau_1-\tau_2)}\frac{K(\tau_2)K(\tau_1-\tau)}{K(\tau_1)K(\tau_2-\tau)}+e^{i2\pi\mathcal{N}}K(\tau_1-\tau_2)\frac{K(-\tau_2)K(\tau_1-\tau)}{K(\tau_1)K(\tau-\tau_2)}+\mathrm{c.c.}\right], \tag{6.28}$$

where function $K(\tau)$ is defined by Eq. (4.16b), and $\mathbf{C}$ is the Euler constant.

Before performing the analytic continuation [see Eq. (6.14)] we have to transform integrals over imaginary times in Eq. (6.28) to the integrals over real time. In order to do so, we use Lehmann representation (3.20) for the kernel $R(\tau)$:

$$\Pi_{\mathrm{el}}(\tau)=\frac{2\pi|K(\tau)|^2}{\nu v_F E_C^2 e^{2\mathbf{C}}}\int\frac{dt_1}{2\pi}\int\frac{dt_2}{2\pi}[R^R(t_1)-R^A(t_1)][R^R(t_2)-R^A(t_2)]^*$$
$$\times\int_0^\beta d\tau_1 d\tau_2\frac{\pi^2T^2}{\sinh[\pi T(t_1+i\tau_1-i\tau)]\sinh[\pi T(t_2+i\tau_2)]}\left[\frac{\pi T}{\sin\,\pi T(\tau_1-\tau_2)}\frac{K(\tau_2)K(\tau_1-\tau)}{K(\tau_1)K(\tau_2-\tau)}\right.$$
$$\left.+e^{i2\pi\mathcal{N}}K(\tau_1-\tau_2)\frac{K(-\tau_2)K(\tau_1-\tau)}{K(\tau_1)K(\tau-\tau_2)}+\mathrm{c.c.}\right]. \tag{6.29}$$

Integration can be now performed in a manner similar to Sec.V A. Using the fact that function $K(\tau_1)$ is analytical within the lower complex semiplane Im $\tau_1<0$, we deform the contour of integration as shown in Fig. 7.

Because of the periodicity of the integrand, the integrals over the parts of the contour running parallel to the imaginary axis cancel out. As the result, only the pole contribution at $\tau_1=it_1+\tau$ remains at $t_1<0$. At $t_1>0$ the pole contribution disappears. Analogously, the complex conjugated terms are contributed by pole $\tau_1=it_1+\tau$ at $t_1>0$. As a result, we obtain from Eq. (6.29)

$$\Pi_{\mathrm{el}}(\tau)=\frac{2\pi|K(\tau)|^2}{\nu v_F E_C^2 e^{2\mathbf{C}}}\int\frac{dt_1dt_2}{2\pi}[R^R(t_2)-R^A(t_2)]^*\int_0^\beta d\tau_2\frac{\pi T}{\sinh[\pi T(t_2-i\tau_2)]}$$
$$\times\left[\frac{\pi T}{\sin\,\pi T(\tau-\tau_2+it_1)}\left(\frac{R^A(t_1)K(\tau_2)K(it_1)}{K(it_1+\tau)K(\tau_2-\tau)}+\frac{R^R(t_1)K(-\tau_2)K(-it_1)}{K(-it_1-\tau)K(\tau-\tau_2)}\right)\right.$$
$$\left.+e^{i2\pi\mathcal{N}}K(\tau-\tau_2+it_1)\frac{R^A(t_1)K(-\tau_2)K(it_1)}{K(it_1+\tau)K(\tau-\tau_2)}-e^{-i2\pi\mathcal{N}}K(\tau_2-\tau-it_1)\frac{R^R(t_1)K(\tau_2)K(-it_1)}{K(-it_1-\tau)K(\tau_2-\tau)}\right], \tag{6.30}$$

where we wrote explicit expressions for all the terms. Integration over τ_2 can be now easily performed by deformation of the integration contours shown in Fig. 8, and we obtain

$$\Pi_{\rm el}(\tau)=\frac{2\pi|K(\tau)|^2}{\nu v_F E_C^2 e^{2\mathbf{C}}}\int dt_1 dt_2[R^R(t_1)[R^R(t_2)]^*+R^A(t_1)[R^A(t_2)]^*]\frac{\pi T}{\sin[\pi T(it_2-it_1-\tau)]}-\frac{2\pi|K(\tau)|^2}{\nu v_F E_C^2 e^{2\mathbf{C}}}$$
$$\times\int dt_1 dt_2\Bigg[\frac{\pi T}{\sin\pi T(\tau-it_2+it_1)}\left(\frac{R^A(t_1)[R^A(t_2)]^*K(it_2)K(it_1)}{K(it_1+\tau)K(it_2-\tau)}+\frac{R^R(t_1)[R^R(t_2)]^*K(-it_2)K(-it_1)}{K(-it_1-\tau)K(\tau-it_2)}\right)$$
$$+e^{i2\pi\mathcal{N}}K(\tau-it_2+it_1)\frac{R^A(t_1)[R^R(t_2)]^*K(-it_2)K(it_1)}{K(it_1+\tau)K(\tau-it_2)}$$
$$-e^{-i2\pi\mathcal{N}}K(it_2-it_1-\tau)\frac{R^R(t_1)[R^A(t_2)]^*K(it_2)K(-it_1)}{K(-it_1-\tau)K(it_2-\tau)}\Bigg]. \tag{6.31}$$

One can see from Eq. (6.31) that function $\Pi_{\rm el}(\tau)$ is indeed analytic in the strip $0<\mathrm{Re}\,\tau<\beta$, which justifies the steps leading to Eq. (6.14).

Finally, we substitute Eq. (6.31) into Eq. (6.14). For small temperatures $T\ll E_C$, we have from Eq. (4.16b) $K(\beta/2+it)=\pi T/\cosh\pi Tt$. As a result, the first term in Eq. (6.31) produces a contribution $\propto T^2$ and can be neglected. The remainder can be recast into the formula

$$G=\frac{2\pi G_R}{\nu v_F E_C^2 e^{2\mathbf{C}}}\left|\int_{-\infty}^{0}dt\,K(it)[R^A(t)e^{i2\pi\mathcal{N}}+R^R(-t)]\right|^2, \tag{6.32}$$

which gives nonaveraged conductance of the dot. Here we used the fact that the characteristic scale of the integration over $t_1,t_2\simeq 1/E_C$ is much smaller than β. Equation (6.32) is reminiscent of the Landauer formula. However, the form factor $K(it)$ entering into this formula indicates that a large number of states in the dot participate in the transport, unlike the case of noninteracting electrons.

Now, we are prepared to study the statistics of the conductance. Using the explicit expression (4.16b) for function K and formula (6.21b), we find the average conductance

$$\overline{G}=G_R\frac{2\Delta}{E_C}e^{-2\mathbf{C}}\Lambda(0), \tag{6.33}$$

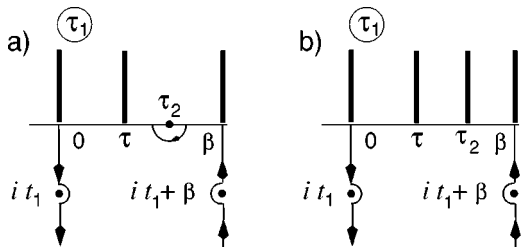

FIG. 7. The integration contour used in the evaluation of the conductance in the spinless case, for the first (a) and the second term (b) in Eq. (6.29). Branch cuts of the integrand are shown by thick lines. Contribution of the semipole at $\tau_1=\tau_2$ in the first term in brackets in Eq. (6.29) is canceled by the term complex conjugated to it.

where $\mathbf{C}\approx 0.577$ is the Euler constant, and $\Lambda(0)\approx 1.398$ is given by Eq. (5.6). This expression is analogous to the elastic cotunneling for the case of weak coupling.[10,11]

For the correlation function of the mesoscopic fluctuations of the conductance, we find with the help of Eqs. (6.21)

$$\frac{\overline{\delta G(1)\delta G(2)}}{\overline{G}^2}=\left(\frac{\cos\pi n}{\Lambda(0)}\right)^2\left[\Lambda^2\left(\frac{H_-^2}{H_c^2}\right)+\Lambda^2\left(\frac{H_+^2}{H_c^2}\right)\right], \tag{6.34}$$

where we use again the shorthand notations $i\equiv\mathcal{N}_i,H_i$, $n=\mathcal{N}_1-\mathcal{N}_2$, and $H_\pm=H_1\pm H_2$. Correlation magnetic field H_c is defined in Eq. (2.23), and the dimensionless function $\Lambda(x)$ is given by Eq. (5.6) and is plotted in Fig. 4. Once again, we see that even though the averaged conductance does not any longer oscillate with the gate voltage, the discreteness of charge manifests itself in the oscillatory behavior of the conductance correlation function. It is also noteworthy that the mesoscopic conductance fluctuations are of the order of the average, similarly to the weak coupling regime.[11]

2. Finite reflection in the contact

So far, we have shown that the conductance in the tunneling setup is nonvanishing at $T\to 0$, which is analogous to the elastic cotunneling in the weak tunneling regime. However, the oscillatory dependence of the conductance showed up not in the average conductance but rather in the correlation function of mesoscopic fluctuations. On the other hand, as we saw in Sec. V finite backscattering leads to the oscillatory dependence in the averaged quantities. The purpose of this subsection is to study how the finite reflection in the contact

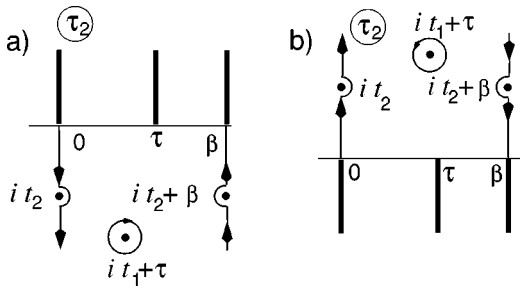

FIG. 8. The integration contours used in the evaluation of the integral over τ_2 in Eq. (6.30) for (a) the first and third terms in brackets, and (b) for the second and fourth term. Only first and second terms have poles at $\tau_2=\tau+it_1$.

affects the elastic cotunneling, and to demonstrate that it indeed leads to the oscillatory dependence of the averaged conductance on the gate voltage.

To treat the finite reflection in the contact, we have to expand the denominator and numerator in Eq. (6.26b) up to the first order in the backscattering Hamiltonian (4.11). Performing averaging over the bosonic fields, we obtain with the help of Eqs. (4.14), (4.8), (6.27), and (4.16b):

$$\Pi_{\rm el}(\tau)=-|r|\frac{|K(\tau)|^2}{2\pi\nu v_F E_C e^{\mathbf{C}}}\int_0^\beta d\tau_1 d\tau_2 d\tau_3 R(\tau_1-\tau)R^*(-\tau_2)\frac{\pi T}{\sin\,\pi T(\tau_1-\tau_2)}$$
$$\times\left[\frac{K(\tau_2)K(\tau_1-\tau)}{K(\tau_1)K(\tau_2-\tau)}\left\{\frac{e^{-i2\pi\mathcal{N}}K(\tau_3)K(\tau-\tau_3)}{K(-\tau_3)K(\tau_3-\tau)}\frac{\sin\,\pi T(\tau_2-\tau_3)K(\tau_2-\tau_3)}{\sin\,\pi T(\tau_1-\tau_3)K(\tau_1-\tau_3)}\right.\right.$$
$$\left.\left.+\frac{e^{i2\pi\mathcal{N}}K(-\tau_3)K(\tau_3-\tau)}{K(\tau_3)K(\tau-\tau_3)}\frac{\sin\,\pi T(\tau_1-\tau_3)K(\tau_1-\tau_3)}{\sin\,\pi T(\tau_2-\tau_3)K(\tau_2-\tau_3)}-2\cos 2\pi\mathcal{N}\right\}+\text{c.c.}\right]. \tag{6.35}$$

Here we retained only the terms that do not vanish after ensemble averaging. Then, we can use the Lehmann representation for the kernel $R(\tau)$ and perform the integration over $\tau_{1,2}$ in the manner of the previous subsection. It yields

$$\Pi_{\rm el}(\tau)=-|r|\frac{|K(\tau)|^2}{2\pi\nu v_F E_C e^{\mathbf{C}}}\int dt_1 dt_2\int_0^\beta d\tau_3\frac{\pi T}{\sin\,\pi T(\tau-it_2+it_1)}\left[\frac{R^A(t_1)[R^A(t_2)]^*K(it_2)K(it_1)}{K(it_1+\tau)K(it_2-\tau)}\right. \tag{6.36}$$
$$\times\left\{\frac{e^{-i2\pi\mathcal{N}}K(\tau_3)K(\tau-\tau_3)}{K(-\tau_3)K(\tau_3-\tau)}\frac{\sin\,\pi T(it_2-\tau_3)K(it_2-\tau_3)}{\sin\,\pi T(\tau+it_1-\tau_3)K(\tau+it_1-\tau_3)}\right.$$
$$\left.\left.+\frac{e^{i2\pi\mathcal{N}}K(-\tau_3)K(\tau_3-\tau)}{K(\tau_3)K(\tau-\tau_3)}\frac{\sin\,\pi T(\tau+it_1-\tau_3)K(\tau+it_1-\tau_3)}{\sin\,\pi T(it_2-\tau_3)K(it_2-\tau_3)}-2\cos 2\pi\mathcal{N}\right\}+\text{c.c.}\right]. \tag{6.37}$$

We deform the integration contour over τ_3, as shown in Fig. 9, and substitute the result into Eq. (6.14). Then, we average the product of the Green functions $R^A[R^A]^*$ using Eq. (6.21b). As a result, we find the oscillating part of the ensemble averaged conductance

$$G=\alpha_1 G_R\left(\frac{|r|\Delta}{E_C}\right)\cos 2\pi\mathcal{N}. \tag{6.38}$$

Here α_1 is the numerical coefficient given by

$$\alpha_1=\frac{4e^{-\mathbf{C}}}{\pi}\int_0^\infty\frac{dxdy}{x^2}e^{2e^x Ei(-x)}\sin(\pi e^{-y})$$
$$\times\sinh[e^{-y}Ei(y)+e^{x+y}Ei(-x-y)-e^y Ei(-y)]$$
$$\approx 1.458,$$

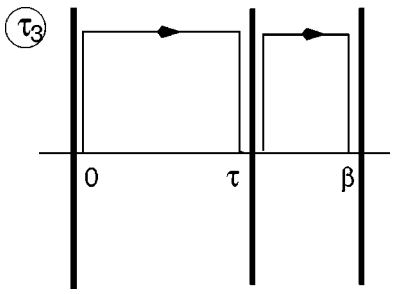

FIG. 9. The integration contour used in the evaluation of the integral over τ_3 in Eq. (6.36). Integral along the part of the contour parallel to the real axis cancels out the $2\cos 2\pi\mathcal{N}$ term.

with $Ei(x)$ being the exponential-integral function.[40]

Equation (6.38) confirms our expectation that the finite backscattering leads to the oscillatory dependence of the averaged conductance on the gate voltage. Although the amplitude of oscillations (6.38) is small compared to the average value of the conductance (6.33), it still exceeds at low temperatures the contribution of the inelastic cotunneling[27] to the conductance oscillations.

C. Electrons with spin

We use formulas of Sec. IV B to bosonize the chiral fermionic fields. In order to account for the appearance of the operator $\hat{n}$ in the Hamiltonian [compare Eqs. (3.15) with Eq. (6.23)], we change the transformation (4.19):

$$\hat{\varphi}_L^i(x)=\frac{\hat{\varphi}_+^i(x)+\hat{\varphi}_-^i(x)+\hat{\Phi}^i-\delta_{i\rho}\pi(\mathcal{N}-\hat{n})}{\sqrt{2}},$$
$$\hat{\varphi}_R^i(x)=\frac{\hat{\varphi}_+^i(-x)-\hat{\varphi}_-^i(-x)-\hat{\Phi}^i-\delta_{i\rho}\pi(\mathcal{N}-\hat{n})}{\sqrt{2}}, \tag{6.39}$$

where $i=\rho,\sigma$, and operator $\hat{n}$ commutes with the bosonic fields $\hat{\varphi}_\pm^{\rho,\sigma},\hat{\Phi}^{\rho,\sigma}$. To preserve the commutation relation $[\hat{F}^\dagger,\hat{\varphi}_{L,R}^{\rho,\sigma}]=0$, we change the operators $\hat{F}^\dagger,\hat{F}$ similarly to Eq. (6.25)

$$\hat{F}^\dagger\mapsto\hat{F}^\dagger e^{-i\hat{\Phi}^\rho},\quad \hat{F}\mapsto\hat{F}e^{i\hat{\Phi}^\rho}. \tag{6.40}$$

Substitution of Eqs. (4.17), (6.39), and (6.40) into Eqs. (6.22b) results in the formulas similar to Eq. (6.26):

$$\Pi_{\rm in}(\tau)=-\frac{2\mathcal{G}(-\tau;\mathbf{r}_t,\mathbf{r}_t)}{\nu\langle T_\tau e^{-\hat{S}}\rangle}\langle T_\tau e^{-\hat{S}}\hat{\tilde{F}}(\tau)\hat{F}(0)e^{i[\hat{\Phi}(0)-\hat{\Phi}(\tau)]}\rangle, \tag{6.41a}$$

$$\begin{aligned}\Pi_{\rm el}(\tau)=&\frac{1}{\pi\nu\lambda\langle T_\tau e^{-\hat{S}}\rangle}\int_0^\beta d\tau_1 d\tau_2 R(\tau_1-\tau)R^*(-\tau_2)\sum_{\alpha=\pm1}\Big\langle T_\tau e^{-\hat{S}}\hat{\tilde{F}}(\tau)\hat{F}(0)\,\hat{\eta}_\alpha(\tau_1)\,\hat{\eta}_\alpha(\tau_2)e^{i[\hat{\Phi}^\rho(0)-\hat{\Phi}^\rho(\tau)]}\\
&\times e^{(i/2)\alpha[\hat{\varphi}^\sigma_-(\tau_1)-\hat{\varphi}^\sigma_-(\tau_2)]}e^{(i/2)\alpha[\hat{\Phi}^\sigma(\tau_1)-\hat{\Phi}^\sigma(\tau_2)]}e^{(i/2)[\hat{\varphi}^\rho_-(\tau_1)-\hat{\varphi}^\rho_-(\tau_2)]}e^{(i/2)[\hat{\Phi}^\rho(\tau_1)-\hat{\Phi}^\rho(\tau_2)]}\\
&\times\Big\{\sin\Big[\frac{\hat{\varphi}^\rho_+(\tau_1)-\hat{\varphi}^\rho_+(\tau_2)}{2}+\alpha\frac{\hat{\varphi}^\sigma_+(\tau_1)-\hat{\varphi}^\sigma_+(\tau_2)}{2}+\frac{\pi}{2}[\hat{n}(\tau_1)-\hat{n}(\tau_2)]\Big]\\
&-\cos\Big[\frac{\hat{\varphi}^\rho_+(\tau_1)+\hat{\varphi}^\rho_+(\tau_2)}{2}+\alpha\frac{\hat{\varphi}^\sigma_+(\tau_1)+\hat{\varphi}^\sigma_+(\tau_2)}{2}+\frac{\pi}{2}[\hat{n}(\tau_1)+\hat{n}(\tau_2)]-\pi\mathcal{N}\Big]\Big\}\Big\rangle,\end{aligned} \tag{6.41b}$$

for the inelastic and the elastic cotunneling, respectively. However, for the calculation it is more convenient to proceed directly to the low-energy effective theory (4.28), because the main contribution to the conductance comes from the energy scale smaller than the charging energy E_C. First, we integrate out the symmetric charge mode $\hat{\varphi}^\rho_+$. Then, we wish to use the substitution (4.26). The important difference brought into the problem by accounting for the second junction is that Eqs. (6.41) contain the charged field $\hat{\Phi}^\rho$ itself, and not only the combination $\hat{\Phi}^\rho-\phi^\rho_-(x=0)$, as we had before. Fortunately, the corresponding change can be simply accounted for by the introduction of one more chiral field $\hat{\phi}$, so that we have

$$\begin{aligned}&\hat{\varphi}^\rho_-(x=0)+\hat{\Phi}^\rho\to\sqrt{2}\,\hat{\varphi}_\rho(x=0),\\
&\hat{\Phi}^\rho-\hat{\varphi}^\rho_-(x=0)\to\sqrt{2}\,\hat{\phi}(x=0)\end{aligned} \tag{6.42}$$

instead of Eq. (4.26). The field $\hat{\phi}$ enters neither the effective action, nor the backscattering Hamiltonian, so it can be immediately integrated out, and we find the low-energy representation

$$e^{i[\hat{\Phi}(\tau)-\hat{\Phi}(0)]}\mapsto\langle e^{i[\hat{\phi}(\tau)-\hat{\phi}(0)]/\sqrt{2}}\rangle e^{i[\hat{\varphi}^\rho(\tau)-\hat{\varphi}^\rho(0)]/\sqrt{2}}=\frac{\pi}{E_C e^{\mathbf{C}}}\sqrt{\frac{v_F}{\tilde{\lambda}}}\Big(\frac{\pi T}{\sin\,\pi T\tau}\Big)^{1/2}e^{i[\hat{\varphi}^\rho(\tau)-\hat{\varphi}^\rho(0)]/\sqrt{2}}. \tag{6.43}$$

The prefactor in the last formula can be found by requiring the averages calculated with the help of the effective theory and the initial theory to coincide. Using Eqs. (6.42) and (6.43), we obtain from Eq. (6.41)

$$\Pi_{\rm in}(\tau)=-\frac{2\mathcal{G}(-\tau;\mathbf{r}_t,\mathbf{r}_t)}{\nu\langle T_\tau e^{-\hat{S}}\rangle}\frac{\pi}{E_C e^{\mathbf{C}}}\sqrt{\frac{v_F}{\tilde{\lambda}}}\Big(\frac{\pi T}{\sin\,\pi T\tau}\Big)^{1/2}\langle T_\tau e^{-\hat{S}}\hat{\tilde{F}}(\tau)\hat{F}(0)e^{i[\hat{\varphi}^\rho(\tau)-\hat{\varphi}^\rho(0)]/\sqrt{2}}\rangle, \tag{6.44a}$$

$$\begin{aligned}\Pi_{\rm el}(\tau)=&\frac{1}{\pi\nu\langle T_\tau e^{-\hat{S}}\rangle}\frac{\pi}{E_C e^{\mathbf{C}}}\sqrt{\frac{v_F}{\tilde{\lambda}^3}}\Big(\frac{\pi T}{\sin\,\pi T\tau}\Big)^{1/2}\int_0^\beta d\tau_1 d\tau_2 R(\tau_1-\tau)R^*(-\tau_2)\sum_{\alpha=\pm1}\Big\langle T_\tau e^{-\hat{S}}\hat{\tilde{F}}(\tau)\hat{F}(0)\\
&\times\hat{\eta}_\alpha(\tau_1)\,\hat{\eta}_\alpha(\tau_2)e^{i[\hat{\varphi}^\rho(\tau)-\hat{\varphi}^\rho(0)]/\sqrt{2}}e^{(i/2)\alpha[\hat{\varphi}^\sigma_-(\tau_1)-\hat{\varphi}^\sigma_-(\tau_2)]}e^{(i/2)\alpha[\hat{\Phi}^\sigma(\tau_1)-\hat{\Phi}^\sigma(\tau_2)]}\\
&\times\Big\{\cos\Big[\alpha\frac{\hat{\varphi}^\sigma_+(\tau_1)+\hat{\varphi}^\sigma_+(\tau_2)}{2}+\frac{\pi}{2}[\hat{n}(\tau_1)+\hat{n}(\tau_2)]-\pi\mathcal{N}\Big]\\
&+\cos\Big[\frac{\pi}{4}+\alpha\frac{\hat{\varphi}^\sigma_+(\tau_1)-\hat{\varphi}^\sigma_+(\tau_2)}{2}+\frac{\pi}{2}[\hat{n}(\tau_1)-\hat{n}(\tau_2)]\Big]\Big\}\Big\rangle,\end{aligned} \tag{6.44b}$$

where the averaging is performed with respect to the Hamiltonian (4.27). The effective action (4.29) acquires the form

$$\hat{S}=\frac{1}{\pi\widetilde{\lambda}}\int_0^\beta d\tau_1 d\tau_2 L(\tau_1-\tau_2)\sum_{\alpha=\pm1}\hat{\eta}_\alpha(\tau_1)\hat{\eta}_\alpha(\tau_2)e^{(i/2)\alpha[\hat{\varphi}_-^\sigma(\tau_1)-\hat{\varphi}_-^\sigma(\tau_2)]}e^{(i/2)\alpha[\hat{\Phi}^\sigma(\tau_1)-\hat{\Phi}^\sigma(\tau_2)]}e^{(i/\sqrt{2})[\hat{\varphi}_\rho(\tau_1)-\hat{\varphi}_\rho(\tau_2)]}$$
$$\times\left\{\cos\left[\alpha\frac{\hat{\varphi}_+^\sigma(\tau_1)+\hat{\varphi}_+^\sigma(\tau_2)}{2}+\frac{\pi}{2}[\hat{n}(\tau_1)+\hat{n}(\tau_2)]-\pi\mathcal{N}\right]+\cos\left[\frac{\pi}{4}+\alpha\frac{\hat{\varphi}_+^\sigma(\tau_1)-\hat{\varphi}_+^\sigma(\tau_2)}{2}+\frac{\pi}{2}[\hat{n}(\tau_1)-\hat{n}(\tau_2)]\right]\right\},\tag{6.45}$$

and the backscattering Hamiltonian $\hat{H}_{\rm bs}$ is given by[27]

$$\hat{H}_{\rm bs}=\frac{2|r|}{\pi}\left(\frac{E_C e^{\mathbf{C}} v_F}{\pi\widetilde{\lambda}}\right)^{1/2}(-1)^{\hat{n}}\cos\pi\mathcal{N}\cos\hat{\varphi}_+^\sigma(0),\tag{6.46}$$

cf. Eq. (4.28). The cutoff $\widetilde{\lambda}$ in Eqs. (6.43)–(6.46) should be of the order of v_F/E_C, because the charging energy E_C is the largest energy scale that can be considered with the help of Hamiltonian (4.27).

In the following subsections we will apply effective description (6.44)–(6.46) and (6.14) to find the tunneling conductance of the dot in the asymmetric setup.

1. Reflectionless contact

Let us consider first the elastic contribution (6.44b) (we will see below that inelastic contribution should be taken into account in order to obtain the correct temperature dependence). In the lowest-order approximation we neglect the action $\hat{S}$, and obtain with the help of Eqs. (4.30):

$$\Pi_{\rm el}^{(0)}(\tau)=\frac{1}{\nu v_F E_C e^{\mathbf{C}}}\frac{\pi T}{\sin\pi T\tau}\int_0^\beta d\tau_1 d\tau_2$$
$$\times R(\tau_1-\tau)R^*(-\tau_2)\frac{\pi T}{\sin\pi T(\tau_1-\tau_2)}$$
$$\times\sum_{\gamma=\pm1}\left(\frac{\sin\pi T\tau_1\sin\pi T(\tau_2-\tau+i\gamma 0)}{\sin\pi T\tau_2\sin\pi T(\tau_1-\tau+i\gamma 0)}\right)^{1/2}.\tag{6.47}$$

When deriving Eq. (6.47), we used an expression similar to Eq. (6.27),

$$\left\langle T_\tau\hat{\bar{F}}(\tau)\hat{F}(0)\cos\left[\frac{\pi}{2}(\hat{n}(\tau_1)-\hat{n}(\tau_2))\right]\right\rangle$$
$$=\cos\left[\frac{\pi}{2}[\theta(\tau-\tau_1)-\theta(\tau-\tau_2)]\right].\tag{6.48}$$

All the further manipulations with Eq. (6.47) are absolutely analogous to the steps of Sec. VI A in the derivation of Eq. (6.32) from Eq. (6.28). Instead of Eq. (6.32), here we find

$$G=\frac{G_R}{\nu v_F E_C e^{\mathbf{C}}}\int_{E_C^{-1}}^\infty dt_1 dt_2\frac{\pi T}{(\sinh\pi T t_1\sinh\pi T t_1)^{1/2}}$$
$$\times\{R^A(-t_1)[R^A(-t_2)]^*+R^R(t_1)[R^R(t_2)]^*\},\tag{6.49}$$

where the divergences (as we will see, logarithmic) should be cut off at times of the order of $1/E_C$. Notice that there is no $\mathcal{N}$ dependence of the nonaveraged conductance. The reason is similar to the absence of the oscillations of the capacitance in the first order in level spacing Δ—the oscillations are washed out by the quantum fluctuations of the spin mode, which is not pinned. We will see later that the oscillatory term in the conductance is smaller than the leading nonoscillatory contribution to the conductance by a factor $\simeq(\Delta/T)^{1/2}$.

Let us now proceed with the statistics of the elastic cotunneling conductance (6.49). Ensemble averaging performed with the help of Eq. (6.21a) gives for the average conductance

$$\bar{G}=G_R\frac{2\Delta e^{-\mathbf{C}}}{E_C}\ln\left(\frac{E_C}{T}\right),\tag{6.50}$$

where $\mathbf{C}\approx0.577$ is the Euler constant. At very low temperatures, T should be substituted by $\Delta\ \ln(E_C/\Delta)$, see discussion in Sec. V B.

Equation (6.50) deserves some discussion. Firstly, we notice the presence of the large logarithmic factor in comparison with Eq. (6.33). It can be understood using the arguments of the orthogonality catastrophe[46] similar to those applied in Ref. 27 for the inelastic cotunneling. Consider the elastic cotunneling process where an electron is introduced at time $t=0$, and then taken away at time $t\gtrsim E_C^{-1}$. Because the introduction of an electron costs extra energy $\simeq E_C$, all the other electrons tend to redistribute themselves by moving one electron charge through the left point contact, Fig 5. One can describe such a tendency as sudden change of the boundary condition in each of the spin channels. Because all the spin channels are symmetric, each spin mode should transfer charge $e/2$. According to the Friedel sum rule, it corresponds to the additional scattering phase shift $\delta=\pm\pi/2$ in each spin mode. It is known[47] that such a sudden change causes creation of a large number of electron-hole excitations, so that the resulting state is orthogonal to the ground-state. The probability for the system to retain its initial state during time t is $P(t)\simeq1/(tE_C)^\chi$, where the index χ is related to the phase shift in all channels, $\chi=\Sigma(\delta/\pi)^2$. In our case we have four spin modes (two in the dot and two in the reservoir), therefore $\chi=1$. In order to find the total conductance, we have to sum over all possible times that the electron spends in the dot: $G\propto\int_{E_C^{-1}}^\beta dt/(E_C t)$, which results in the logarithmic temperature dependence (6.50). The similar argument for the spinless electrons gives the phase shift $\delta=\pi$ in each

of the two channels. Thus, $\chi=2$, all the relevant dynamics occurs during the times smaller than $1/E_C$, and the divergent factor disappears.

Secondly, even though the elastic contribution is dominant in the value of the conductance, in order to find the temperature dependence, one has to take into account the inelastic contribution (6.44a), which yields[48]

$$G_{\rm in}=G_R\frac{\pi^3 T e^{-\mathbf{C}}}{2E_C}. \tag{6.51}$$

We see that this term has a stronger temperature dependence than Eq. (6.50) and, therefore, the resulting conductance $\overline{G}+G_{\rm in}$ always grows as the temperature increases.

Mesoscopic fluctuations of the contribution (6.49) to the conductance can be obtained with the help of Eq. (6.21),

$$\frac{\overline{\delta G(H_1)\,\delta G(H_2)}}{\overline{G}^2}=\frac{1}{2}\sum_{\gamma=\pm}\left(1-\frac{\ln\max(1;[H_\gamma/H_c^<]^2)}{\ln(E_C/T)}\right)^2. \tag{6.52}$$

Here the correlation field $H_c^<$ is defined by Eq. (5.16), and the field combinations $H_\pm=H_1\pm H_2$ are assumed to be much smaller than H_c [the charging correlation field H_c is given by Eq. (2.23)]. The correlation function of the conductance fluctuations starts to decrease fast, as $1/H_\pm^4$, only at fields $H_\pm\gtrsim H_c$. Similarly to the case of capacitance fluctuations discussed in the previous section, to obtain a representative statistics of the conductance, the magnetic field should be varied in a range wider than H_c.

Equation (6.52) shows that the amplitude of conductance fluctuations is of the order of its average value, as in the case of the spinless fermions. However, unlike Eq. (6.34), the correlation function (6.52) does not reveal any oscillations with the gate voltage $\mathcal{N}$.

In order to reveal this oscillatory dependence on $\mathcal{N}$, one has to expand $\Pi_{\rm el}(\tau)$ from Eq. (6.44b) up to the first order in action (6.45). The procedure of averaging over all the relevant operators is absolutely similar to the derivation of Eq. (6.47), and we obtain

$$\begin{aligned}\Pi_{\rm el}^{(1)}(\tau)=&-\frac{1}{\nu v_F^2 E_C e^{\mathbf{C}}}\frac{\pi T}{\sin\pi T\tau}\int_0^\beta d\tau_1\cdots d\tau_4 R(\tau_1-\tau)R^*(-\tau_2)L(\tau_3-\tau_4)\\&\times\sum_{\gamma=\pm1}e^{i2\pi\gamma\mathcal{N}}\left(\frac{\sin\pi T\tau_1\sin\pi T(\tau_2-\tau-i\gamma0)}{\sin\pi T\tau_2\sin\pi T(\tau_1-\tau+i\gamma0)}\frac{\sin\pi T(\tau_4-\tau-i\gamma0)\sin\pi T\tau_3}{\sin\pi T\tau_4\sin\pi T(\tau_3-\tau+i\gamma0)}\right)^{1/2}\\&\times\frac{\pi^2T^2}{[\sin\pi T(\tau_1-\tau_2+i\gamma0)\sin\pi T(\tau_3-\tau_4+i\gamma0)\sin\pi T(\tau_3-\tau_2+i\gamma0)\sin\pi T(\tau_1-\tau_4+i\gamma0)]^{1/2}}.\end{aligned} \tag{6.53}$$

Integration over imaginary times in Eq. (6.53) is rather straightforward, and technically very close to that in the Sec. VI B 2. Unlike Eq. (6.49), here the result for the nonaveraged conductance is $\mathcal{N}$ dependent. We obtain for the oscillating contribution:

$$G_{\rm osc}=\frac{G_R}{\nu v_F^2 E_C e^{\mathbf{C}}}\frac{\alpha_2}{(2\pi^2T)^{1/2}}\int_{E_C^{-1}}^\infty\left[\prod_{i=1}^3 dt_i\left(\frac{\pi T}{\sinh\pi T t_i}\right)^{1/2}\right]\{ie^{-i2\pi\mathcal{N}}R^R(t_1)[R^A(t_2)]^*L^R(t_3)+\text{c.c.}\}, \tag{6.54}$$

where α_2 is a numerical coefficient:

$$\alpha_2=\int_{-\infty}^\infty\frac{dx\,dy}{|\sinh y|^{1/2}(\cosh x)^{3/2}[\cosh(y-x)]^{1/2}}\approx11.31. \tag{6.55}$$

Ensemble averaging of Eq. (6.54) is then performed with the help of Eqs. (3.25) and (6.21), and the final result is

$$\begin{aligned}\frac{\overline{\delta G_{\rm osc}(1)\,\delta G_{\rm osc}(2)}}{G_R^2}&=\alpha_3\frac{\Delta}{T}\left(\frac{\Delta}{E_C}\right)^2\ln^3\left(\frac{E_C}{T}\right)\cos2\pi n(\Lambda_++\Lambda_-)(\Lambda_+^2+\Lambda_-^2),\\ \Lambda_\pm&=1-\frac{\ln\max(1;[H_\pm/H_c^<]^2)}{\ln(E_C/T)},\end{aligned} \tag{6.56}$$

where the shorthand notation for the conductance arguments is $i=\mathcal{N}_i,H_i$, $H_\pm=H_1\pm H_2$, $n=\mathcal{N}_1-\mathcal{N}_2$, correlation magnetic field $H_c^<$ is given by Eq. (5.16), and the numerical coefficient α_3 is given by $\alpha_3=\alpha_2^2e^{-2\mathbf{C}}/(2\pi^4)\approx0.207$.

The variance of the conductance fluctuations (6.56) in the unitary limit ($H\gtrsim H_c$) is suppressed by a factor of four compared to its zero-field value.

2. Finite reflection in the contact

For the spinless electrons, finite reflection leads to the oscillations in the averaged conductance already in the first order of perturbation theory in $r\ll1$. On the contrary, for the electrons with spin, backscattering leads only to the enhancement of the

TABLE I. The ensemble-averaged differential capacitance (Ref. 14) and the correlation function of the mesoscopic fluctuations in the Coulomb blockade regime; only the contributions oscillating with the gate voltage $\mathcal{N}$ are presented in this table. Here $|r|^2 \ll 1$ is the reflection coefficient in an almost open channel, and $\beta = 1,2$ for the orthogonal and unitary ensembles, respectively. For more details see Eqs. (5.7), (5.9), (5.17), and (5.22).

	$\overline{\delta C_{\rm diff}(\mathcal{N})}/C$	$\overline{\delta C_{\rm diff}(\mathcal{N}_1)\,\delta C_{\rm diff}(\mathcal{N}_2)}/C^2$
$s=0$	$3.56\lvert r\rvert \cos 2\pi\mathcal{N}$	$\frac{5.59}{\beta}\left(\frac{\Delta}{E_C}\right)\cos 2\pi(\mathcal{N}_1-\mathcal{N}_2)$
$s=1/2$	$4.53\lvert r\rvert^2 \cos 2\pi\mathcal{N} \ln\left(\frac{E_C}{T}\right)$	$\frac{0.54}{\beta}\left(\frac{\Delta}{E_C}\right)\ln^3\left(\frac{E_C}{T}\right)\left[\left(\frac{\Delta}{E_C}\right)\ln\left(\frac{E_C}{T}\right)+7.12\lvert r\rvert^2\right]\cos 2\pi(\mathcal{N}_1-\mathcal{N}_2)$

oscillating part of the correlation function of the mesoscopic fluctuations. In order to demonstrate this, we expand Eq. (6.44b) up to the first order in the backscattering Hamiltonian (6.46). We obtain

$$\Pi_{\rm el}^{(b)}(\tau) = -\frac{1}{\nu v_F E_C e^{\mathbf{C}}}\sqrt{\frac{E_C e^{\mathbf{C}}}{\pi}}\frac{\pi T}{\sin \pi T\tau}\int_0^\beta d\tau_1\cdots\tau_3 R(\tau_1-\tau)R^*(-\tau_2)\sum_{\gamma=\pm 1} e^{i2\pi\gamma\mathcal{N}} \times\left(\frac{\sin \pi T\tau_1 \sin \pi T(\tau_2-\tau-i\gamma 0)}{\sin \pi T\tau_2 \sin \pi T(\tau_1-\tau+i\gamma 0)}\right)^{1/2}\frac{(\pi T)^{3/2}}{[\sin \pi T(\tau_1-\tau_2+i\gamma 0)\sin \pi T(\tau_3-\tau_2+i\gamma 0)\sin \pi T(\tau_1-\tau_3+i\gamma 0)]^{1/2}}. \tag{6.57}$$

Performing the contour deformation for the integration over $\tau_{1,2}$, as we did before, and the analytic continuation (6.14), we find

$$G = \frac{G_R}{\pi\nu v_F E_C e^{\mathbf{C}}}\frac{\alpha_2|r|\sqrt{E_C e^{\mathbf{C}}}}{(2\pi^2 T)^{1/2}} \times\int_{E_C^{-1}}^\infty dt_1 dt_2 \frac{\pi T}{(\sinh \pi T t_1 \sinh \pi T t_2)^{1/2}} \times\{ie^{-i2\pi\mathcal{N}}R^R(t_1)[R^A(t_2)]^* + \text{c.c.}\}, \tag{6.58}$$

where the numerical coefficient α_2 is given by Eq. (6.55). Average of Eq. (6.58) obviously vanishes, and for the mesoscopic fluctuations we obtain with the help of Eqs. (6.21)

$$\frac{\overline{\delta G(1)\,\delta G(2)}}{G_R^2} = \alpha_4\frac{|r|^2\Delta^2}{E_C T}\ln^2\left(\frac{E_C}{T}\right)(\Lambda_+^2+\Lambda_-^2)\cos 2\pi n, \tag{6.59}$$

where we use the same shorthand notation as in Eq. (6.56). The numerical coefficient α_4 in Eq. (6.59) is given by $\alpha_4 = \alpha_2^2 e^{-\mathbf{C}}/\pi^4 \approx 0.737$.

Calculation of the contribution of the backscattering into the average conductance requires accounting of Eq. (6.46) in the second-order perturbation theory. On dimensional grounds we expect this contribution to be

$$\overline{G}_{\rm osc}(\mathcal{N}) \simeq G_R\frac{|r|^2\Delta}{T}\cos 2\pi\mathcal{N}.$$

The low-temperature power-law divergence in this formula and in Eq. (6.58) should be cut off at the energy[27] $\epsilon^* \simeq |r|^2 E_C \cos^2 \pi\mathcal{N}$. Calculation of the precise behavior of the conductance at $T \lesssim \epsilon^*$, which can be performed with the help of refermionization technique of Ref. 27 is beyond the scope of the present paper. However, the perturbation theory results indicate that the modulation of the conductance $\overline{G}_{\rm osc}(\mathcal{N})$ at low temperature should be of the order of the average conductance $\overline{G}$.

TABLE II. Conductance of the quantum dot in a strongly asymmetric setup, see Fig. 5, and the correlation function of its mesoscopic fluctuations, oscillating with gate voltage $\mathcal{N}$. Tunneling conductance G_R is much smaller than $e^2/(2\pi\hbar)$. For the detailed results, see Eqs. (6.33), (6.34), (6.38), (6.50)–(6.52), (6.56), and (6.59).

	$\overline{G(\mathcal{N})}/G_R$	$\overline{\delta G(\mathcal{N}_1)\,\delta G(\mathcal{N}_2)}/G_R^2$
$s=0$	$\frac{\Delta}{E_C}(0.63+1.46\lvert r\rvert\cos 2\pi\mathcal{N})$	$\frac{0.78}{\beta}\left(\frac{\Delta}{E_C}\right)^2\cos 2\pi(\mathcal{N}_1-\mathcal{N}_2)$
$s=1/2$	$\frac{1.12\Delta}{E_C}\left[\ln\left(\frac{E_C}{T}\right)+7.75\frac{T}{\Delta}+\mathcal{O}(\lvert r\rvert^2)\right]$	$\left(\frac{\Delta^2}{E_C T}\right)\ln^2\left(\frac{E_C}{T}\right)\left[\frac{0.83}{\beta^2}\left(\frac{\Delta}{E_C}\right)\ln\left(\frac{E_C}{T}\right)+\frac{1.48\lvert r\rvert^2}{\beta}\right]\cos 2\pi(\mathcal{N}_1-\mathcal{N}_2)$

VII. CONCLUSION

In this paper, we considered mesoscopic effects in the Coulomb blockade (CB) regime. The emphasis was put on the case when the quantum dot is connected to a lead by a perfectly transparent single-mode channel. We have demonstrated that the earlier conclusion that the CB vanishes under this condition[14] is only an approximation, which resulted from neglecting the electron trajectories returning to the channel after traversing the dot. We have shown that the CB persists, and its period is still determined by a single electron charge. However, CB oscillations in all the observable quantities acquire a random phase and therefore it is revealed in the correlation functions of mesoscopic fluctuations. We constructed an analytic, well-controlled theory describing those fluctuations.

Our results are substantially different from the known results in noninteracting models of mesoscopic systems. The correlated ground state involves all the one-electron wave functions in the energy strip of the order of the charging energy E_C. The number of states in this strip is large, $n \sim E_C/\Delta \gg 1$ (here Δ is the level spacing). Therefore, the amplitude of the differential capacitance fluctuations exceeds parametrically the estimate[17] obtained in the noninteracting model. The correlation magnetic flux for the mesoscopic fluctuations $\Phi = \Phi_0 \sqrt{E_T/E_C}$ is controlled by the energy scale E_C, rather than by level spacing Δ. The large number of states in the relevant energy strip leads to the robustness of the oscillatory dependence over about E_C/Δ peaks, which is yet another difference from a noninteracting model.

We obtained the closed analytic expression for some experimentally relevant characteristics. Final results are summarized in Table I for the thermodynamic quantities (differential capacitance of an almost open dot), and in Table II for the transport quantities (tunneling conductance of an almost open dot).

Up to now, only one experiment studying the effect of the opening of the channel on the Coulomb blockade was published.[49] It was found that at the quantized value of the channel conductance, the Coulomb blockade oscillations disappeared completely, in disagreement with our predictions. We attribute this finding to a relatively simple geometry of the dot,[49] allowing for an adiabatic (rather than chaotic) propagation of an electron through the entire confined region. Quantum chaos of electron states in dots of sufficiently complicated geometries was studied previously in the regimes of strong Coulomb blockade and of ballistic transport.[5–7,12] These dots have the right parameters for the observation of mesoscopic charge quantization. The first experiments on the dot conductance in a strongly asymmetric setup (considered above in Sec. VI) are under way now.[43]

ACKNOWLEDGMENTS

We are grateful to B.L. Altshuler, P.W. Brouwer, A.I. Larkin, and K.A. Matveev for useful discussions and to S.M. Cronenwett and C.M. Marcus for valuable information. Hospitality of the Aspen Center for Physics and of the International Centre for Theoretical Physics in Trieste is also acknowledged. The work at the University of Minnesota is supported by NSF Grants No. DMR-9423244 and No. DMR-9731756 .

APPENDIX A: DERIVATION OF EQ. (3.7)

Let us discretize the space in the direction along the channel axis. The fermionic Hamiltonian $\hat{H}_F$ acquires the form

$$\hat{H}_F = \int d\mathbf{r}_\perp \sum_n \frac{(\psi_n^\dagger - \psi_{n+1}^\dagger)(\psi_n - \psi_{n+1})}{2ma} + a\psi_n^\dagger \hat{H}_\perp \psi_n , \tag{A1}$$

where the transverse part of the motion is described by the operator

$$\hat{H}_\perp = -\frac{\nabla_{\mathbf{r}}^2}{2m} + U_n(\mathbf{r}) - \mu, \tag{A2}$$

and a is the discretization step. Fermionic operators in Eq. (A1) satisfy the anticommutation relation $\{\psi_n^\dagger(\mathbf{r})\psi_{n'}(\mathbf{r}')\} = a^{-1}\delta_{nn'}\delta(\mathbf{r}_\perp - \mathbf{r}_\perp')$. The continuous limit of $a \to 0$, which will be taken in the end of the calculation, corresponds to the usual Schrödinger equation. Let us separate the space into two regions; region ''1'' includes all the lattice sites with $n \leqslant 0$ and region ''2'' includes sites with $n > 0$. The terms entering into decomposition of the Hamiltonian [see also Eq. (3.6)], $\hat{H}_F = \hat{H}_1 + \hat{H}_2 + \hat{H}_{12}$, have the form

$$\hat{H}_1 = \int d\mathbf{r}_\perp \sum_{n<0} \left[\frac{(\psi_n^\dagger - \psi_{n+1}^\dagger)(\psi_n - \psi_{n+1})}{2ma} + a\psi_n^\dagger \left(\hat{H}_\perp + \frac{\delta_{0,n}}{2ma} \right) \psi_n \right], \tag{A3a}$$

$$\hat{H}_2 = \int d\mathbf{r}_\perp \sum_{n\geqslant 1} \left[\frac{(\psi_n^\dagger - \psi_{n+1}^\dagger)(\psi_n - \psi_{n+1})}{2ma} + a\psi_n^\dagger \left(\hat{H}_\perp + \frac{\delta_{1,n}}{2ma} \right) \psi_n \right], \tag{A3b}$$

$$\hat{H}_{12} = -\int d\mathbf{r}_\perp \frac{\psi_0^\dagger \psi_1 + \psi_1^\dagger \psi_0}{2ma}. \tag{A3c}$$

We obtain the average in Eq. (3.6) using Eq. (A3c):

$$\frac{1}{2}\langle T_\tau \hat{H}_{12}(\tau_1)\hat{H}(\tau_2)\rangle_2 = \int \frac{d\mathbf{r}_\perp d\mathbf{r}_\perp'}{4m^2a^2} \langle T_\tau \psi_0(\mathbf{r};\tau_1)\overline{\psi}_0(\mathbf{r}',\tau_2)\rangle \times T_\tau \psi_1(\mathbf{r}',\tau_2)\overline{\psi}_1(\mathbf{r},\tau_1). \tag{A4}$$

Using the definition of the Matsubara Green function

$$-\langle \psi_n(\tau)\overline{\psi}_m(0)\rangle_2 = \mathcal{G}_{nm}(\tau) = \left[\frac{1}{\partial_\tau - \hat{H}_2} \right]_{nm} \tag{A5}$$

and the low-energy representation for the fermionic operator [only one transverse mode $\phi(\mathbf{r}_\perp)$ in the channel]

$$\psi_0(\mathbf{r}_\perp) = \psi_0 \phi(\mathbf{r}_\perp),$$

we rewrite Eq. (A4) in the form

$$\frac{1}{2}\langle T_\tau \hat{H}_{12}(\tau_1)\hat{H}(\tau_2)\rangle_2$$

$$= -T_\tau \psi_0(\tau_1)\overline{\psi}_0(\tau_2)\frac{1}{4m^2a^2}\int d\mathbf{r}_\perp d\mathbf{r}'_\perp \phi(\mathbf{r}_\perp)\phi(\mathbf{r}'_\perp) \times \mathcal{G}_{11}(\tau_1-\tau_2;\mathbf{r}_\perp,\mathbf{r}'_\perp). \quad \text{(A6)}$$

As it follows from Eqs. (A3) and (A5), the Green function satisfies the equation

$$\left\{(\partial_\tau - \hat{H}_\perp)\delta_{nn'} - \frac{2\delta_{nn'}-\delta_{nn'+1}-\delta_{nn'-1}}{2ma^2}\right\}\mathcal{G}_{n'm} = a^{-1}\delta_{nm}\delta(\mathbf{r}_1-\mathbf{r}_2), \quad n>1; \quad \text{(A7a)}$$

$$\left\{(\partial_\tau - \hat{H}_\perp)\delta_{nn'} - \frac{2\delta_{nn'}-\delta_{nn'-1}}{2ma^2}\right\}\mathcal{G}_{n'm} = a^{-1}\delta_{nm}\delta(\mathbf{r}_1-\mathbf{r}_2), \quad n=1. \quad \text{(A7b)}$$

We see that the difference between Eq. (A7a) and Eq. (A7b) can be described by the boundary condition

$$\mathcal{G}_{0n}=0, \quad \mathcal{G}_{n0}=0. \quad \text{(A8)}$$

Now, we introduce coordinate $x=an$, and take the continuous limit $a\to 0$. Substituting $\mathcal{G}_{11}=a^2\partial^2_{xx'}\mathcal{G}(x,x')|_{x,x'=+0}$ into Eq. (A6), we obtain Eq. (3.7).

APPENDIX B: DERIVATION OF EQS. (4.14)

We introduce correlation functions more general than Eq. (4.13):

$$\mathcal{D}_-(\tau;x_1,x_2)=\langle T_\tau \hat{\varphi}_-(\tau;x_1)\hat{\varphi}_-(0;x_2)\rangle, \quad \text{(B1a)}$$

$$\mathcal{D}_+(\tau;x_1,x_2)=\langle T_\tau \hat{\varphi}_+(\tau;x_1)\hat{\varphi}_+(0;x_2)\rangle, \quad \text{(B1b)}$$

$$\mathcal{D}_\Phi(\tau)=\langle T_\tau \hat{\Phi}(\tau)\hat{\Phi}(0)\rangle, \quad \text{(B1c)}$$

$$\mathcal{D}_{\Phi+}(\tau;x)=\langle T_\tau \hat{\Phi}(\tau)\hat{\varphi}_+(0,x)\rangle. \quad \text{(B1d)}$$

Correlation functions (4.13) are related to those from Eq. (B1) by

$$\mathcal{D}_\pm(\tau)=\int_{-\infty}^{\infty}\frac{dx}{\pi}\frac{\lambda\mathcal{D}_\pm(\tau;0,x)}{\lambda^2+x^2}, \quad \mathcal{D}_{\Phi+}(\tau)=\mathcal{D}_{\Phi+}(\tau;0), \quad \text{(B2)}$$

where the high momenta cutoff is introduced consistently with Eqs. (4.1). Equations of motion for propagators (B1) follow from Eqs. (4.8) and (4.10) and they are given by

$$(\partial_\tau + iv_F\partial_x)\mathcal{D}_-(\tau;x,y) = -i\pi\delta(\tau)\mathrm{sgn}(x-y); \quad \text{(B3a)}$$

$$(\partial_\tau + iv_F\partial_x)\mathcal{D}_+(\tau;x,y) = i\,\mathrm{sgn}\,x\frac{E_C}{2\pi}\mathcal{D}_+(\tau;0,y) - i\pi\delta(\tau)\mathrm{sgn}(x-y), \quad \text{(B3b)}$$

$$\partial_\tau\mathcal{D}_\Phi(\tau)=i\frac{E_C}{2\pi}\mathcal{D}_{\Phi+}(\tau;0), \quad \text{(B3c)}$$

$$\partial_\tau\mathcal{D}_{\Phi+}(\tau;x)=i\pi\delta(\tau)-i\frac{E_C}{2\pi}\mathcal{D}_+(\tau;0,x). \quad \text{(B3d)}$$

Performing imaginary time Fourier transform $\mathcal{D}(\tau)=T\Sigma_{\Omega_n}e^{-i\Omega_n\tau}\mathcal{D}(\Omega_n)$ (here $\Omega_n=2\pi nT$ is the bosonic Matsubara frequency) we find the solution of Eq. (B3b):

$$\mathcal{D}_+(\Omega_n;x,y) = \frac{\pi}{\Omega_n}\{\mathrm{sgn}(x-y)+2\theta[\Omega_n(y-x)]e^{(\Omega_n/v_F)(x-y)}\} - \frac{E_C}{2\pi}\mathcal{D}_+(\Omega_n;0,y)\{\mathrm{sgn}\,x+2\theta(-\Omega_n x)e^{(\Omega_n/v_F)x}\}. \quad \text{(B4)}$$

Substituting $x=0$ in the both sides of Eq. (B4), we find $\mathcal{D}_+(\Omega_n;0,y)$ and, then Eq. (B2) yields:

$$\mathcal{D}_+(\Omega_n)=\frac{\pi}{|\Omega_n|+E_C/2\pi}f\left(\frac{|\Omega_n|\lambda}{v_F}\right). \quad \text{(B5a)}$$

Propagator $\mathcal{D}_-$ is found by putting $E_C=0$ in Eq. (B5a),

$$\mathcal{D}_-(\Omega_n)=\frac{\pi}{|\Omega_n|}f\left(\frac{|\Omega_n|\lambda}{v_F}\right), \quad \text{(B5b)}$$

and remaining propagators are found from the time Fourier transform of Eqs. (B3c)–(B3d) and Eq. (B5a):

$$\mathcal{D}_\Phi(\Omega_n)=\frac{E_C}{2\pi|\Omega_n|}\frac{\pi}{|\Omega_n|+E_C/2\pi}, \quad \text{(B5c)}$$

$$\mathcal{D}_{\Phi+}(\Omega_n)=\frac{\pi\,\mathrm{sgn}\,\Omega_n}{|\Omega_n|+E_C/2\pi}. \quad \text{(B5d)}$$

In Eqs. (B5), the cutoff function $f(x)$ is defined as

$$f(x)=\int_0^\infty\frac{2dy}{\pi}\frac{e^{-xy}}{1+y^2}. \quad \text{(B6)}$$

Inverse Fourier transform of Eqs. (B5) gives Eqs. (4.14). Let us write here for completeness the result for the propagator $\mathcal{D}_+(0)$ at arbitrary temperatures:

$$\mathcal{D}_+(0)=\ln\left(\frac{2\pi v_F}{\lambda E_C e^{\mathrm{C}}}\right)+\int_0^\infty dx\left[\cot x-\frac{1}{x}\right]e^{-xE_C/2\pi^2T}. \tag{B7}$$

At small temperatures $T\ll E_C$, Eq. (B7) reduces to Eq. (4.14c). At large temperatures, $T\gg E_C$, we obtain

$$\mathcal{D}_+(0)=\ln\left(\frac{v_F}{2\pi T\lambda}\right)+\frac{2\pi^2T}{E_C}.$$

All the results associated with the Coulomb blockade [see, e.g., Eq. (4.15b)] contain exponential terms of the form $e^{-\mathcal{D}_+(0)}$. This gives the suppression of the charge quantization at high temperature by a factor of $e^{-2\pi^2T/E_C}$. This clearly indicates that the effects considered in this paper and in Refs. 14 and 27 cannot be obtained in any order of perturbation theory in charging energy E_C.

*Present address: SUNY at Stony Brook, Stony Brook, NY 11794.

[1] H. R. Zeller and I. Giaever, Phys. Rev. **181**, 789 (1969); I. O. Kulik and R. I. Shekhter, Zh. Éksp. Teor. Fiz. **62**, 623 (1975) [Sov. Phys. JETP **41**, 308 (1975)]; for the review see Refs. 2, 3.

[2] D. V. Averin and K. K. Likharev, in *Mesoscopic Phenomena in Solids*, edited by B. L. Altshuler, P. A. Lee, and R. A. Webb (North-Holland, New York, 1991).

[3] L. P. Kouwenhoven, C. M. Marcus, P. L. McEuen, S. Tarucha, R. M. Westervelt, and N. S. Wingreen, in *Mesoscopic Electron Transport*, Vol. 345 of *NATO Advanced Studies Institute E: Applied Sciences*, edited by L. Sohn, L. P. Kouwenhoven, and G. Schön (Kluwer, Dordrecht, 1997).

[4] R. Jalabert, A. D. Stone, and Y. Alhassid, Phys. Rev. Lett. **68**, 3468 (1992); Y. Alhassid and H. Attias, *ibid.* **76**, 1711 (1996).

[5] C. M. Marcus, A. J. Rimberg, R. M. Westerwelt, P. F. Hopkins, and A. C. Gossard, Phys. Rev. Lett. **69**, 506 (1992); C. M. Markus, R. M. Westerwelt, P. F. Hopkins, and A. C. Gossard, Phys. Rev. B **48**, 2460 (1993); Chaos **3**, 643 (1993).

[6] A. M. Chang, H. U. Baranger, L. N. Pfeiffer, K. W. West, and T. Y. Chang, Phys. Rev. Lett. **76**, 1695 (1996).

[7] J. A. Folk, S. R. Patel, S. F. Godijn, A. G. Huibers, S. M. Cronenwett, C. M. Marcus, K. Campman, and A. C. Gossard, Phys. Rev. Lett. **76**, 1699 (1996).

[8] *Statistical Theories of Spectra: Fluctuations*, edited by C. E. Porter (Academic Press, New York, 1965).

[9] M. L. Mehta, *Random Matrices* (Academic, New York, 1991).

[10] D. V. Averin and Yu. N. Nazarov, Phys. Rev. Lett. **65**, 2446 (1990).

[11] L. L. Aleiner and L. I. Glazman, Phys. Rev. Lett. **77**, 2057 (1996).

[12] S. M. Cronenwett, S. R. Patel, C. M. Marcus, K. Campman, and A. C. Gossard, Phys. Rev. Lett. **79**, 2312 (1997).

[13] L. I. Glazman and K. A. Matveev, Zh. Éksp. Teor. Fiz. **98**, 1834 (1990) [Sov. Phys. JETP **71**, 1031 (1990)]; K. A. Matveev, *ibid.* **99**, 1598 (1991) [*ibid.* **72**, 892 (1991)].

[14] K. A. Matveev, Phys. Rev. B **51**, 1743 (1995).

[15] K. Flensberg, Phys. Rev. B **48**, 11 156 (1993); Physica B **203**, 432 (1994).

[16] M. Büttiker, H. Thomas, and A. Pretre, Z. Phys. B **94**, 133 (1994); M. Büttiker, Nuovo Cimento B **110**, 509 (1995); J. Phys.: Condens. Matter **5**, 9361 (1993).

[17] V. A. Gopar, P. A. Mello, and M. Büttiker, Phys. Rev. Lett. **77**, 3005 (1996); P. W. Brouwer and M. Büttiker, Europhys. Lett. **37**, 441 (1997).

[18] P. Nozieres, J. Low Temp. Phys. **17**, 31 (1974).

[19] B. L. Altshuler and B. D. Simons, in *Mesoscopic Quantum Physics*, Les Houches Summer School Course LXI, edited by E. Akkermans, G. Montambaux, J.-L. Pichard, and J. Zinn-Justin (Elsevier, Amsterdam, 1995).

[20] M. C. Gutzwiller, *Chaos in Classical and Quantum Mechanics* (Springer-Verlag, New York, 1990).

[21] M. V. Berry, Proc. R. Soc. London, Ser. A **400**, 229 (1985).

[22] This subsection was motivated by discussions with Piet Brouwer.

[23] B. L. Altshuler and D. E. Khmelnitskii, Pis'ma Zh. Éksp. Teor. Fiz. **42**, 291 (1985) [JETP Lett. **42**, 359 (1985)].

[24] I. L. Aleiner and A. I. Larkin, Phys. Rev. B **54**, 14 423 (1996).

[25] P. W. Brouwer, Phys. Rev. B **51**, 16 878 (1995).

[26] M. L. Mehta and A. Pandey, J. Phys. A **16**, 2655 (1983).

[27] A. Furusaki and K. A. Matveev, Phys. Rev. Lett. **75**, 709 (1995); Phys. Rev. B **52**, 16 676 (1995).

[28] K. B. Efetov, *Supersymmetry in Disorder and Chaos* (Cambridge University Press, New York, 1997).

[29] For recent review, see C. W. J. Beenakker, Rev. Mod. Phys. **69**, 731 (1997).

[30] B. L. Altshuler and B. I. Shklovskii, Zh. Éksp. Teor. Fiz. **91**, 220 (1986) [Sov. Phys. JETP **64**, 127 (1986)].

[31] B. L. Altshuler, Y. Gefen, A. Kamenev, and L. S. Levitov, Phys. Rev. Lett. **78**, 2803 (1997); O. Agam, N. S. Wingreen, B. L. Altshuler, D. C. Ralph, and M. Tinkham, *ibid.* **78**, 1956 (1997); Ya. M. Blanter, Phys. Rev. B **54**, 12 807 (1996).

[32] Ya. M. Blanter and A. D. Mirlin, Phys. Rev. E **55**, 6514 (1997).

[33] U. Sivan, R. Berkovits, Y. Aloni, O. Prus, A. Auerbach, and G. Ben-Yoseph, Phys. Rev. Lett. **77**, 1123 (1996); R. Berkovits and U. Sivan, cond-mat/9707138.

[34] A. A. Koulakov, F. G. Pikus, and B. I. Shklovskii, Phys. Rev. B **55**, 9223 (1997).

[35] F. D. M. Haldane, J. Phys. C **14**, 2585 (1981); I. Affleck, Nucl. Phys. B **265**, 448 (1986).

[36] D. V. Averin and A. A. Odintsov, Phys. Lett. A **140**, 251 (1989).

[37] L. W. Molenkamp, K. Flensberg, and M. Kemerink, Phys. Rev. Lett. **75**, 4282 (1995).

[38] N. B. Zhitenev, R. C. Ashoori, L. N. Pfeiffer, and K. W. West, Phys. Rev. Lett. **79**, 2308 (1997); N. V. Zhitenev and R. C. Ashoori (private communication).

[39] I. L. Aleiner and L. I. Glazman (unpublished).

[40] I. S. Gradshteyn and I. M. Ryzhik, *Table of Integrals, Series, and Products*, 5th ed. (Academic Press, New York, 1994).

[41] In a recent work (Ref. 42), an attempt has been made to describe the Coulomb blockade for an open channel by replacing the averaging over a grand canonical ensemble by the averaging over a canonical ensemble. We do not see any grounds for such an approach because the quantum fluctuations of the number of electrons in the dot are parametrically large, $\langle(\delta\hat{Q}/e)^2\rangle \simeq \ln(\epsilon_F/E_C)$.

[42] P. W. Brouwer, S. A. van Langen, K. M. Frahm, M. Büttiker, and C. W. J. Beenakker, Phys. Rev. Lett. **79**, 913 (1997).

[43] C. M. Marcus (private communication).

[44] See, e.g., G. D. Mahan, *Many-Particle Physics* (Plenum Press, New York, 1990).

[45] The same formulas can be obtained also starting from the random matrix formulation of Sec. III B and correlation function (6.7) in the form $\Pi(\tau) = -\Delta M \langle T_\tau \psi_\alpha(\tau) \overline{\psi}_\alpha(0) \rangle$ where α is an arbitrary state of the dot.

[46] P. W. Anderson, Phys. Rev. Lett. **18**, 1049 (1967).

[47] P. Nozieres and C. T. de Dominicis, Phys. Rev. **178**, 1097 (1969).

[48] Numerical coefficient in Eq. (6.51) differs from Ref. 27 because we define G_R as the conductance per one spin and our definition of the charging energy E_C also differs by a factor of 2.

[49] N. C. van der Vaart, A. T. Johnson, L. P. Kouwenhoven, D. J. Maas, W. de Jong, M. P. de Ruyter van Steveninck, A. van der Enden, C. J. P. M. Harmans, and C. T. Foxon, Physica B **189**, 99 (1993).